รายงานวิจัยฉบับสมบูรณ์

โครงการการศึกษาผลกระทบของปฏิสัมพันธ์ระหว่างของไหลภายในท่อกับผนังท่อต่อพฤติกรรมของท่อขุดเจาะและลำเลียงของไหลใต้ทะเล

โดย ดร.ชัยณรงค์ อธิสกุล และคณะ

มิถุนายน 2555

สัญญาเลขที่ MRG5380034

รายงานวิจัยฉบับสมบูรณ์

โครงการ การศึกษาผลกระทบของปฏิสัมพันธ์ระหว่างของไหลภายในท่อกับผนังท่อต่อพฤติกรรมของท่อขุดเจาะและลำเลียงของไหลใต้ทะเล

คณะผู้วิจัย	สังกัด
1.) นายชัยณรงค์ อธิสกุล	ภาควิชาวิศวกรรมโยธา คณะวิศวกรรมศาสตร์ มหาวิทยาลัยเทคโนโลยีพระจอมเกล้าธนบุรี
2.) ศ.ดร.สมชาย ชูชีพสกุล	ภาควิชาวิศวกรรมโยธา คณะวิศวกรรมศาสตร์ มหาวิทยาลัยเทคโนโลยีพระจอมเกล้าธนบุรี

สนับสนุนโดยสำนักงานคณะกรรมการการอุดมศึกษา และสำนักงานกองทุนสนับสนุนการวิจัย

(ความเห็นในรายงานนี้เป็นของผู้วิจัย สกอ. และ สกว. ไม่จำเป็นต้องเห็นด้วยเสมอไป)

บทคัดย่อ

รหัสโครงการ : **MRG5380034**

ชื่อโครงการ : **การศึกษาผลกระทบของปฏิสัมพันธ์ระหว่างของไหลภายในท่อกับผนังท่อต่อพฤติกรรมของท่อขุดเจาะและลำเลียงของไหลใต้ทะเล**

ชื่อนักวิจัย : **ดร.ชัยณรงค์ อธิสกุล**
ศ.ดร.สมชาย ชูชีพสกุล
ภาควิชาวิศวกรรมโยธา คณะวิศวกรรมศาสตร์
มหาวิทยาลัยเทคโนโลยีพระจอมเกล้าธนบุรี

E-mail Address : **chainarong.ath@kmutt.ac.th**

ระยะเวลาโครงการ : 2 ปี (15 มิถุนายน 2553 ถึง 14 มิถุนายน 2555)

งานวิจัยนี้ศึกษาปฏิสัมพันธ์ระหว่างของไหลภายในท่อกับผนังท่อ โดยการศึกษาจะเริ่มจากการสร้างสมการความเร่งของของไหลภายในท่อในพจน์ของการเคลื่อนที่ของท่อและความเร็วการไหลภายในท่อ สมการความเร่งนี้จะใช้ในการคำนวณแรงเฉื่อยของของไหลภายในท่อซึ่งมีการเสียรูปได้มาก แบบจำลองสำหรับการวิเคราะห์ท่อขุดเจาะและลำเลียงของไหลใต้ทะเลจะได้รับการพัฒนาขึ้นภายใต้ทฤษฎีการเสียรูปมากของโครงสร้างอีลาสติกาและหลักการของงานและพลังงาน ในการศึกษานี้จะอาศัยระเบียบวิธีการไฟไนต์เอลิเมนต์ในการหาคำตอบเชิงตัวเลข ผลกระทบของปฏิสัมพันธ์ระหว่างของไหลภายในท่อกับผนังท่อที่มีต่อพฤติกรรมทางสถิตศาสตร์และพลศาสตร์ของท่อขุดเจาะและลำเลียงของไหลใต้ทะเลจะนำเสนอไว้ในรายงานวิจัยนี้

คำหลัก : ท่อขุดเจาะและลำเลียงของไหลใต้ทะเล, ของไหลภายในท่อ,
ปฏิสัมพันธ์ระหว่างของไหลภายในท่อกับผนังท่อ

Abstract

Project Code : **MRG5380034**

Project Title : **Effect of Interaction between Internal Fluid and Pipe Wall on Marine Riser Behavior**

Investigator : **Chainarong Athisakul, Ph.D.**
Prof. Somchai Chucheepsakul, Ph.D.
Department of Civil Engineering, Faculty of Engineering
King Mongkut's University of Technology Thonburi

E-mail Address : **chainarong.ath@kmutt.ac.th**

Project Period : **2 years (15 June 2010 – 14 June 2012)**

The interaction between internal fluid and pipe wall of marine riser is thoroughly addressed. The acceleration of the internal fluid has to be formulated firstly in terms of the displacement of the riser and the internal fluid speed. This acceleration is used to derive the inertia force of transported fluid inside the riser which may be experiencing large displacement and large deformation. The model formulation of extensible marine riser is developed based on the extensible elastica theory and the work-energy principle. The finite element method is used to obtain the numerical solutions. The effect of interaction between internal fluid and pipe wall on static and dynamic behaviors of the extensible marine riser is presented.

Keywords : Marine Riser, Internal Fluid, Fluid and Pipe Wall Interaction

กิตติกรรมประกาศ

ผู้วิจัยขอขอบพระคุณ มหาวิทยาลัยเทคโนโลยีพระจอมเกล้าธนบุรี สำนักงานคณะกรรมการการอุดมศึกษา และสำนักงานกองทุนสนับสนุนการวิจัย สำหรับการสนับสนุนทุนวิจัยทั้งหมดของโครงการวิจัยนี้ และขอกราบขอบพระคุณ ศ.ดร.สมชาย ชูชีพสกุล สำหรับคำสอน คำแนะนำ และการให้คำปรึกษาในทุกด้านจนกระทั่งโครงการวิจัยนี้สามารถสำเร็จลุล่วง ผู้วิจัยขอขอบพระคุณ ภาควิชาวิศวกรรมโยธา คณะวิศวกรรมศาสตร์ มหาวิทยาลัยเทคโนโลยีพระจอมเกล้าธนบุรี ที่ให้การสนับสนุนสถานที่และบุคลากรในการดำเนินโครงการวิจัยในครั้งนี้

ผู้วิจัยขอกราบขอบพระคุณครู และอาจารย์ทุกท่านที่กรุณาให้ความรู้ คำสอนและแนวทางปฏิบัติที่ดีแก่ผู้วิจัยมาโดยตลอด ผู้วิจัยขอขอบคุณ คุณแพมาลา อุทะนุต เจ้าหน้าที่บริหารโครงการ ฝ่ายวิชาการ สกว. และเจ้าหน้าที่ของภาควิชาวิศวกรรมโยธาทุกท่านรวมถึงคุณการันต์ คล้ายฉ่ำ และคุณธงชัย ปัญญาสหะชาติ สำหรับความช่วยเหลือในงานเอกสาร สุดท้ายผู้วิจัยขอกราบขอบพระคุณบิดา มารดา และญาติพี่น้องของผู้วิจัย รวมถึงคุณวราภรณ์ จาตนิล ผู้ซึ่งให้การสนับสนุน และเป็นกำลังใจแก่ผู้วิจัยเสมอมา

Executive Summary

Research Significant and Problem Statement

The increasing demand on energy resources, especially in oil and gas, has driven the offshore production into deepwater and ultra deepwater fields. At present, there are a lot of deepwater offshore structures installed in all parts of the world. The new technologies for deep offshore industry are required and developed continuously. One of a key component for offshore production is the marine riser.

The marine riser is a vertical pipe that extends from the offshore platform down to the well at the sea bed. There are two fundamental types of marine riser: drilling riser and production riser. Drilling riser is used to contain drilling mud and cutting from the borehole to the drilling platform, while production riser is used to transport hydrocarbons from the seabed to the production platform. Nowadays, the oil and gas companies try to develop new technologies for offshore production in over 2000 m of water. A damage of the riser system causes a severe environmental pollution and a significant financial consequence. Therefore, engineers and researchers must have a good understanding of marine riser behaviors.

This report presents the effect of internal fluid and pipe wall interaction on static behavior and dynamic properties of marine riser. The model formulation of an extensible marine riser transporting fluid is developed by a variational approach. The finite element method is used to determine the numerical solutions. The effect of axial extensibility on large displacement and dynamic properties of marine riser are also investigated herein.

Objective of Research

The objectives of this research are as follows:

- To present the concepts of fluid flow inside the extensible marine riser.
- To develop the variational model formulation of the extensible marine riser transporting fluid.
- To develop the finite element model for static and dynamic analysis of the extensible marine riser transporting fluid.
- To investigate the effect of internal fluid and pipe wall interaction on static and dynamic behaviors of marine riser.

Research Methodology and Results

The kinematics of marine riser and internal fluid inside the extensible marine riser has been addressed. The acceleration of the internal fluid has to be formulated firstly in terms of the displacement of the riser and the internal fluid speed. The model formulation of an extensible marine riser is developed by the variational approach based on the elastica theory and the work-energy principle. The strain energy of the riser composes of the strain energy due to large axial deformation, and bending. The large axial strain is described by the total Lagrangian descriptor. The external virtual work of the riser is composed of the virtual work done by the apparent weight, the hydrodynamic forces, and the inertial forces.

The finite element method is used to obtain the numerical solutions. For nonlinear static analysis, the system of finite element equations is solved by iterative numerical method. The static configurations are used as the initial configuration for free vibration analysis of marine riser. In this study, the linear free vibration of the marine riser is investigated. The natural frequencies and their corresponding mode shapes are determined by solving the boundary value problem. This problem is solved by the QR-algorithm.

The numerical examples in this report are presented in order to investigate the effect of internal flow velocity on maximum displacement, maximum bending moment and dynamic properties of marine riser. The results indicate that the increase in internal flow velocity enlarges the riser displacement and changes the position of the maximum displacement down to the seabed. The increase in velocity of transporting fluid increases the maximum bending moment until the velocity reaches a value that induces a peak value of maximum bending moment. Beyond this velocity, the maximum bending moment no longer increases, but it is decreased. However, the maximum displacement continuously increases and the riser tends to have divergence instability. The negative flow velocity affects the nonlinear static behavior of the marine riser as same as the positive flow velocity. The internal flow velocity has an insignificant effect on the axial strain, the true-wall tension, and the apparent tension. The increase in internal flow velocity reduces the natural frequencies and the structural stability of the marine riser. The number of curvature for the mode shape of marine riser could be changed when the internal flow velocity reaches the critical values. The effect of the internal flow can be reduced by increasing the axial deformation.

Contents

1. Introduction

1.1 Statement of the Problem

The increasing demand on energy resources, especially in oil and gas, has driven the offshore production into deepwater and ultra deepwater fields. At present, there are a lot of deepwater offshore structures installed in all parts of the world. The new technologies for deep offshore industry are required and developed continuously. One of a key component for offshore production is the marine riser.

The marine riser is a vertical pipe that extends from the offshore platform down to the well at the sea bed. There are two fundamental types of marine riser: drilling riser and production riser. Drilling riser is used to contain drilling mud and cutting from the borehole to the drilling platform, while production riser is used to transport hydrocarbons from the seabed to the production platform. Nowadays, the oil and gas companies try to develop new technologies for offshore production in over 2000 m of water. A damage of the riser system causes a severe environmental pollution and a significant financial consequence. Therefore, engineers and researchers must have a good understanding of marine riser behaviors.

This report presents the effect of internal fluid and pipe wall interaction on static behavior and dynamic properties of marine riser. The model formulation of an extensible marine riser transporting fluid is developed by a variational approach. The finite element method is used to determine the numerical solutions. The effect of axial extensibility on large displacement and dynamic properties of marine riser are also investigated herein.

1.2 Literature Review

The analysis of marine riser has received considerable attention over the past several years. The first riser was installed in Mohole Project in 1949. St. Denis and Armijo [1] presented the first technical paper on dynamic analysis of the Mohole riser. From then on, many other interesting papers have been published on marine riser problems to increase the understanding of the static and dynamic behavior of the marine riser.

In the literature, there are many papers related to analysis of marine riser as reviewed by Chakrabarti and Frampton [2], Ertas and Kozik [3], Jain [4] and Patel and Seyed [5]. A comprehensive review of the literature shows that the development of a model

formulation and computational technique is the main concern in riser analysis. The internal fluid transportation is a main function of marine riser, however, the effect of internal fluid and pipe wall interaction on the riser behavior has received a little attention.

The effects of the internal fluid flow have been long investigated in many research studies dealing with the pipe conveying fluid. The vibrations of straight and curved pipes are presented in many papers, for example, Housner [6], Gregory and Païdoussis [7], Païdoussis [8], and Doll and Mote [9]. They stated that the liquid flow in the curve pipe would affect the tangential force. As a result, the internal flow can induce the flutter instability or the snaking behavior of cantilever pipes, and can generate the divergence instability or the statical buckling of simply supported pipes.

In the early of 1980s, many papers have investigated the effects of the internal flow on the marine riser. They simplified that the internal flow induces only the friction force acting on the pipe wall and this force is vanished from the equation of motion. This simplification may not be sufficient for the large sagged pipes, because the internal friction force does not act directly on the riser pipe. It transmits the internal pressure into the pipe wall. This pressure reduces the internal tension of the marine riser [6-11]. In addition, the internal flow generated not only the effects of the pressure, but also other fictitious forces such as Coriolis and centrifugal forces.

The misconception of the internal flow effect has been dispelled in the end of 1980s because many researchers in that period put their interest in this effect. Irani et al. [12] presented the dynamic analysis of the riser with internal flow and nutation dampers. They suggested that the steadily internal flow reduces the stiffness of the marine risers, and provides a negative damping mechanism.

Patel and Seyed [13] presented a method for the analysis of the flexible risers subjected to a time varying internal flow. They concluded that the effect of the slug flow is significant for moderate to large water depths or in the large pressure area, and the slug flow caused additional source of the cyclic fatigue loading.

Moe and Chucheepsakul [14] used the asymptotic method and finite element method to obtain the natural frequencies of the flexible marine riser. They mentioned that the natural frequencies of the pipes are reduced when the internal flow velocity increase. This finding is also confirmed by Wu and Lou [15].

Chucheepsakul and Huang [16] investigated the effect of the steadily transported mass on the two-dimensional riser. They reported that the internal flow induces additional large displacements of the marine riser. At the state of low top-tensioning and low elastic modulus, the high flow rate leads to the divergence instability of the marine riser [17]. Chucheepsakul and Monprapussorn [18] investigated the nonlinear buckling of marine elastica pipes/risers transporting fluid. They solved the boundary value problem of the model by shooting optimization technique. Their results confirm that the effect of the internal flow velocity is to increase the large displacement and the critical top tension, and to decrease the critical pipe's weight and the structural stability of the marine pipes/risers.

Although the model formulations of the flexible marine riser transporting fluid have been presented by several scholars [19-22], their model formulations have not yet considered the geometric nonlinearity and the axial deformation of the marine riser. These themes have been taken into account in large strain model formulations of the extensible flexible marine pipes/risers by Chucheepsakul et al. [23]. This research aims to develop this model formulation for investigating the effects of internal fluid and pipe wall interaction on static and dynamic behavior of the extensible marine riser.

1.3 Objectives

The objectives of this research are as follows:

- To present the concepts of fluid flow inside the extensible marine riser.
- To develop the variational model formulation of the extensible marine riser transporting fluid.
- To develop the finite element model for static and dynamic analysis of the extensible marine riser transporting fluid.
- To investigate the effect of internal fluid and pipe wall interaction on static and dynamic behaviors of marine riser.

1.4 Assumptions

The following assumptions are established in order to limit the scope of this study.

- The material of the marine riser is linearly elastic.
- At the undeformed state, the marine riser is straight, and has no residual stresses.
- The riser's cross sections remain circular after the change of cross-sectional size due to the axial deformation effect.
- Every cross-section remains plane perpendicular to the axis.
- The effect of the shear strain is small and can be neglected.
- The effect of torsion is not considered.
- The marine riser connections are presumed to be homogeneous with the riser body, and have the same properties.
- The marine riser stiffness is determined from the cross-section of the riser only, the contribution from the drilling pipe and the surrounding kill and choke lines are not considered.
- The internal and external fluids are inviscid, incompressible and irrotational.

2. Theoretical Concepts and Model Formulation

In this chapter, theory and model formulation of the extensible marine risers are presented. A variational formulation is developed based on the extensible elastica theory and the work-energy principle. The strain energy due to bending, axial stretching and virtual work done by hydrostatic pressure and other external forces are involved in the variational model. The virtual work done by inertial forces of the riser and internal fluid are also included in the formulation. The outstanding feature of the model is the flexibility of the independent variable that is used to define elastic curves of the riser. The independent variable can be chosen between $s, x, y,$ or z to make it suitable for the particular problem.

2.1 Kinematics of Marine Riser

The riser configurations in each state can be described by using the position of the riser's centroidal line as shown in the figure (2.1). At the top end, the riser is connected to the surface vessel with an appropriately tension (N_{aH}) in order to prevent buckling due to its self weight and environmental loads. A connection of riser at the top end is a slip joint, which allows the relative motion between the moving surface vessel and the stationary seabed. At the seabed, the riser is connected to a ball joint locating inside the upper portion of the blowout preventer, or "BOP" stack. The horizontal offset of the vessel measured from the bottom end is represented by x_H (figure 2.1).

In this study, the two-dimensional Cartesian coordinate system is used to define position, motion, and deformation of the riser's centroidal line. The Cartesian coordinate system x, y with unit vector $\hat{i}, \hat{j}$ is used as the global coordinate. The local coordinate system is represented by the tangential vector $\hat{t}$ and normal vector $\hat{n}$.

The first configuration of the riser is the undeformed configuration, which is an ideal configuration. The material point on the riser cross-section at the undeformed configuration can be defined by the position vector $\vec{\mathbf{r}}_\mathbf{o}$ as shown below.

$$\vec{\mathbf{r}}_\mathbf{o} = x_o(\alpha)\hat{i} + y_o(\alpha)\hat{j} \tag{2.1}$$

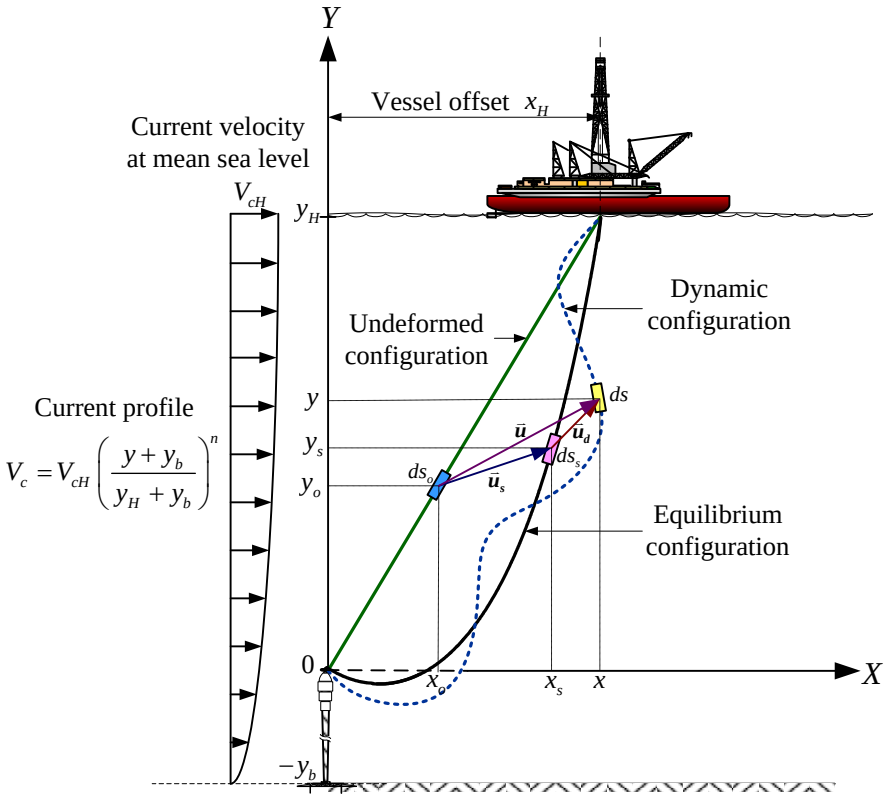

Figure 2.1 Three configuration states of an extensible marine riser.

The parameter α is used to define the riser configuration. This parameter is employed in the formulation for the sake of generality. Therefore, the users can choose any convenient coordinates such as $x_o, x_s, x, y_o, y_s, y, z_o, z_s, z, s_o, s_s, s$ to define the centroidal curve instead of parameter α .

According to time independent loads (such as the apparent weight, the quasi-static load due to current, and the tangential force due to internal flow rate), the riser configuration is changed from the undeformed configuration to the equilibrium configuration. The material point on the riser cross-section at the equilibrium configuration is defined by the following position vector.

$$\vec{\mathbf{r}}_{\mathbf{s}}(\alpha) = \vec{\mathbf{r}}_{\mathbf{0}}(\alpha) + \vec{\mathbf{u}}_{\mathbf{s}}(\alpha) = x_s(\alpha)\hat{i} + y_s(\alpha)\hat{j} \tag{2.2}$$

The vector $\vec{\mathbf{u}}_{\mathbf{s}}(\alpha)$ represents a static displacement vector of marine riser, which is measured from the undeformed state.

$$\vec{\mathbf{u}}_{\mathbf{s}}(\alpha) = u_s(\alpha)\hat{i} + v_s(\alpha)\hat{j} \tag{2.3}$$

When the riser is excited by the time dependent load such as wave and unsteady flows of transporting fluids, the riser will change its position from equilibrium to the dynamic configuration. As shown in figure 2.1, the position vector of the material point on the riser cross-section at the dynamic configuration is

$$\vec{\mathbf{r}}(\alpha,t)=\vec{\mathbf{r}}_{\mathbf{s}}(\alpha)+\vec{\mathbf{u}}_{\mathbf{d}}(\alpha,t)=x(\alpha,t)\hat{i}+y(\alpha,t)\hat{j} \tag{2.4}$$

The vector $\vec{\mathbf{u}}_{\mathbf{d}}(\alpha,t)$ represents the dynamic displacement vector of marine riser. It is measured from the equilibrium configuration.

$$\vec{\mathbf{u}}_{\mathbf{d}}(\alpha,t)=u_d(\alpha,t)\hat{i}+v_d(\alpha,t)\hat{j} \tag{2.5}$$

Therefore, the position vector for the displaced configuration can be expressed by the following equations.

$$\vec{\mathbf{r}}(\alpha,t)=\vec{\mathbf{r}}_{\mathbf{o}}(\alpha)+\vec{\mathbf{u}}(\alpha,t)=(x+u)\hat{i}+(y+v)\hat{j} \tag{2.6 a}$$

$$\vec{\mathbf{r}}(\alpha,t)=\vec{\mathbf{r}}_{\mathbf{s}}(\alpha)+\vec{\mathbf{u}}_{\mathbf{d}}(\alpha,t)=(x_s+u_d)\hat{i}+(y_s+v_d)\hat{j} \tag{2.6 b}$$

By taking the first and second derivative to equation (2.6) with respect to time t, the velocity $\vec{\mathbf{V}}_{\mathbf{P}}(\alpha,t)$ and acceleration $\vec{\mathbf{a}}_{\mathbf{P}}(\alpha,t)$ of the riser can be derived as follows.

$$\vec{\mathbf{V}}_{\mathbf{P}}=\dot{\vec{\mathbf{r}}}(\alpha,t)=\dot{u}_d(\alpha,t)\hat{i}+\dot{v}_d(\alpha,t)\hat{j} \tag{2.7}$$

$$\vec{\mathbf{a}}_{\mathbf{P}}=\ddot{\vec{\mathbf{r}}}(\alpha,t)=\ddot{u}_d(\alpha,t)\hat{i}+\ddot{v}_d(\alpha,t)\hat{j} \tag{2.8}$$

The superscripts $\dot{(\,)}$ denotes the partial derivative with respect to time t.

2.2 Axial Strain Definition

Based on the differential geometry of plane curve, the derivative of arc-length at the undeformed state(s_o), the equilibrium state(s_s), and the dynamic state (s) can be expressed by the following equations.

$$s_o'=\sqrt{x_o'^2+y_o'^2} \tag{2.9}$$

$$s_s'=\sqrt{x_s'^2+y_s'^2}=\sqrt{(x_o'+u_s')^2+(y_o'+v_s')^2} \tag{2.10}$$

$$s'=\sqrt{x'^2+y'^2}=\sqrt{(x_o'+u')^2+(y_o'+v')^2}=\sqrt{(x_o'+u_s'+u_d')^2+(y_o'+v_s'+v_d')^2} \tag{2.11}$$

Based on the mechanics of deformable body, the axial strain can be defined by the total Lagrangian descriptor as follows

Total strain: $$\varepsilon_t = \frac{s' - s'_o}{s'_o} = \frac{s'}{s'_o} - 1 = \sqrt{1 + 2L_t} - 1 \quad (2.12a)$$

Static strain: $$\varepsilon_s = \frac{s'_s - s'_o}{s'_o} = \frac{s'_s}{s'_o} - 1 = \sqrt{1 + 2L_s} - 1 \quad (2.12b)$$

Dynamic strain: $$\varepsilon_d = \frac{s' - s'_s}{s'_o} = \sqrt{1 + 2L_t} - \sqrt{1 + 2L_s} \quad (2.12c)$$

The Green strains (L_t, L_s) in equations (2.12) can be derived in the terms of riser displacements as follows.

$$L_t = \frac{1}{s'^2_o}\left(x'_o u' + y'_o v' + \frac{u'^2}{2} + \frac{v'^2}{2} \right) \quad (2.13a)$$

$$L_s = \frac{1}{s'^2_o}\left(x'_o u'_s + y'_o v'_s + \frac{u'^2_s}{2} + \frac{v'^2_s}{2} \right) \quad (2.13b)$$

2.3 The Change of Differential Arc-length, Cross-Sectional Properties, and Internal Flow Velocity due to the Large Axial Strain

The large axial strain of the riser cross-section leads to the change of differential arc-length. Because the riser volume is conserved, the cross-sectional properties of the riser also change from the original to the deformed quantity. Moreover, the internal flow velocity is changed based on the continuity property of transporting fluid. Consequently, the differential arc-length, the cross-sectional properties, and internal flow velocity at each state are related to each other through the axial strain as follows.

- ***Differential Arc-length***

The relations of large axial strain to the differential arc-length can be expressed as

$$ds_o = \frac{ds_s}{1 + \varepsilon_s} = \frac{ds}{1 + \varepsilon_t} \quad (2.14)$$

- ***Cross-Sectional Properties***

If the large axial stain occurs on the riser, the differential arc-length is changed from its original quantity. Therefore, the volumetric strain of the riser is expressed as

$$\varepsilon_v = \frac{d\forall_P - d\forall_{Po}}{d\forall_{Po}} = \frac{A_P s'}{A_{Po} s'_o} - 1 = \frac{A_P\left(1+\varepsilon_t\right)}{A_{Po}} - 1 \tag{2.15}$$

Since the riser volume is conserved, the volumetric strain of the riser becomes zero. Therefore, the cross-sectional area of the riser in three states can be related to each other as

$$A_{Po} = A_{Ps}\left(1+\varepsilon_s\right) = A_P\left(1+\varepsilon_t\right) \tag{2.16}$$

From equation (2.16), one can obtain the relationships of diameter (D_{Po}, D_{Ps}, D_P), and moment of inertia (I_{Po}, I_{Ps}, I_P) of the riser in each state as follows.

$$D_{Po} = D_{Ps}\sqrt{1+\varepsilon_s} = D_P\sqrt{1+\varepsilon_t} \tag{2.17}$$

$$I_{Po} = I_{Ps}\left(1+\varepsilon_s\right)^2 = I_P\left(1+\varepsilon_t\right)^2 \tag{2.18}$$

- ***Internal Flow Velocity***

Based on the fluid mechanics [24], the continuity equation for incompressible fluid can be expressed as

$$A_{io}V_{io} = A_{is}\left(s_s\right)V_{is}\left(s_s\right) = A_i\left(s,t\right)V_i\left(s,t\right) \tag{2.19}$$

From equation (2.19), one can see that the internal flow velocity is not uniform but it varies along the arc-length of the riser due to the change of the cross-sectional size. By using equation (2.16), the internal flow velocity at three states can be related to each other as

$$V_{io} = \frac{V_{is}}{\left(1+\varepsilon_s\right)} = \frac{V_i}{\left(1+\varepsilon_t\right)} \tag{2.20}$$

where V_{io}, V_{is}, V_i are the average velocity over a cross-section at undeformed, equilibrium, and dynamic state, respectively.

2.4 Hydrodynamic Forces due to Current and Wave

Based on the Morison equation [25], the hydrodynamic forces can be expressed as follows.

$$\vec{\mathbf{f}}_{\mathbf{H}} = \begin{Bmatrix} f_{Hn} \\ f_{Ht} \end{Bmatrix} = \underbrace{0.5\rho_e D_e \begin{Bmatrix} C_{Dn}\gamma_n |\gamma_n| \\ \pi C_{Dt}\gamma_t |\gamma_t| \end{Bmatrix}}_{\text{Viscous drag force}} + \underbrace{\rho_e A_e C_a \begin{Bmatrix} \dot{\gamma}_n \\ \dot{\gamma}_t \end{Bmatrix}}_{\substack{\text{Hydrodynamic} \\ \text{mass force}}} + \underbrace{\rho_e A_e \begin{Bmatrix} \dot{V}_{Hn} \\ \dot{V}_{Ht} \end{Bmatrix}}_{\substack{\text{Froude-Krylov} \\ \text{force}}} \tag{2.21}$$

where C_{Dn}, and C_{Dt} represent the normal drag coefficient, and the tangential drag coefficient, respectively. The constant C_a is an added mass coefficient. The parameters D_e and A_e represent the external diameter and the external cross-sectional area, respectively. The relative current and wave velocities in normal and tangential directions can be represented by $\gamma_n = V_{Hn} - \dot{v}_n$ and $\gamma_t = V_{Ht} - \dot{u}_t$, respectively. The parameters $\dot{v}_n$ and $\dot{u}_t$ are the riser velocities in normal and tangential directions, respectively. The parameters V_{Hn} and V_{Ht} represent the current and wave velocity in normal and tangential directions, respectively.

In order to eliminates the absolute functions. The signum function is introduced

$$\operatorname{sgn}(\gamma) = \begin{cases} 1 & if\ \gamma \geq 0 \\ -1 & if\ \gamma < 0 \end{cases} \tag{2.22}$$

By using the signum function, equation (2.21) can be arranged into the form as

$$\vec{\mathbf{f}}_{\mathbf{H}} = \begin{Bmatrix} f_{Hn} \\ f_{Ht} \end{Bmatrix} = -\underbrace{\begin{bmatrix} C_a^* & 0 \\ 0 & C_a^* \end{bmatrix} \begin{Bmatrix} \ddot{v}_n \\ \ddot{u}_t \end{Bmatrix}}_{\text{Added mass force}} - \underbrace{\begin{bmatrix} C_{eqn}^* & 0 \\ 0 & C_{eqt}^* \end{bmatrix} \begin{Bmatrix} \dot{v}_n \\ \dot{u}_t \end{Bmatrix}}_{\text{Hydrodynamic damping}} + \underbrace{\begin{Bmatrix} C_{Dn}^* V_{Hn}^2 + C_M^* \dot{V}_{Hn} \\ C_{Dt}^* V_{Ht}^2 + C_M^* \dot{V}_{Ht} \end{Bmatrix}}_{\text{Hydrodynamic excitation}} \tag{2.23}$$

where, the coefficients of equivalent normal damping C_{eqn}^*, normal drag force C_{Dn}^*, tangential damping C_{eqt}^*, tangential drag force C_{Dt}^*, and the equivalent coefficients of added mass C_a^* and inertia forces C_M^* are

$$C_{eqn}^* = C_{Dn}^* \left[2V_{Hn} - \dot{v}_n \right],\ C_{Dn}^* = 0.5\rho_e D_e C_{Dn} \cdot \operatorname{sgn}(\gamma_n) \tag{2.24 a-b}$$

$$C_{eqt}^* = C_{Dt}^* \left[2V_{Ht} - \dot{u}_t \right],\ C_{Dt}^* = 0.5\rho_e D_e \pi C_{Dt} \cdot \operatorname{sgn}(\gamma_t) \tag{2.24 c-d}$$

$$C_a^* = \rho_e A_e C_a,\ C_M^* = \rho_e A_e C_M \tag{2.24 e-f}$$

in which $C_M = C_a + 1$ is the inertia coefficient.

With some manipulations, equation (2.23) can be transformed to an equation in the Cartesian coordinate system as follows.

$$\bar{\mathbf{f}}_{\mathbf{H}} = \begin{Bmatrix} f_{Hx} \\ f_{Hy} \end{Bmatrix} = -\underbrace{\begin{bmatrix} C_a^* & 0 \\ 0 & C_a^* \end{bmatrix}\begin{Bmatrix} \ddot{x} \\ \ddot{y} \end{Bmatrix}}_{\text{Added mass force}} - \underbrace{\begin{bmatrix} C_{eqx}^* C_{eqxy}^* \\ C_{eqxy}^* C_{eqy}^* \end{bmatrix}\begin{Bmatrix} \dot{x} \\ \dot{y} \end{Bmatrix}}_{\text{Hydrodynamic damping force}} + \underbrace{\begin{Bmatrix} C_{Dx}^* V_{Hx}^2 + 2C_{Dxy1}^* V_{Hx} V_{Hy} + C_{Dxy2}^* V_{Hy}^2 + C_M^* \dot{V}_{Hx} \\ C_{Dy}^* V_{Hy}^2 + 2C_{Dxy2}^* V_{Hx} V_{Hy} + C_{Dxy1}^* V_{Hx}^2 + C_M^* \dot{V}_{Hy} \end{Bmatrix}}_{\text{Hydrodynamic excitation}} \quad (2.25)$$

where V_{Hx} and V_{Hy} are the components of current and wave velocities in x and y direction. Since the current and wave are normally in the horizontal direction, the components of current and wave velocities become

$$V_{Hx} = V_c + V_w, \;\; V_{Hy} = 0 \quad (2.26a\text{-}b)$$

The profile of current velocity $V_c = V_c(y)$ is a polynomial function as shown below.

$$V_c = V_{cH}\left(\frac{y + y_b}{y_H + y_b}\right)^n \quad (2.27)$$

where V_{cH} is the current velocity at mean sea level, and y_b and y_H are defined in figure (2.1). The degree n can be varied from 0 to1 depending on the current profile. In this study, $n = 1/7$ is employed for the tidal current profile [26].

The velocity of wave particle V_w can be determined based on the Airy's wave theory. According to the direction of x and y axes as indicated in figure 2.1, the horizontal velocity of wave particle at any time t can be expressed as shown below [27].

$$V_w = V_{wa}\cos\omega_w t \quad (2.28)$$

The wave frequency ω_w is defined by

$$\omega_w = \frac{2\pi}{T} \quad (2.29)$$

where T is the wave period.

The velocity amplitude V_{wa} is a function of y as

$$V_{wa} = \varsigma_a \omega_w e^{k\left[(y+y_b)-(y_H+y_b)\right]} \quad (2.30)$$

This equation is used for deep water, $\left(y_H + y_b\right)/\lambda \geq 0.5$. The wave amplitude ς_a is small in comparison with the wave length λ and the water depth $\left(y_H + y_b\right)$. The wave amplitude is defined by

$$\varsigma_a = \frac{H}{2} \tag{2.31}$$

where H is the wave height. The wave number k is defined in term of the wave length by

$$k = \frac{2\pi}{\lambda} \tag{2.32}$$

According to equation (2.25), the coefficients of equivalent hydrodynamic damping force in x and y direction are

$$C^*_{eqx} = C^*_{eqn}\cos^2\theta + C^*_{eqt}\sin^2\theta \tag{2.33a}$$

$$C^*_{eqy} = C^*_{eqn}\sin^2\theta + C^*_{eqt}\cos^2\theta \tag{2.33b}$$

the coupling coefficients of equivalent hydrodynamic damping force in $x-y$ plane can be expressed as

$$C^*_{eqxy} = \left(-C^*_{eqn} + C^*_{eqt}\right)\sin\theta\cos\theta \tag{2.34}$$

the coefficients of equivalent of drag force in x and y directions are

$$C^*_{Dx} = C^*_{Dn}\cos^3\theta + C^*_{Dt}\sin^3\theta \tag{2.35a}$$

$$C^*_{Dy} = -C^*_{Dn}\sin^3\theta + C^*_{Dt}\cos^3\theta \tag{2.35b}$$

and the coupling coefficients of drag force in $x-y$ plane can be expressed as

$$C^*_{Dxy1} = -C^*_{Dn}\sin\theta\cos^2\theta + C^*_{Dt}\sin^2\theta\cos\theta \tag{2.36a}$$

$$C^*_{Dxy2} = C^*_{Dn}\sin^2\theta\cos\theta + C^*_{Dt}\sin\theta\cos^2\theta \tag{2.36b}$$

For static analysis, the flow of external fluid is considered as a steady flow. Therefore, the hydrodynamic forces can be reduced to

$$\vec{\mathbf{f}}_{\mathbf{Hs}} = \begin{Bmatrix} f_{Hns} \\ f_{Hts} \end{Bmatrix} = \begin{Bmatrix} C^*_{Dns}V^2_{Hns} \\ C^*_{Dts}V^2_{Hts} \end{Bmatrix} \tag{2.37}$$

$$\vec{\mathbf{f}}_{\mathbf{Hs}} = \begin{Bmatrix} f_{Hxs} \\ f_{Hys} \end{Bmatrix} = \begin{Bmatrix} C^*_{Dxs}V^2_{Hxs} + 2C^*_{Dxy1s}V_{Hxs}V_{Hys} + C^*_{Dxy2s}V^2_{Hys} \\ C^*_{Dys}V^2_{Hys} + 2C^*_{Dxy2s}V_{Hxs}V_{Hys} + C^*_{Dxy1s}V^2_{Hxs} \end{Bmatrix} \tag{2.38}$$

2.5 Fluid and Pipe Wall Interaction

The hydrostatic pressure due to the external fluid and internal fluid has an influence on the axial tension inside the riser. The internal fluid flow inside the riser can induce the instability of marine riser. Consequently, the effect of fluid and pipe wall interaction on marine riser's behavior has to be carefully investigated. The theoretical concepts of fluid and pipe wall interaction for analysis of marine riser can be briefly presented in this section.

2.5.1 Hydrostatic pressure and concept of the apparent tension

Based on the Archimedes' law and superposition technique [28], the real system of the riser can be transformed to the apparent system as shown in figure 2.2. By using the superposition technique, the forces on the real system of the riser in figure 2.2(a) can be separated into two groups as shown in figures 2.2(b1) and 2.2(b2).

Because the Archimedes' law can be applied directly only to pressure fields that are completely closed, the missing pressures are added into both ends of the riser segment in figure 2.2(c1). In order to balance the missing pressures, the same value of the missing pressures have to be added into both ends of the riser segment in figure 2.2(c2). As a result in figure 2.2(c1), the pressure fields are closed and Archimedes' law is now applicable.

The enclosing external and internal pressure fields induce the buoyancy force w_e, and the internal fluid weight w_i. Moreover, these pressure fields also induce the triaxial stresses which provoke the axial force N_{tri} [23]. Therefore, the pressure fields in figure 2.2(c1) can be replaced by the apparent weight and the axial force N_{tri} as shown in figure 2.2(d1). In which, the apparent weight that is the net weight per unit length of the riser can be expressed in three deformation descriptor as

$$w_a = \left(\rho_p A_p - \rho_e A_e + \rho_i A_i\right) g \tag{2.39}$$

where $\rho_p, \rho_e,$ and ρ_i are the densities of the riser, the external fluid, and the internal fluid respectively.

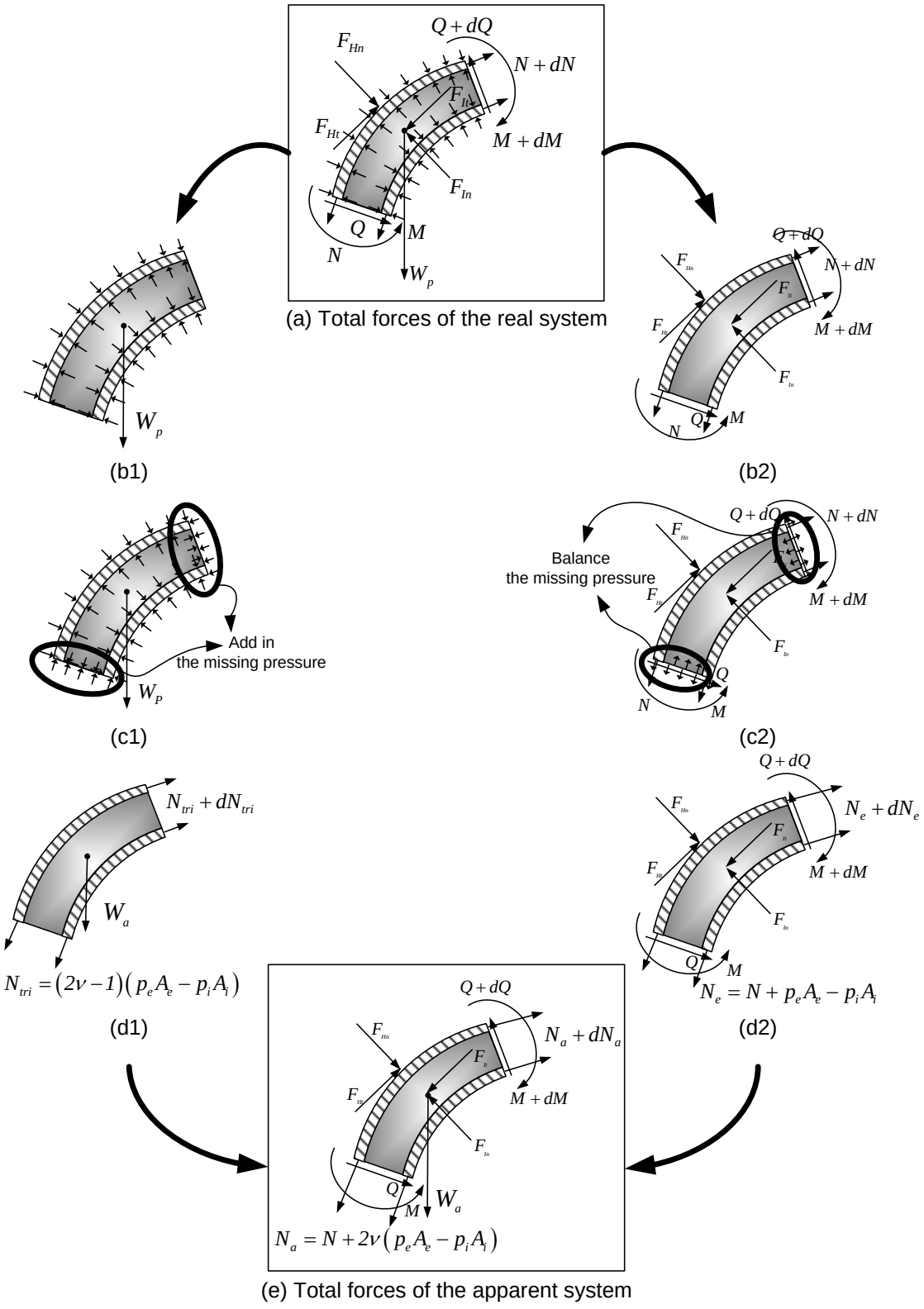

Figure 2.2 Transformation of the real system into the apparent system

Based on the theory of elasticity [29], the axial force $\left(N_{tri}\right)$ that appears in figure 2.2(d1) can be expressed as

$$N_{tri} = \left(2\nu - 1\right)\left(p_e A_e - p_i A_i\right) \tag{2.40}$$

where p_e is the external hydrostatic pressure around the riser, and p_i is the internal hydrostatic pressures in the riser. By the addition of the balance forces due to the missing pressure on the riser segment in figure 2.2(c2), one obtains the effective tension [28] which is the sum of the true wall tension N and balance forces as shown in figure 2.2(d2). The expression of the effective tension is

$$N_e = N + p_e A_e - p_i A_i \tag{2.41}$$

Finally, by adding the two groups of forces in figures 2.2(d1) and 2.2(d2), the apparent system of marine riser can be depicted as figure 2.2(e). Consequently, the apparent tension $\left(N_a\right)$ can be derived as follows.

$$N_a = N_e + N_{tri} = N + 2\nu\left(p_e A_e - p_i A_i\right) = EA_p\varepsilon \tag{2.42}$$

2.5.2 Kinematics of the incompressible fluid flow inside the marine riser

The flow inside riser is assumed to be the one dimensional fully developed plug flow. The flow is also simplified that all points of the internal fluid having a velocity V_{FP} relative to the riser. Consequently, the absolute velocity of internal fluid flow can be expressed as

$$\vec{\mathbf{V}}_{\mathbf{F}} = \vec{\mathbf{V}}_{\mathbf{p}} + V_{FP}\hat{t} \tag{2.43}$$

where $\vec{\mathbf{V}}_{\mathbf{P}}$ is the velocity of the riser. The unit tangent vector $\hat{t}$ is defined by

$$\hat{t} = \frac{x'}{s'}\hat{i} + \frac{y'}{s'}\hat{j} = \frac{1}{s'}\left[\frac{\partial x}{\partial \alpha}\hat{i} + \frac{\partial y}{\partial \alpha}\hat{j}\right] \tag{2.44}$$

Consequently, the velocity of transported fluid can be written in the normal and tangential coordinates as

$$\vec{\mathbf{V}}_{\mathbf{F}} = \left(\dot{u}_t\hat{t} + \dot{v}_n\hat{n}\right) + V_{FP}\hat{t} = \left(\dot{u}_t + V_{FP}\right)\hat{t} + \dot{v}_n\hat{n} \tag{2.45}$$

where u_t ,and v_n are the components of riser displacement vector in tangential and normal directions, respectively.

The velocity of transported fluid can also be written in the fixed Cartesian coordinate as

$$\vec{\mathbf{V}}_{\mathbf{F}} = \left[\frac{\partial x}{\partial t}\hat{i} + \frac{\partial y}{\partial t}\hat{j}\right] + \frac{V_{FP}}{s'}\left[\frac{\partial x}{\partial \alpha}\hat{i} + \frac{\partial y}{\partial \alpha}\hat{j}\right] \tag{2.46}$$

Consequently,

$$\vec{\mathbf{V}}_{\mathbf{F}} = \left(\frac{\partial}{\partial t} + \frac{V_{FP}}{s'}\frac{\partial}{\partial \alpha}\right)\left(x\hat{i} + y\hat{j}\right) \equiv \frac{D\vec{\mathrm{r}}}{Dt} \tag{2.47}$$

where $\dfrac{D}{Dt} = \left(\dfrac{\partial}{\partial t} + \dfrac{V_{FP}}{s'}\dfrac{\partial}{\partial \alpha}\right)$ is the material derivative for the fluid element. Therefore,

$$\vec{\mathbf{V}}_{\mathbf{F}} = \left[\dot{x} + V_{FP}\frac{x'}{s'}\right]\hat{i} + \left[\dot{y} + V_{FP}\frac{y'}{s'}\right]\hat{j} \tag{2.48}$$

In a same manner, the acceleration of the internal fluid [30] is found to be

$$\vec{\mathbf{a}}_{\mathbf{F}} = \frac{D\left(\vec{V}_F\right)}{Dt} = \frac{D^2\vec{\mathrm{r}}}{Dt^2} \tag{2.49}$$

Consequently,

$$\vec{\mathbf{a}}_{\mathbf{F}} = \underbrace{\frac{\partial^2\left(\vec{\mathbf{r}}_{\mathbf{P}}\right)}{\partial t^2}}_{(1)} + \underbrace{\left(\frac{2V_{FP}}{s'}\right)\frac{\partial^2\left(\vec{\mathbf{r}}_{\mathbf{P}}\right)}{\partial \alpha \partial t}}_{(2)} + \underbrace{\left(\frac{V_{FP}}{s'}\right)^2\frac{\partial^2\left(\vec{\mathbf{r}}_{\mathbf{P}}\right)}{\partial \alpha^2}}_{(3)} + \left[\underbrace{\frac{\dot{V}_{FP}}{s'}}_{(4)} + \underbrace{\frac{V_{FP}V'_{FP}}{s'^2}}_{(5)} - \underbrace{\frac{V_{FP}\dot{s}'}{s'^2} - \frac{V_{FP}^2 s''}{s'^3}}_{(6)}\right]\frac{\partial\left(\vec{\mathbf{r}}_{\mathbf{P}}\right)}{\partial \alpha} \tag{2.50}$$

where term (1) is the acceleration of riser, term (2) is the coriolis acceleration, term (3) is the centripetal acceleration, term (4) is the local acceleration due to unsteady flow, term (5) is the convective acceleration due to non-uniform flow, and term (6) is the relative accelerations due to local coordinate rotation and displacement. The magnitude of V_{FP} is changed depend on the change of axial strain at each states as show in equation (2.20), therefore $V_{FP} = V_{io}$ at the undeformed state, $V_{FP} = V_{is}$ at the equilibrium state, and $V_{FP} = V_i$ at the displaced state.

According to the differential geometry of plane curve, one obtains following expressions.

$$\vec{\mathbf{r}}' = s'\hat{t}\ ,\ \frac{\hat{t}'}{s'} = \kappa\hat{n}\ ,\ \kappa = \frac{\theta'}{s'} = \frac{x''y' - x'y''}{s'^3}\ ,\ \frac{x'}{s'} = \sin\theta,\ \frac{y'}{s'} = \cos\theta \qquad \text{(2.51 a-e)}$$

$$\frac{\partial^2 \vec{\mathbf{r}}}{\partial \alpha^2} = s'^2 \kappa \hat{n} + s'' \hat{t} \ , \ \frac{\partial^2 \vec{\mathbf{r}}}{\partial \alpha \partial \mathrm{t}} = \frac{\partial \left(s' \hat{t} \right)}{\partial t} = \dot{s}' \hat{t} + s' \frac{\partial \hat{t}}{\partial s} \cdot \frac{\partial s}{\partial t} = \dot{s}' \hat{t} + \dot{s} s' \kappa \hat{n} \qquad \text{(2.51 f-g)}$$

$$s's'' = x'x'' + y'y'' \ , \ s'\dot{s}' = x'\dot{x}' + y'\dot{y}' \qquad \text{(2.51 h-i)}$$

By using equations (2.51), the acceleration of transported fluid at the displaced state can be written in the normal and tangential coordinates as follows.

$$\vec{\mathbf{a}}_{\mathbf{F}} = \left[\ddot{u}_t + \frac{V_i \dot{s}'}{s'} + \dot{V}_i + \frac{V_i V_i'}{s'} \right] \hat{t} + \left[\ddot{v}_n + 2 V_i \dot{s} \kappa + V_i^2 \kappa \right] \hat{n} \qquad (2.52)$$

With some manipulations, the acceleration of transported fluid at the displaced state can also be written in the fixed Cartesian coordinate as follows.

$$\begin{aligned} \vec{\mathbf{a}}_{\mathbf{F}} = & \left\{ \ddot{x} + \left[\left(\frac{2}{s'} - \frac{x'^2}{s'^3} \right) \dot{x}' - \left(\frac{x'y'}{s'^3} \right) \dot{y}' \right] V_i + \left(\frac{\kappa y'}{s'} \right) V_i^2 + \left(\frac{DV_i}{Dt} \right) \frac{x'}{s'} \right\} \hat{i} \\ & + \left\{ \ddot{y} + \left[- \left(\frac{x'y'}{s'^3} \right) \dot{x}' + \left(\frac{2}{s'} - \frac{y'^2}{s'^3} \right) \dot{y}' \right] V_i - \left(\frac{\kappa x'}{s'^4} \right) V_i^2 + \left(\frac{DV_i}{Dt} \right) \frac{y'}{s'} \right\} \hat{j} \end{aligned} \qquad (2.53)$$

By eliminating time dependent terms in equations (2.45), (2.48), (2.52), and (2.53), one obtains the velocity and the acceleration of the transported fluid at equilibrium state in the normal and tangential coordinates as

$$\vec{\mathbf{V}}_{\mathbf{Fs}} = V_{is} \hat{t}_s \ , \ \vec{\mathbf{a}}_{\mathbf{F}} = \left(\frac{V_{is} V_{is}'}{s_s'} \right) \hat{t}_s + \left(V_{is}^2 \kappa_s \right) \hat{n}_s \qquad \text{(2.54 a,b)}$$

and in the fixed Cartesian coordinate system as

$$\vec{\mathbf{V}}_{\mathbf{Fs}} = \left(\frac{V_{is} x_s'}{s_s'} \right) \hat{i} + \left(\frac{V_{is} y_s'}{s_s'} \right) \hat{j} \qquad (2.55)$$

$$\vec{\mathbf{a}}_{\mathbf{Fs}} = \left\{ \left[\frac{\kappa_s y_s'}{s_s'} \right] V_{is}^2 + \left(\frac{V_{is} V_{is}'}{s_s'} \right) \frac{x_s'}{s_s'} \right\} \hat{i} + \left\{ - \left[\frac{\kappa_s x_s'}{s_s'} \right] V_{is}^2 + \left(\frac{V_{is} V_{is}'}{s_s'} \right) \frac{y_s'}{s_s'} \right\} \hat{j} \qquad (2.56)$$

2.6 Variational Model Formulation

The model formulation used in this study is developed by the variational approach. Theoretically, the strain energy includes those contributions from axial deformation and bending deformation. The external virtual work of the riser system is composed of the virtual works done by the effective weight, hydrodynamic loading and inertial forces of the riser mass and the transported fluid mass. These expressions can be shown briefly in the following subtopics.

2.6.1 Strain energy due to axial deformation

Based on the total Lagrangian description [23], the strain energy due to axial deformation of the apparent system of the riser is

$$U_a = \int_0^{s_t} \frac{EA_{po}\varepsilon_t^2}{2} ds \tag{2.57}$$

Since the riser is a submerged structure, the effect of pressure fields from external and internal fluid has to be considered [13,23,28]. Based on theory of elasticity, the total axial strain ε_t for elastic isotropic riser can be expressed in terms of the true wall tension N and fluid pressures by equation (2.58).

$$\varepsilon_t = \frac{1}{EA_{po}}\left[N + 2\nu\left(p_e A_{eo} - p_i A_{io} \right) \right] \tag{2.58}$$

By rearranging the equation (2.58), the apparent tension can be written again as

$$N_a = N + 2\nu\left(p_e A_{eo} - p_i A_{io} \right) = EA_{po}\varepsilon_t \tag{2.59}$$

By taking the first variation to equation (2.57) and adopting equation (2.59), one obtains the virtual strain energy due to axial deformation as shown below.

$$\delta U_a = \int_{\alpha_o}^{\alpha_t} \left[N_a \frac{x'}{s'} \delta u' + N_a \frac{y'}{s'} \delta v' \right] d\alpha \tag{2.60}$$

2.6.2 Strain energy due to bending

According to the total Lagrangian description, the strain energy due to bending can be expressed as

$$U_b = \int_0^s \frac{M^2}{2EI_{Po}} ds \tag{2.61}$$

Based on the elastica theory of extensible risers/pipes [23], the moment-curvature relation of the riser system can be written in the following form:

$$M = EI_{Po}(1+\varepsilon)\kappa \tag{2.62}$$

By substituting equation (2.62) into Eq. (2.61), one obtains

$$U_b = \int_0^{s_t} \frac{1}{2} EI_{Po}\kappa^2 \left(1+\varepsilon\right)^2 ds \tag{2.63}$$

The virtual strain energy due to bending is derived by taking a first variation of equation (2.63) and changing variable ds to be $d\alpha$. The virtual strain energy due to bending can be written as

$$\delta U_b = \int_{\alpha_o}^{\alpha_t} M\,\delta\theta' d\alpha \tag{2.64}$$

By substituting equations (2.51) and (2.62) into equation (2.64), one obtains

$$\begin{aligned}\delta U_b = \int_{\alpha_o}^{\alpha_t} \Bigg\{ & \frac{B\kappa}{s'}\left(\frac{y'}{s'}\right)\delta u'' + \left[-B\kappa^2\left(\frac{x'}{s'}\right) - B\kappa\frac{s''}{s'^2}\left(\frac{y'}{s'}\right)\right]\delta u' \\ & - \frac{B\kappa}{s'}\left(\frac{x'}{s'}\right)\delta v'' + \left[-B\kappa^2\left(\frac{y'}{s'}\right) + B\kappa\frac{s''}{s'^2}\left(\frac{x'}{s'}\right)\right]\delta v' \Bigg\} d\alpha\end{aligned} \tag{2.65}$$

where $B = EI_p\left(1+\varepsilon\right)$ is the bending rigidity of the riser.

2.6.3 External virtual work

The external virtual work of the riser is composed of the virtual work done by the apparent weight, the hydrodynamic forces, and the inertial forces. The expressions of these virtual works can be expressed in the fixed Cartesian coordinate system as follows.

The virtual work done by the apparent weight of the riser can be expressed as

$$\delta W_w = -\int_0^{s_t} w_a \delta v ds = -\int_{\alpha_o}^{\alpha_t} w_a s' \delta v d\alpha \tag{2.66}$$

The virtual work done by hydrodynamic force can be expressed as follows

$$\delta W_H = \int_{\alpha_o}^{\alpha_t} \left[f_{Hx} s' \delta u + f_{Hy} s' \delta v \right] d\alpha \tag{2.67}$$

Based on the Newton's second law, the inertial force from internal flow velocity is defined as

$$\vec{F} = -\int_{\alpha_o}^{\alpha_t} m_i \vec{a}_i s' d\alpha \tag{2.68}$$

The external virtual work done by the inertial forces of the riser and transporting fluid is

$$\delta W_I = -\int_{\alpha} \left[\left(m_p a_{px} + m_i a_{Fx} \right) s' \delta u + \left(m_p a_{py} + m_i a_{Fy} \right) s' \delta v \right] d\alpha \tag{2.69}$$

where m_p is the mass of riser per unit length, m_i is the mass of transported fluid per unit length, a_{px}, and a_{py} are the components of the riser acceleration vector (equation (2.8)), and a_{Fx}, and a_{Fy} are the components of the transporting fluid acceleration vector (equation (2.53)).

2.6.4 Total virtual work equation

Based on the virtual work principle, the total virtual work-energy of the riser system is

$$\delta\pi = \left(\delta U_a + \delta U_b\right) - \left(\delta W_w + \delta W_H + \delta W_I\right) \tag{2.70}$$

By substituting equations (2.60), (2.65), (2.66), (2.67), and (2.69) into equation (2.70), one obtains the total virtual work equation as shown below.

$$\begin{aligned}
\delta\pi = &\int_{\alpha_o}^{\alpha_t}\left\{\frac{B\kappa}{s'}\left(\frac{y'}{s'}\right)\delta u'' + \left[\left(N_a - B\kappa^2\right)\left(\frac{x'}{s'}\right) - B\kappa\frac{s''}{s'^2}\left(\frac{y'}{s'}\right)\right]\delta u'\right\}d\alpha \\
&+\int_{\alpha_o}^{\alpha_t}\left\{-\frac{B\kappa}{s'}\left(\frac{x'}{s'}\right)\delta v'' + \left[\left(N_a - B\kappa^2\right)\left(\frac{y'}{s'}\right) + B\kappa\frac{s''}{s'^2}\left(\frac{x'}{s'}\right)\right]\delta v'\right\}d\alpha \\
&-\int_{\alpha}\left\{s'\left[f_{Hx} - m_p a_{px} - m_i a_{Fx}\right]\delta u\right\}d\alpha \\
&-\int_{\alpha}\left\{s'\left[-w_a + f_{Hy} - m_p a_{py} - m_i a_{Fy}\right]\delta v\right\}d\alpha
\end{aligned} \tag{2.71}$$

For static analysis of marine riser, the time dependent terms in equation (2.71) are eliminated. Consequently, equation (2.71) can be reduced to

$$\begin{aligned}
\delta\pi_s = &\int_{\alpha_o}^{\alpha_t}\left\{\frac{B_s\kappa_s}{s_s'}\left(\frac{y_s'}{s_s'}\right)\delta u_s'' + \left[\left(N_{as} - B_s\kappa_s^2\right)\left(\frac{x_s'}{s_s'}\right) - B\kappa\frac{s''}{s_s'^2}\left(\frac{y_s'}{s_s'}\right)\right]\delta u_s'\right\}d\alpha \\
&+\int_{\alpha_o}^{\alpha_t}\left\{-\frac{B_s\kappa_s}{s_s'}\left(\frac{x_s'}{s_s'}\right)\delta v_s'' + \left[\left(N_{as} - B_s\kappa_s^2\right)\left(\frac{y_s'}{s_s'}\right) + B_s\kappa_s\frac{s_s''}{s_s'^2}\left(\frac{x_s'}{s_s'}\right)\right]\delta v_s'\right\}d\alpha \\
&+\int_{\alpha_o}^{\alpha_t} -\left[f_{Hn}y_s' + f_{Ht}x_s' - m_i\kappa_s y_s' V_i^2\right]\delta u_s d\alpha \\
&+\int_{\alpha_o}^{\alpha_t} -\left[-\frac{w_a s_s'}{1+\varepsilon_s} - f_{Hn}x_s' + f_{Ht}y_s' + m_i\kappa_s x_s' V_i^2\right]\delta v_s d\alpha
\end{aligned} \tag{2.72}$$

Equation (2.72) is used for calculating the static equilibrium configuration of marine riser. This equation is suitable for the case of the applied top tension is specified and the total arc-length of riser is an unknown. The arc-length of the riser depends on the coordinate of the riser configuration and it can be determined by using equations (2.10) and (2.14).

2.6.5 Constraint equation and Modified total virtual work equation

In the case of the total arc-length is specified, the top tension that is sufficient to maintain the equilibrium of riser is an unknown. The assumed top tension may be guessed and then adjust the value until the arc-length reaches to the specified value. However, this method is not efficient for numerical computation. Therefore, a better technique, which is the Lagrange multiplier method, is used.

According to equation (2.10), the total arc-length of the riser can be calculated as shown below.

$$\int_{\alpha} ds = \int_{\alpha} \left\{ \sqrt{y'^2 + x'^2} \right\} d\alpha = S_{total} \tag{2.73}$$

In the procedure, a Lagrange multiplier is introduced in the constraint condition. When the value of stretched arc-length $\left(S_{total}\right)$ is specified, this introduces the constraint condition which is written as

$$g = \int_{\alpha} \left\{ \sqrt{y'^2 + x'^2} \right\} d\alpha - S_{total} = 0 \tag{2.74}$$

Based on the virtual work principle, the total virtual work of the riser system is equal to zero when the riser system is in equilibrium. Therefore, equation (2.72) has to be minimized to zero with the constraint equation (2.74). According to the Lagrange multiplier technique, the unknown variable λ is added to the system and the total virtual work equation is modified as follows.

$$\delta\pi^* = \delta\pi + \delta\left(\lambda g\right) \tag{2.75}$$

where $\delta\pi^*$ is the modified total virtual work. After performing variation of the second term in equation (2.75), one obtains

$$\begin{aligned}
\delta\pi^* = & \int_{\alpha} \left\{ \frac{B\kappa}{s'}\left(\frac{y'}{s'}\right)\delta u'' + \left[\left(N_a - B\kappa^2\right)\left(\frac{x'}{s'}\right) - B\kappa\frac{s''}{s'^2}\left(\frac{y'}{s'}\right) \right]\delta u' \right\} d\alpha \\
& + \int_{\alpha} \left\{ -\frac{B\kappa}{s'}\left(\frac{x'}{s'}\right)\delta v'' + \left[\left(N_a - B\kappa^2\right)\left(\frac{y'}{s'}\right) + B\kappa\frac{s''}{s'^2}\left(\frac{x'}{s'}\right) \right]\delta v' \right\} d\alpha \\
& + \int_{\alpha} \left\{ -s'\left[f_{Hx} - m_P a_{Px} - m_i a_{Fx} \right]\delta u - s'\left[-W_a + f_{Hy} - m_P a_{Py} - m_i a_{Fy} \right]\delta v \right\} d\alpha \\
& + \int_{\alpha} \left\{ \lambda\left[\left(\frac{x'}{s'}\right)\delta u' + \left(\frac{y'}{s'}\right)\delta v' \right] \right\} d\alpha + \left(\int_{\alpha} \left\{ \sqrt{x'^2 + y'^2} \right\} d\alpha - S_{total} \right)\delta\lambda = 0
\end{aligned} \tag{2.76}$$

3. Finite Element Model

Based on the theoretical formulation in chapter 2, there are several nonlinear terms in the formulation. Because of this, one cannot evaluate the closed-form solution for marine riser problems. Therefore, the numerical techniques are required to investigate this complicate problem. In this study, the finite element method is used to evaluate the numerical solutions in both static and dynamic problems.

3.1 Finite Element Model for Nonlinear Static Analysis

In general, the riser will vibrate around its static configuration which is commonly nonlinear. Therefore, the nonlinear static solutions have to be evaluated before calculating the dynamic properties of the riser.

Because the top end of the riser can slide through the slip joint, the total arc-length of the riser measured from the seabed to the slip joint may not be known until the equilibrium configuration is determined. Therefore, the discretization along the arc-length may not be convenient to set up the boundary condition at the top end. In order to eliminate this problem, the discretization of the riser element along the sea water level is applied instead of the total unknown arc-length as shown in Fig. 3.1.

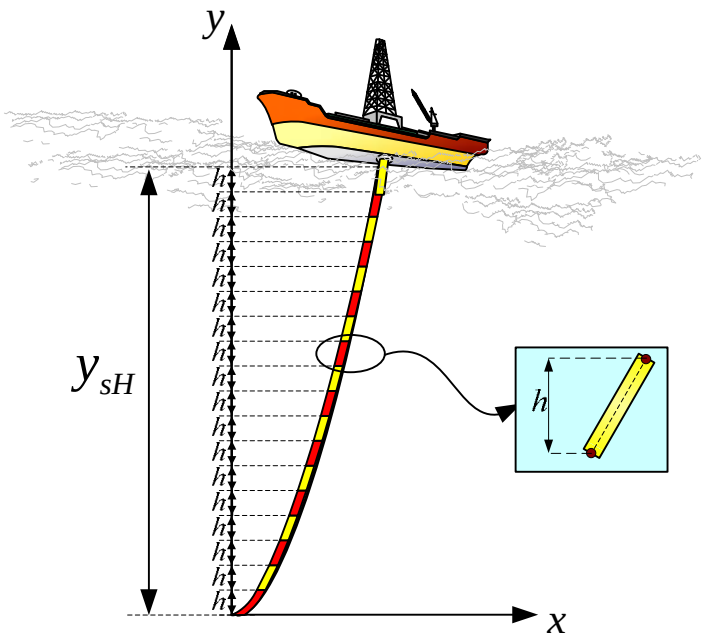

Figure 3.1 The discretization of the riser along the water depth.

3.1.1The applied top tension is specified

For the case of the applied top tension is specified, the sea water level (y_s) is used as an independent variable (α). Therefore, the virtual work energy of the riser at equilibrium state can be expressed as

$$\delta\pi = \int_0^{y_H} \left\{ \frac{B_s\kappa_s}{s_s'^2}\delta u_s'' + \left[\frac{N_{as}x_s'}{s_s'} - 2\frac{B_s\kappa_s x_s'' x_s'}{s_s'^4} \right] \delta u_s' \right\} dy_s + \int_0^{y_H} -\left[f_{Hn} + f_{Ht}x_s' - m_i\kappa_s V_i^2 \right] \delta u_s dy_s \tag{3.1}$$

wherethe axial tension inside the riser can be determined by

$$N_{as}(y_{so}) = N_{as}(y_{sH}) + \int_{y_{so}}^{y_{sH}} \left[(B_s\kappa_s)'\kappa_s + s_s' \left(-\frac{w_a}{s_s'} + f_{Hts} - m_{is}a_{Fts} \right) \right] dy_s \tag{3.2}$$

The large displacement of the riser (x_s) is composed of two components. First is the linear component (x_{sl}), which can be directly calculated by linear interpolation. Second is the nonlinear component (u_s), which is approximated by the fifth degree polynomial. Hence, the large displacement of the riser can be written as shown below.

$$x_s = x_{sl} + u_s \tag{3.3}$$

$$u_s = [N_s]\{d_{si}\} \tag{3.4}$$

Vanishing of the virtual work-energy functional expressed in equation (3.1) yields the following system of nonlinear equilibrium equations ($\delta\pi = (\partial\pi / \partial d_{si})\delta d_{si} = 0$).

$$\frac{\partial\pi_s}{\partial d_{si}} = \int_o^h \left\{ \frac{\lfloor N'' \rfloor^T B_s\kappa_s}{s_s'^2} + \lfloor N' \rfloor^T \left[\frac{N_{as}x_s'}{s_s'} - \frac{2B_s\kappa_s x_s'' x_s'}{s_s'^4} \right] - \lfloor N \rfloor^T \left[f_{ns} + f_{ts}x_s' - \rho_i A_{is}\kappa_s V_{is}^2 \right] \right\} dy_s = 0 \tag{3.5}$$

The effect of external moments at top and bottom end is taken into account by the following natural boundary conditions.

$$-[N']^T \frac{M_A}{(1+y'^2)}\bigg|^{x=0} - [N']^T \frac{M_B}{(1+y'^2)}\bigg|^{x=L} = 0 \tag{3.6}$$

The essential boundary conditions or geometric boundary conditions are up to the riser supports. At top end, the riser is held by the slip joint that allows the riser to change its length when the vessel heaves and moves laterally. At the seabed, the riser is connected to a ball joint located inside the blowout preventer. Therefore, the boundary conditions of the riser system are

(at bottom end, $y_s = 0$) $\quad u_s = 0, u_s'' = 0$ (3.7a,b)

(at top end, $y_s = y_{sH}$) $\quad u_s = 0, u_s'' = 0, N_{as} = N_{asH}$, (3.7c-e)

Equation (3.5) is a system of nonlinear equations which requires a computer program to find the solutions. The followings are the solution steps of the program.

1. Read the input data from the data file.
2. Assume the initial guessed values of all degrees of freedom.
3. Calculate the constant parameters.
4. Label node numbers for all elements.
5. Form the system of finite element equations by using equations (3.2)-(3.5).
6. Assemble the element equations to obtain the finite element model of the global system.
7. Impose the boundary conditions of the problem, equations (3.6)-(3.7).
8. Solve the finite element model of the global system which is the system of nonlinear equations. In this study, the subroutine DNEQNF, which is one of the fortran routines in IMSL math library, is used to solve this system of nonlinear equations. This routine uses a modified Powell hybrid algorithm and a finite-difference approximation to the Jacobian[31]. The routine will correct and update the guessed values of degrees of freedom and repeat steps 5-7 until the stopping error criterion is satisfied.
9. Save the numerical results in the result files.

In this study, the computer program is written in the Fortran-90 language.

3.1.2The total arc-length of the riser is specified

For the case of the total arc-length is specified, the Lagrange multiplier technique is applied. The modified total virtual work equation is

$$\delta\pi^* = \int_0^{y_H} \left\{ \frac{B_s\kappa_s}{s_s'^2}\delta u_s'' + \left[\frac{T_{as}x_s'}{s_s'} - 2\frac{B_s\kappa_s x_s'' x_s'}{s_s'^4} \right] \delta u_s' \right\} dy_s$$
$$+ \int_0^{y_H} -\left[f_{Hn} + f_{Ht}x_s' - m_i\kappa_s V_i^2 \right] \delta u_s dy_s$$
$$+ \int_0^{y_H} \left\{ \frac{\lambda(1-\varepsilon_s)x_s'}{s_s'} \delta u_s' \right\} dy_s + \left(\int_0^{y_H} \left\{ (1-\varepsilon_s)\sqrt{1+x_s'^2} \right\} dy_s - S_{total} \right) \delta\lambda \tag{3.8}$$

According to the virtual work principle, equation (3.8) is equal to zero for equilibrium position. Therefore,

$$\delta\pi^* = \left(\frac{\partial\pi^*}{\partial d_i} \right) \delta d_i + \left(\frac{\partial\pi^*}{\partial\lambda} \right) \delta\lambda = 0 \tag{3.9}$$

Since δd_i and $\delta\lambda$ are not equal to zero, thus

$$\left(\frac{\partial\pi^*}{\partial d_i} \right) = \int_0^{y_H} \left\{ \frac{\left[N''\right]^T B_s\kappa_s}{s_s'^2} + \left[N'\right]^T \left[\frac{T_{as}x_s'}{s_s'} - 2\frac{B_s\kappa_s x_s'' x_s'}{s_s'^4} \right] \right\} dy_s$$
$$- \int_0^{y_H} \left[N\right]^T \left(f_{Hn} + f_{Ht}x_s' - \rho_i A_{is}\kappa_s V_i^2 \right) dy_s$$
$$+ \int_0^{y_H} \left\{ \left[N'\right]^T \left(\frac{\lambda(1-\varepsilon_s)x_s'}{s_s'} \right) \right\} dy_s = 0 \tag{3.10}$$

$$\left(\frac{\partial\pi^*}{\partial\lambda} \right) = \left(\int_0^{y_H} (1-\varepsilon_s)\sqrt{1+x_s'^2} dy_s - S_{total} \right) = 0 \tag{3.11}$$

Because equations (3.10) and (3.11) are the system of nonlinear equations, the iterative procedure is used to obtain the numerical solutions. According to Taylor's series approximation, equations (3.10) and (3.11) can be approximated by neglecting the second-order terms as shown below

$$\left\{ \frac{\partial\pi_k^*}{\partial d_i} \right\}^{(n+1)} = \left\{ \frac{\partial\pi_k^*}{\partial d_i} \right\}^{(n)} + \left\{ \frac{\partial}{\partial d_j} \left(\frac{\partial\pi_k^*}{\partial d_i} \right) \right\}^{(n)} \Delta d^{(n)} + \left\{ \frac{\partial}{\partial\lambda} \left(\frac{\partial\pi_k^*}{\partial d_i} \right) \right\}^{(n)} \Delta\lambda^{(n)} = 0 \tag{3.12}$$

$$\left\{ \frac{\partial\pi_k^*}{\partial\lambda} \right\}^{(n+1)} = \left\{ \frac{\partial\pi_k^*}{\partial\lambda} \right\}^{(n)} + \left\{ \frac{\partial}{\partial d_i} \left(\frac{\partial\pi_k^*}{\partial\lambda} \right) \right\}^{(n)} \Delta d^{(n)} + \left\{ \frac{\partial}{\partial\lambda} \left(\frac{\partial\pi_k^*}{\partial\lambda} \right) \right\}^{(n)} \Delta\lambda^{(n)} = 0 \tag{3.13}$$

where $\{\Delta d\}^n = \{d_i^{n+1}\} - \{d_i^n\}$, $\Delta\lambda^{(n)} = \lambda^{(n+1)} - \lambda^{(n)}$, and n = number of iteration.

Equations (3.12) and (3.13) can be arranged into the matrix form as follows

$$\begin{bmatrix} [K_{NL}]_{N\times N} & \{K_\lambda\}_{N\times 1} \\ \{K_\lambda\}^T_{1\times N} & 0 \end{bmatrix} \begin{Bmatrix} \{\Delta d_i\} \\ \Delta\lambda \end{Bmatrix} = \begin{Bmatrix} -\{R_i\} \\ -R_\lambda \end{Bmatrix} \tag{3.14}$$

The integer value N is the number of nodal displacements of the riser system. The matrix $[K_{NL}]$ is the assemblage of the matrices $\{\partial^2\pi_k^*/\partial d_i\partial d_j\}$ from all elements. The vector $\{K_\lambda\}$ represents the assemblage of the element vectors $\{\partial^2\pi_k^*/\partial\lambda\partial d_i\}$. The vector $\{R_i\}$ is the element vectors $\{\partial\pi_k^*/\partial d_i\}$. The parameter R_λ is the value of $\partial\pi^*/\partial\lambda$. The increment vector of nodal displacements $\{\Delta d_i\}$ and the increment value $\Delta\lambda$ are the unknown to be determined. By adding the increment vector $\{\Delta d_i\}$ to $\{d_i\}$ and adding the value of $\Delta\lambda$ to λ, the adjusted values of $\{d_i\}$ and λ are obtained. Use these values for computation the next iteration. Repeat this process until it is terminated when $\{\Delta d_i\}$ and $\Delta\lambda$ approach zero.

3.2Finite Element Model for Dynamic Analysis

The weak formulation of Equation (2.71) is employed for the dynamic analysis as well. From $\delta\pi = 0$, hence Equation (2.71) may be decomposed into the following two nonlinear equilibrium equations.

$$\int_{\alpha_o}^{\alpha_t} \left\{ \frac{B\kappa}{s'}\left(\frac{y'}{s'}\right)\delta u'' + \left[\left(N_a - B\kappa^2\right)\left(\frac{x'}{s'}\right) - B\kappa\frac{s''}{s'^2}\left(\frac{y'}{s'}\right)\right]\delta u' \right\} d\alpha$$
$$\int_{\alpha_o}^{\alpha_t} \left\{ s_s'\left[f_{Hx} - m_{ps}a_{px} - m_{is}a_{Fx}\right]\delta u \right\} d\alpha = 0 \tag{3.15a}$$

$$\int_{\alpha_o}^{\alpha_t} \left\{ -\frac{B\kappa}{s'}\left(\frac{x'}{s'}\right)\delta v'' + \left[\left(N_a - B\kappa^2\right)\left(\frac{y'}{s'}\right) + B\kappa\frac{s''}{s'^2}\left(\frac{x'}{s'}\right)\right]\delta v' \right\} d\alpha$$
$$\int_{\alpha_o}^{\alpha_t} \left\{ s_s'\left[-w_a + f_{Hy} - m_{ps}a_{py} - m_{is}a_{Fy}\right]\delta v \right\} d\alpha = 0 \tag{3.15b}$$

For the vibrations with infinitesimal amplitudes, the axial force can be approximated by

$$N_a = EA_{Ps}\left(\varepsilon_s + \varepsilon_d\right) \approx N_{as} + EA_{Ps}\left(\frac{x_s' u_d' + y_s' v_d'}{s_s'^2}\right) \tag{3.16}$$

By substituting Equations (2.8), (2.25), (2.53), and (3.16) into Equations (3.15a-b) together with neglecting the higher order terms,eliminating the time-independent terms and using the relation that

$$-B\kappa^2\left(\frac{x'}{s'}\right) - B\kappa\frac{s''}{s'^2}\left(\frac{y'}{s'}\right) = -\frac{B\kappa}{s'^4}\left[\left(2x'y'\right)x'' + \left(y'^2 - x'^2\right)y''\right] \tag{3.17a}$$

$$-B\kappa^2\left(\frac{y'}{s'}\right) + B\kappa\frac{s''}{s'^2}\left(\frac{x'}{s'}\right) = \frac{B\kappa}{s'^4}\left[\left(y'^2 - x'^2\right)x'' - \left(2x'y'\right)y''\right] \tag{3.17b}$$

$$\int\left[s_s' m_{is} V_i^2 \frac{\kappa y'}{s'}\right]\delta u\, d\alpha = \left[\frac{s_s'}{s'} m_{is} V_i^2 \delta u \frac{x'}{s'}\right]_{\alpha_o}^{\alpha_t} - \int_{\alpha_o}^{\alpha_t}\left(\frac{s_s'}{s'} m_{is} V_i^2 \delta u\right)'\frac{x'}{s'} d\alpha \tag{3.17c}$$

$$\int\left[s_s' m_{is} V_i^2\left(-\frac{\kappa x'}{s'}\right)\right]\delta v\, d\alpha = \left[\frac{s_s'}{s'} m_{is} V_i^2 \delta v \frac{y'}{s'}\right]_{\alpha_o}^{\alpha_t} - \int_{\alpha_o}^{\alpha_t}\left(\frac{s_s'}{s'} m_{is} V_i^2 \delta v\right)'\frac{y'}{s'} d\alpha \tag{3.17d}$$

$$\dot{s}' = \frac{x'\dot{u}' + y'\dot{v}'}{s'} \tag{3.17e}$$

$$\kappa = \frac{x''y' - x'y''}{s'^3} \tag{3.17f}$$

Equations (3.15a-b) can be expressed as

$$\begin{aligned}
&\int_{\alpha_o}^{\alpha_t}\left\{\frac{B_s}{s_s'^5}\left[\left(y_s'^2\right)u'' - \left(x_s' y_s'\right)v''\right]\delta u'' + \left[\frac{\left(N_{as} - m_{is}V_{is}^2\right)u'}{s_s'}\right]\delta u'\right\} d\alpha \\
&+\int_{\alpha_o}^{\alpha_t}\left\{\frac{EA_{Ps}}{s_s'^3}\left[\left(x_s'^2\right)u' + \left(x_s' y_s'\right)v'\right] - \frac{B_s\kappa_s}{s_s'^4}\left[\left(2x_s' y_s'\right)u'' + \left(y_s'^2 - x_s'^2\right)v''\right]\right\}\delta u' d\alpha \\
&+\int_{\alpha_o}^{\alpha_t}\left\{-s_s'\left[-C_{as}^*\ddot{u} - C_{eqxs}^*\dot{u} - C_{eqxys}^*\dot{v} + C_{Dxs}^*\left(2V_c V_w + V_w^2\right) + C_{Ms}^*\dot{V}_w\right]\delta u\right\} d\alpha \\
&+\int_{\alpha_o}^{\alpha_t}\left\{s_s'\left[\left(m_{Ps} + m_{is}\right)\ddot{u} + m_{is}V_{is}\left(\frac{2}{s_s'} - \frac{x_s'^2}{s_s'^3}\right)\dot{u}' - m_{is}V_{is}\left(\frac{x_s' y_s'}{s_s'^3}\right)\dot{v}'\right]\delta\dot{u}\right\} d\alpha \\
&+\int_{\alpha_o}^{\alpha_t}\left\{s_s'\left[\left(\frac{m_{is}V_{is}V_{is}'}{s_s'^2}\right)u' + \frac{m_{is}x_s'}{s_s'}\frac{DV_{id}}{Dt}\right]\delta u\right\} d\alpha + \left[\frac{m_{is}V_{is}^2 u'}{s_s'}\delta u\right]_{\alpha_o}^{\alpha_t} = 0
\end{aligned} \tag{3.18a}$$

$$\int_{\alpha_o}^{\alpha_t}\left\{\frac{B_s}{s_s'^5}\left[-\left(x_s'y_s'\right)u''+\left(x_s'^2\right)v''\right]\delta v''+\left[\frac{\left(N_{as}-m_{is}V_{is}^2\right)v'}{s_s'}\right]\delta v'\right\}d\alpha$$
$$+\int_{\alpha_o}^{\alpha_t}\left\{\frac{EA_{Ps}}{s_s'^3}\left[\left(x_s'y_s'\right)u'+\left(y_s'^2\right)v'\right]-\frac{B_s\kappa_s}{s_s'^4}\left[\left(y_s'^2-x_s'^2\right)u''-\left(2x_s'y_s'\right)v''\right]\right\}\delta v'd\alpha$$
$$+\int_{\alpha_o}^{\alpha_t}\left\{-s_s'\left[-C_{as}^*\ddot{v}-C_{eqys}^*\dot{v}-C_{eqxys}^*\dot{u}+C_{Dxy1s}^*\left(2V_cV_w+V_w^2\right)\right]\delta v\right\}d\alpha$$
$$+\int_{\alpha_o}^{\alpha_t}\left\{s_s'\left[\left(m_{Ps}+m_{is}\right)\ddot{v}-m_{is}V_{is}\left(\frac{x_s'y_s'}{s_s'^3}\right)\dot{u}'+m_{is}V_{is}\left(\frac{2}{s_s'}-\frac{y_s'^2}{s_s'^3}\right)\dot{v}'\right]\right\}\delta\dot{v}d\alpha$$
$$+\int_{\alpha_o}^{\alpha_t}\left\{s_s'\left[\left(\frac{m_{is}V_{is}V_{is}'}{s_s'^2}\right)v'+\frac{m_{is}y_s'}{s_s'}\frac{DV_{id}}{Dt}\right]\delta v\right\}d\alpha+\left[\frac{m_{is}V_{is}^2v'}{s_s'}\delta v\right]_{\alpha_o}^{\alpha_t}=0 \qquad (3.18b)$$

The solution form of the Equation (3.18a-b) can be obtained by separation of variables. Therefore, the displacement vector is assumed as

$$\{\mathbf{d}\}=\{u_d \quad v_d\}^T=\left[\mathbf{N}\left(y_s\right)\right]\{\mathbf{d_{nd}}(t)\} \qquad (3.19)$$

In Equation (3.19), the nodal degree of freedoms $\{\mathbf{d_{nd}}\}$ is function of time only, i.e.

$$\{\mathbf{d_{nd}}\}=\{u_1 \quad u_1' \quad u_1'' \quad v_1 \quad v_1' \quad v_1' \quad u_2 \quad u_2' \quad u_2'' \quad v_2 \quad v_2' \quad v_2''\} \qquad (3.20)$$

and the shape function matrix $[\mathbf{N}]$ is function of y_s which can be expressed as

$$[\mathbf{N}]=\begin{bmatrix} N_{51} & N_{52} & N_{53} & 0 & 0 & 0 & N_{54} & N_{55} & N_{56} & 0 & 0 & 0 \\ 0 & 0 & 0 & N_{51} & N_{52} & N_{53} & 0 & 0 & 0 & N_{54} & N_{55} & N_{56} \end{bmatrix} \qquad (3.21)$$

Note that, N_{5i} are the coefficients of the fifth order polynomial shape functions.

Based on the virtual displacements, $\delta\pi=0$, Equations (3.18a-b) can be decomposed into two equations of motion for riser elements. These equations can be rearranged into the matrix form as

$$\left[\mathbf{m}^e\right]\left\{\ddot{\mathbf{d}}_{\mathbf{nd}}\right\}+\left(\left[\mathbf{c}^e\right]+\left[\mathbf{g}^e\right]\right)\left\{\dot{\mathbf{d}}_{\mathbf{nd}}\right\}+\left[\mathbf{k}^e\right]\left\{\mathbf{d}_{\mathbf{nd}}\right\}=\left\{\mathbf{f}^e\right\} \qquad (3.22)$$

where the element mass matrix is

$$\left[\mathbf{m}^e\right]_{12\times12} = \int_0^{y_H} \left\{ \left[\mathbf{N}\right]_{12\times2}^T s_s' \left(m_{Ps} + m_{is} + C_{as}^* \right) \begin{bmatrix} 1 & 0 \\ 0 & 1 \end{bmatrix} \left[\mathbf{N}\right]_{2\times12} \right\} dy_s \tag{3.23}$$

The element hydrodynamic damping is

$$\left[\mathbf{c}^e\right]_{12\times12} = \int_0^{y_H} \left\{ \left[\mathbf{N}\right]_{12\times2}^T s_s' \begin{bmatrix} C_{eqxs}^* & C_{eqxys}^* \\ C_{eqxys}^* & C_{eqys}^* \end{bmatrix} \left[\mathbf{N}\right]_{2\times12} \right\} dy_s \tag{3.24}$$

The element hydrodynamic damping is

$$\left[\mathbf{g}^e\right]_{12\times12} = \int_0^{y_H} \left\{ \left[\mathbf{N}\right]_{12\times2}^T m_{is} V_{is} \begin{bmatrix} 2 - \dfrac{x_s'^2}{s_s'^2} & -\dfrac{x_s'}{s_s'} \\ -\dfrac{x_s'}{s_s'} & 2 - \dfrac{1}{s_s'^2} \end{bmatrix} \left[\mathbf{N}'\right]_{2\times12} \right\} dy_s \tag{3.25}$$

The element stiffness matrix is

$$\left[\mathbf{k}^e\right]_{12\times12} = \left[\mathbf{k}_{b1}^e\right] + \left[\mathbf{k}_{b2}^e\right] + \left[\mathbf{k}_{t1}^e\right] + \left[\mathbf{k}_{t2}^e\right] \tag{3.26}$$

In which the bending stiffness matrix of fourth order derivative is

$$\left[k_{b1}^e\right]_{12\times12} = \int_0^{y_H} \left\{ \left[\mathbf{N}''\right]_{12\times2}^T \frac{B_s}{s_s'^5} \begin{bmatrix} 1 & -x_s' \\ -x_s' & x_s'^2 \end{bmatrix} \left[\mathbf{N}''\right]_{2\times12} \right\} dy_s \tag{3.27a}$$

The bending stiffness matrix of third order derivative is

$$\left[k_{b2}^e\right]_{12\times12} = \int_0^{y_H} \left\{ \left[\mathbf{N}'\right]_{12\times2}^T \frac{B_s \kappa_s}{s_s'^4} \begin{bmatrix} 2x_s' & 1 - x_s'^2 \\ 1 - x_s'^2 & -2x_s' \end{bmatrix} \left[\mathbf{N}''\right]_{2\times12} \right\} dy_s \tag{3.27b}$$

The axial stiffness matrix of the second order derivative is

$$\begin{aligned} \left[k_{t1}^e\right]_{12\times12} = & \int_0^{y_H} \left\{ \left[\mathbf{N}'\right]_{12\times2}^T \left(\frac{N_{as} - m_{is} V_{is}^2}{s_s'} \right) \begin{bmatrix} 1 & 0 \\ 0 & 1 \end{bmatrix} \left[\mathbf{N}'\right]_{2\times12} \right\} dy_s \\ & + \int_0^{y_H} \left\{ \left[\mathbf{N}'\right]_{12\times2}^T \frac{EA_{Ps}}{s_s'^3} \begin{bmatrix} x_s'^2 & x_s' \\ x_s' & 1 \end{bmatrix} \left[\mathbf{N}'\right]_{2\times12} \right\} dy_s \end{aligned} \tag{3.28a}$$

The axial stiffness matrix of the first order derivative is

$$\left[k_{t2}^{e}\right]_{12\times12}=\int_{0}^{y_H}\left\{\left[\mathbf{N}'\right]_{12\times2}^{T}\left(\frac{m_{is}V_{is}V_{is}'}{s_s'^2}\begin{bmatrix}1&0\\0&1\end{bmatrix}\right)\left[\mathbf{N}\right]_{2\times12}\right\}dy_s \tag{3.28b}$$

The element hydrodynamic excitation vector is

$$\left\{\mathbf{f}^{e}\right\}=\int_{0}^{y_H}\left[\mathbf{N}\right]_{12\times2}^{T}s_s'\begin{Bmatrix}C_{Dxs}^{*}\left(2V_cV_w+V_w^2\right)+C_{Ms}^{*}\dot{V}_w-\dfrac{m_{is}x_s'}{s_s'}\dfrac{DV_{id}}{Dt}\\C_{Dxy1s}^{*}\left(2V_cV_w+V_w^2\right)-\dfrac{m_{is}}{s_s'}\dfrac{DV_{id}}{Dt}\end{Bmatrix}dy_s \tag{3.29}$$

By assembling the element equations of motion, one obtains the equations of motion for entire riser as

$$\left[\mathbf{M}\right]\left\{\ddot{\mathbf{D}}_{\mathbf{nd}}\right\}+\left(\left[\mathbf{C}^{e}\right]+\left[\mathbf{G}\right]\right)\left\{\dot{\mathbf{D}}_{\mathbf{nd}}\right\}+\left[\mathbf{K}\right]\left\{\mathbf{D}_{\mathbf{nd}}\right\}=\left\{\mathbf{F}\right\} \tag{3.30}$$

The global nodal displacement $\left\{\mathbf{D}_{\mathbf{nd}}\right\}$, velocity $\left\{\dot{\mathbf{D}}_{\mathbf{nd}}\right\}$, and $\left\{\ddot{\mathbf{D}}_{\mathbf{nd}}\right\}$ vectors can be obtained by assembling the element nodal displacement, therefore

$$\left\{\mathbf{D}_{\mathbf{nd}}\right\}=\sum_{i=1}^{nelem}\left\{\mathbf{d}_{\mathbf{nd}}\right\},\ \left\{\dot{\mathbf{D}}_{\mathbf{nd}}\right\}=\sum_{i=1}^{nelem}\left\{\dot{\mathbf{d}}_{\mathbf{nd}}\right\},\ \left\{\ddot{\mathbf{D}}_{\mathbf{nd}}\right\}=\sum_{i=1}^{nelem}\left\{\ddot{\mathbf{d}}_{\mathbf{nd}}\right\} \tag{3.31a-c}$$

In the same manner, the total mass matrix is

$$\left[\mathbf{M}\right]=\sum_{i=1}^{nelem}\left[\mathbf{m}^{e}\right] \tag{3.32a}$$

the total hydrodynamic damping matrix is

$$\left[\mathbf{C}\right]=\sum_{i=1}^{nelem}\left[\mathbf{c}^{e}\right] \tag{3.32b}$$

the total gyroscopic matrix is

$$\left[\mathbf{G}\right]=\sum_{i=1}^{nelem}\left[\mathbf{g}^{e}\right] \tag{3.32c}$$

the total stiffness matrix is

$$\left[\mathbf{K}\right] = \sum_{i=1}^{nelem} \left[\mathbf{k}^{e}\right] \tag{3.32d}$$

and the total hydrodynamic excitation vector is

$$\left\{\mathbf{F}\right\} = \sum_{i=1}^{nelem} \left\{\mathbf{f}^{e}\right\} \tag{3.32e}$$

Note that, "*nelem*" is the abbreviation for the number of finite element.

Equation (3.30) is the system of nonlinear equation of motion for two-dimensional marine riser system. The nonlinearity of the system is still occurred by the hydrodynamic damping forces although the amplitude of the vibration is assumed to be small. In order to solve this equation, the identity $\left\{\dot{\mathbf{D}}_{\mathbf{nd}}\right\} = \left\{\dot{\mathbf{D}}_{\mathbf{nd}}\right\}$ has to be added into the system of Equation (3.30). Therefore, the system of nonlinear equations of motion of marine riser can be rearranged into matrix form

$$\begin{bmatrix} \mathbf{I} & \mathbf{0} \\ \mathbf{0} & \mathbf{M} \end{bmatrix} \begin{Bmatrix} \dot{\mathbf{D}}_{\mathbf{nd}} \\ \ddot{\mathbf{D}}_{\mathbf{nd}} \end{Bmatrix} + \begin{bmatrix} \mathbf{0} & \mathbf{-I} \\ \mathbf{K} & \mathbf{C+G} \end{bmatrix} \begin{Bmatrix} \mathbf{D}_{\mathbf{nd}} \\ \dot{\mathbf{D}}_{\mathbf{nd}} \end{Bmatrix} = \begin{Bmatrix} \mathbf{0} \\ \mathbf{F} \end{Bmatrix} \tag{3.33}$$

Equations (3.33) can be cast it the state form [32] as

$$\left\{\dot{\mathbf{X}}_{\mathbf{nd}}\right\} = \left[\mathbf{A}\right]\left\{\mathbf{X}_{\mathbf{nd}}\right\} + \left[\mathbf{b}\right]\left\{\mathbf{F}\right\} = \left[\mathbf{A}\right]\left\{\mathbf{X}_{\mathbf{nd}}\right\} + \left\{\mathbf{B}\right\} \tag{3.34}$$

where $\left\{\mathbf{X}_{\mathbf{nd}}\right\}_{2n\times 1} = \left\{\mathbf{D}_{\mathbf{nd}} \quad \dot{\mathbf{D}}_{\mathbf{nd}}\right\}^{T}$ is the $2n-$dimensional state vector, and

$$\left[\mathbf{A}\right] = \begin{bmatrix} \mathbf{0} & \mathbf{I} \\ \mathbf{-M^{-1}K} & \mathbf{-M^{-1}\left(C+G\right)} \end{bmatrix}_{2n\times 2n}, \quad \left\{\mathbf{B}\right\} = \begin{Bmatrix} \mathbf{0} \\ \mathbf{M^{-1}F} \end{Bmatrix}_{2n\times 1} \tag{3.35a,b}$$

are the $2n\times 2n$ real nonsymmetric coefficient matrix and the $2n\times 1$ deterministic input matrix respectively. It has to note that n is total degree of freedoms of the riser system and $\left[\mathbf{b}\right]_{2n\times n} = \begin{bmatrix} \mathbf{0} & \mathbf{M^{-1}} \end{bmatrix}^{T}$.

The state equation (3.34) is used for the natural frequency analysis and for the nonlinear vibration analysis. In this study, the natural frequency analysis is presented in next section.

3.3Natural Frequency Analysis of Marine Riser

For natural frequency analysis of marine riser, the damping matrix $[\mathbf{C}]$ and the hydrodynamic excitation vector $\{\mathbf{F}\}$ are neglected. Consequently, Equation (3.33) is reduced to the free vibration equations in the standard state form

$$\{\dot{\mathbf{X}}_{\mathbf{nd}}\} = [\mathbf{A}]\{\mathbf{X}_{\mathbf{nd}}\} \tag{3.36}$$

and the $2n \times 2n$ real nonsymmetric coefficient matrix is reduced to

$$[\mathbf{A}] = \begin{bmatrix} \mathbf{0} & \mathbf{I} \\ \mathbf{-M^{-1}K} & \mathbf{-M^{-1}G} \end{bmatrix}_{2n \times 2n} \tag{3.37}$$

The solution of Equation (3.36) has the exponential form

$$\{\mathbf{X}_{\mathbf{nd}}\} = e^{\lambda t}\{\mathbf{X}_{\mathbf{na}}\} \tag{3.38}$$

The parameter λ is the complex eigenvalues of Equation (3.38), i.e.

$$\lambda = \alpha \pm i\omega \tag{3.39}$$

where ω is the frequency of the riser system and $\{\mathbf{X}_{\mathbf{na}}\}$ is a constant $2n$ complex vector. Inserting Equation (3.38) into Equation (3.36) and dividing though by $e^{\lambda t}$, one obtain the general algebraic eigenvalue problem as follow.

$$[\mathbf{A}]\{\mathbf{X}_{\mathbf{nd}}\} = \lambda\{\mathbf{X}_{\mathbf{nd}}\} \tag{3.40}$$

The boundary conditions are imposed as follows

(i) At bottom end, $y_s = 0$.

$$u_d = v_d = 0,\ u_d'' = v_d'' = 0 \tag{3.41a-b}$$

(ii)At top end, $y_s = y_{sH}$.

$$u_d = v_d = 0,\ u_d'' = v_d'' = 0 \tag{3.42c-d}$$

In this study, the computer program for the eigenvalues and eigenvectors calculation is written though the following steps.

1. By using static solutions, one can evaluate the element mass matrix (Equation (3.23)), the element gyroscopic matrix (Equation (2.24)), and the element stiffness matrix (Equation (2.27)).
2. Assemble the element matrix from step 1 to obtain the global mass matrix, the global gyroscopic matrix, and the global stiffness matrix (Equation (3.32a,c,d)).
3. Impose the boundary conditions of the problem (Equation (3.41)).
4. Form the coefficient matrix of Equation (3.37).
5. Solve the eigenvalue problem of Equation (3.40). In this study, the subroutine DEVCRG, which is one of the fortran routine in IMSL math library, is used to compute the eigenvalues and eigenvectors of real nonsymmetric matrix. This routine uses the implicit double-shifted QR algorithm [33] based on the EISPACK routine HQR2 [34] to compute the eigenvalues and the eigenvectors.
6. Save the numerical results in the result files.

4. Results and Discussions

4.1 Verification of Numerical Results

In order to validate the numerical results of this study, the special test cases of the two-dimensional extensible marine riser transporting fluid [14, 35] have been presented. The parameters used in this example are shown in Table 4.1. In Table 1, the natural frequencies of the rigid production riser are shown and are compared with the analytical solutions and the numerical solutions that were reported by Moe and Chucheepsakul [14], and Monprapussorn et al. [35], respectively. The results from Table 4.1 indicate that the numerical results obtained from this study are in good agreement with the previous reports.

Table 4.1 Input parameters and the in-plane fundamental natural frequencies of the rigid production riser transporting fluid with various speeds of internal flow

Input parameters used for the rigid production riser transporting fluid						
1. Riser top tension (N_{aH})	476,200 N					
2. Water depth (y_H)	300 m					
3. Excursion of the vessel in x direction (x_H)	0 m					
4. Excursion of the vessel in z direction (z_H)	0 m					
5. Outside diameter (D_{epo})	0.26 m					
6. Inside diameter (D_{ipo})	0.20 m					
7. Density of riser (ρ_p)	7850 kg/m^3					
8. Density of sea water (ρ_e)	1025 kg/m^3					
9. Density of mud (ρ_t)	998 kg/m^3					
10. Young's modulus (E)	2.07x10^{11} N/m^2					
11. Poisson's ratio (ν)	0.50					
12. Current velocity at mean sea level (V_{cH})	0 m/sec					
13. Angle between current direction and x-direction	0^o					
14. Normal drag coefficient (C_{Dn})	0.70					
15. Tangential drag coefficient (C_{Dt})	0.03					
16. Added mass coefficient (C_a)	1.00					
Numerical results						
Internal flow velocity (V_{io}) (m/sec)	**The in-plane fundamental natural frequencies of production riser (rad/sec)**					
	Moe and Chucheepsakul (1988) (IA,EBR)		Monprapussorn et al. (2007) (EA)		This study (20 elements) (3-D,EA)	
	Analytical solution	Numerical solution	EBR	IBR	EBR	IBR
0	0.2878	0.2890	0.2891	0.3001	0.2892	0.2988
5	-	-	0.2881	0.2994	0.2883	0.2980
10	0.2838	0.2853	0.2853	0.2972	0.2854	0.2957
15	-	-	0.2804	0.2934	0.2805	0.2917
20	0.2706	0.2730	0.2731	0.2880	0.2732	0.2860
25	-	-	0.2627	0.2809	0.2629	0.2783
30	0.2413	0.2478	0.2478	0.2717	0.2481	0.2684
35	-	-	0.2224	0.2603	0.2230	0.2559

Note: IA = Inextensible Analysis, EA = Extensible Analysis,
3-D = 3-D Analysis, EBR = Excluding Bending Rigidity, IBR = Including Bending Rigidity.

4.2 Effect of Internal Flow Velocity on Maximum Displacement and Maximum Bending Moment of Marine Riser

According to the validation of previous examples, the authors are confident that the model formulation developed herein is applicable and give the sufficient accuracy of the numerical results. In this subsection, the input parameters in Table 4.2 are used. The applied top tension is kept to a constant value of 2,000 kN. The offset of the vessel is equal to 540 m (30% of the sea depth). In general operation, the internal flow velocity in a riser is usually less than 10 m/sec, however, the velocity of greater than this value is used in numerical example as for demonstration purpose. The fluid is pumping up with the consecutive positive internal flow velocities (flow up) from 0 m/s to 65 m/sec. The case of the riser is subjected to negative internal flow velocities (flow down), which may occurr in the drilling riser, are also considered.

Table 4.2 Input parameters for analysis of the marine water riser transporting fluid

Input parameters used for analysis of the marine riser transporting fluid	
1. Riser top tension (N_{aH})	2,000-10,000 kN
2. Water depth (y_H)	1,800 m
3. Offset of the vessel $(\%x_H)$	30%
4. Outside diameter (D_{epo})	0.25 m
5. Inside diameter (D_{ipo})	0.21 m
6. Density of riser (ρ_p)	7850 kg/m^3
7. Density of sea water (ρ_e)	1025 kg/m^3
8. Density of mud (ρ_i)	998 kg/m^3
9. Young's modulus (E)	2.07x10^{11} N/m^2
10. Poisson's ratio (ν)	0.30
11. Internal flow velocity (V_{io})	0-65 m/sec
12. Current velocity at mean sea level (V_{cH})	0.0 m/sec
13. Angle between current direction and x-axis	0^o
14. Normal drag coefficient (C_{Dn})	1.00
15. Tangential drag coefficient (C_{Dt})	0.05
16. Added mass coefficient (C_a)	1.00

Numerical results in Table 4.3 show maximum displacements, maximum moments and their positions form seabed. The results indicate that the maximum displacement increases as the internal flow velocity increases. Moreover, the increase in velocity of

transporting fluid changes the position of the maximum displacement down to the seabed.

The increase in velocity of transporting fluid increases the maximum bending moment until the velocity reaches 60 m/s. Beyond this velocity the maximum bending moment no longer increases, but decreases, however the maximum displacement continuously increases and the riser tends to have a divergence instability.

Table 4.3 Maximum displacements and maximum bending moments of the marine riser with 30% offset

	Maximum displacement (m)	$@\frac{y}{y_H}$	Maximum Moment (N-m)	$@\frac{y}{y_H}$
V_{is} = 0 m/s	150.00	0.31	50987.91	0.01
V_{is} = 5 m/s	150.24	0.31	51213.73	0.01
V_{is} = 10 m/s	150.96	0.31	51902.48	0.01
V_{is} = 15 m/s	152.19	0.30	53089.55	0.01
V_{is} = 20 m/s	153.98	0.30	54839.83	0.01
V_{is} = 25 m/s	156.37	0.30	57258.90	0.01
V_{is} = 30 m/s	159.45	0.30	60516.14	0.01
V_{is} = 35 m/s	163.42	0.29	64897.63	0.01
V_{is} = 40 m/s	168.45	0.28	70953.51	0.01
V_{is} = 45 m/s	174.96	0.27	80037.28	0.01
V_{is} = 50 m/s	183.72	0.26	96943.84	0.01
V_{is} = 55 m/s	196.54	0.25	143487.92	0.01
V_{is} = 60 m/s	221.63	0.21	273943.80	0.01
V_{is} = 65 m/s	241.86	0.19	231910.60	0.01

The effects of the negative flow velocity (flow down) on maximum displacement and maximum bending moment are illustrated in figure 4.1 and figure 4.2 respectively. These figures indicate that the negative flow velocity affects the nonlinear static behavior of the marine riser as same as the positive flow velocity does. This result can be explained as follows.

If the internal flow velocity has the opposite direction to the tangent of the centerline of the riser, the absolute velocity of the riser can be expressed as

$$\vec{\mathbf{V}}_{\mathbf{F}} = \vec{\mathbf{V}}_{\mathbf{p}} - V_{FP}\hat{t} = \frac{D\vec{\mathbf{r}}}{Dt} \tag{4.1}$$

where $\frac{D}{Dt} = \left(\frac{\partial}{\partial t} - \frac{V_{FP}}{s'} \frac{\partial}{\partial \alpha} \right)$ is the material derivative for the fluid element. By direct derivation, yields

$$\vec{\mathbf{a}}_{\mathbf{F}} = \frac{D\vec{\mathbf{V}}_{\mathbf{F}}}{Dt} = \frac{D^2\vec{\mathbf{r}}}{Dt^2} \tag{4.2}$$

Therefore, the acceleration of the transported fluid for negative flow velocity is found to be

$$\vec{\mathbf{a}}_{\mathbf{F}} = \underbrace{\frac{\partial^2(\vec{\mathbf{r}}_{\mathbf{P}})}{\partial t^2}}_{(1)} \underbrace{- \left(\frac{2V_{FP}}{s'} \right) \frac{\partial^2(\vec{\mathbf{r}}_{\mathbf{P}})}{\partial \alpha \partial t}}_{(2)} + \underbrace{\left(\frac{V_{FP}}{s'} \right)^2 \frac{\partial^2(\vec{\mathbf{r}}_{\mathbf{P}})}{\partial \alpha^2}}_{(3)} + \left[\underbrace{- \frac{\dot{V}_{FP}}{s'}}_{(4)} + \underbrace{\frac{V_{FP}V'_{FP}}{s'^2}}_{(5)} + \underbrace{\frac{V_{FP}\dot{s}'}{s'^2}}_{(6)} - \underbrace{\frac{V_{FP}^2 s''}{s'^3}}_{(7)} \right] \frac{\partial(\vec{\mathbf{r}}_{\mathbf{P}})}{\partial \alpha} \tag{4.3}$$

By comparison with equation (2.50), there are three terms having a negative sign namely terms (2), (4), and (6). At equilibrium state, the transported fluid has a steady flow along the tangential line of the riser. Therefore, the time-dependent terms are eliminated from equation (4.3). Consequently, the acceleration of the transported fluid is combined with only the centripetal acceleration (term 3) and the convective acceleration due to non-uniform flow (term 5). One obtains

$$\vec{\mathbf{a}}_{\mathbf{Fs}} = \left(\frac{V_{is}}{s'} \right)^2 \frac{\partial^2(\vec{\mathbf{r}}_{\mathbf{P}})}{\partial \alpha^2} + \frac{V_{is}V'_{is}}{s'^2} \frac{\partial(\vec{\mathbf{r}}_{\mathbf{P}})}{\partial \alpha} = \left(V_{is}^2 \kappa_s \right) \hat{n}_s + \left(\frac{V_{is}V'_{is}}{s'_s} \right) \hat{t}_s \tag{4.4}$$

Equation (4.4) is identical to equation (2.54 b). As a result of this agreement, the direction of the internal flow velocity has no effect on the nonlinear static behavior of the marine riser but the increase in the absolute value of the internal flow velocity induces the large displacement and reduces riser stability.

Moreover, the author also found that the fluid transportation has an insignificant effect on axial strain, true-wall tension, and the apparent tension. The maximum value of the internal flow velocity for this example is 65 m/s. If the internal flow velocity is larger than 65 m/s, the riser will buckle and collapse.

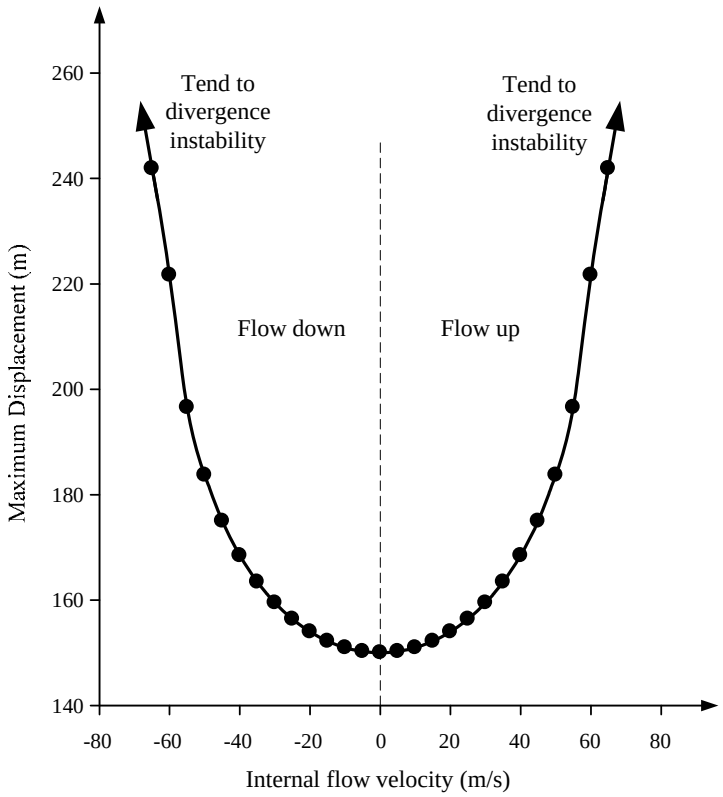

Figure 4.1 Effects of Fluid Transportation on Maximum Displacement of the marine riser with 30% offset.

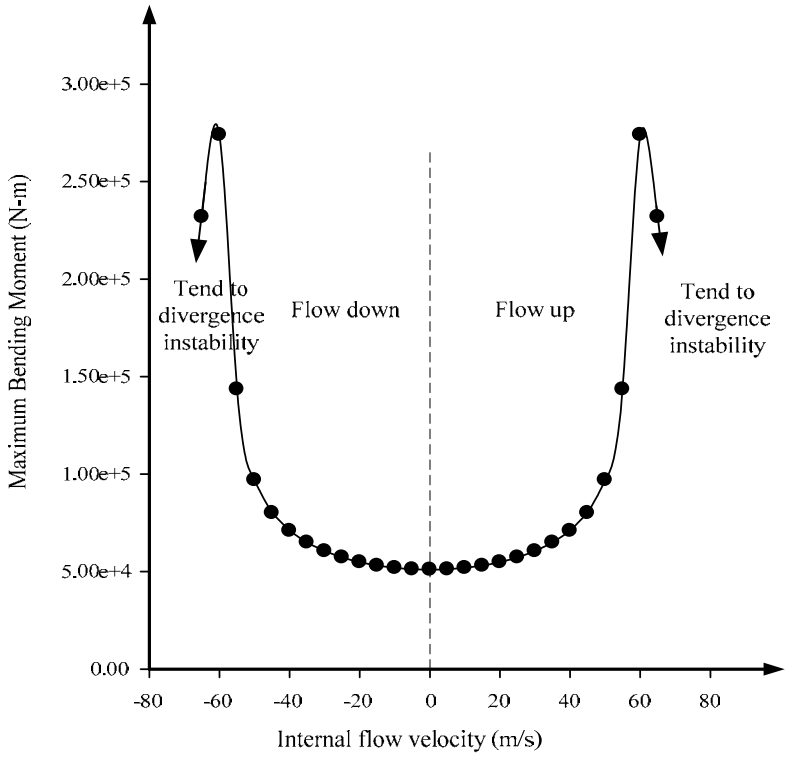

Figure 4.2 Effects of Fluid Transportation on Maximum Bending Moment of the marine riser with 30% offset.

4.3 The Couple Effect of Internal Flow Velocity and Axial Extensibility on Maximum Displacement of Marine Riser

In this section, the couple effect of axial extensibility and internal flow on maximum displacement of marine riser is presented. The data in Table 4.4 is utilized for this example. In case of extensible riser, the flexural rigidity is small as compared with the applied top tension. Therefore, the applied top tension $\left(N_{aH}\right)$ is used as the basis for the parametric normalization. The following dimensionless parameters are introduced in order to comprehend the effect of axial extensibility.

$$\hat{E}_{irv}=\left(\frac{w_a L}{N_{aH}}\right)\sqrt{\frac{EA_{po}}{N_{aH}}},\ \hat{V}_{io}=V_{io}\sqrt{\frac{m_{io}}{N_{aH}}},\ \hat{\omega}=\omega L\sqrt{\frac{m_{to}}{N_{aH}}},\ \hat{y}_s=\frac{y_s}{L},\hat{u}_s=\frac{u_s}{L} \qquad \text{(4.5 a-e)}$$

The parameter $\hat{E}_{irv}$ is recognized as the Irvine's first parameter [36] in cable mechanics. It is utilized to describe the effect of riser's extensibility. The high value of $\hat{E}_{irv}$ implied the low extensibility, but the low value of $\hat{E}_{irv}$ implied the high extensibility condition of the riser. The parameter $\hat{V}_{io}$ denotes the effect of the mean flow velocity of transported fluid. The parameter $\hat{\omega}$ is the nondimensional form of the natural frequency $\left(\omega\right)$ of the riser. The parameter $\hat{y}_s$ represents the position of maximum displacement from sea bed. The parameter $\hat{u}_s$ is the nondimensional form of the lateral displacement of the riser where the span length $L=\sqrt{x_H^2+y_H^2}$.

The combination effect of axial extensibility and internal flow on the maximum displacement of extensible marine riser is shown in figures 4.3 and 4.4. It is evident that the internal flow of transported fluid increases the lateral displacements. The internal flow induces a tangential loading, which destabilizes the riser system. Consequently, the divergent instability could be occurred when speed of internal flow reaches the value of $\hat{V}_{is}=0.3246$ as shown in figure 4.4.

Figure 4.3 and 4.4 also shows that an increase in axial extensibility, by reducing $\hat{E}_{irv}$ from 286.50 to 28.65, enlarges the lateral displacements due to the reduction of bending stiffness. However, the turning point occurs when $\hat{E}_{irv}$ is reduced passing 10.00 to 1.81. In this range, the increase in axial extensibility reduces the lateral displacements.

Table 4.4 The input data utilized for study the effect of axial extensibility and internal flow on maximum displacement of marine riser.

Parameters	Value
Offset of the vessel (x_H)	70 m
Water depth (y_H)	300 m
Normal drag coefficient (C_{Dn})	0.70
Tangential drag coefficient (C_{Dt})	0.03
Added mass coefficient (C_a)	1.00
Current velocity at mean sea level (V_{cH})	0.20 m/s
Elastic modulus (E)	2.07×10^{11} N/m^2
Outside diameter (D_{epo})	0.26 m
Inside diameter (D_{ipo})	0.20 m
Density of pipes/risers (ρ_p)	7850 kg/m^3
Density of sea water (ρ_e)	1025 kg/m^3
Density of internal fluid (ρ_i)	998 kg/m^3

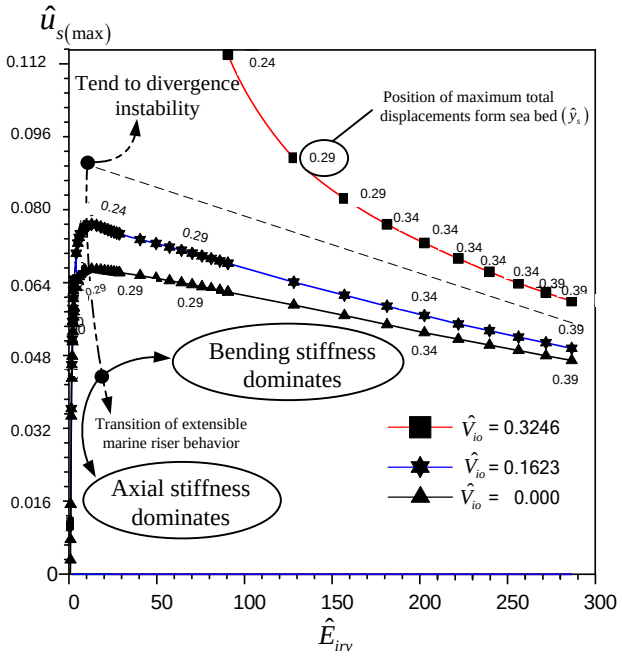

Figure 4.3 Effect of axial extensibility and internal flow on maximum displacement $(\hat{u}_s)$ of extensible marine risers and their positions from sea bed

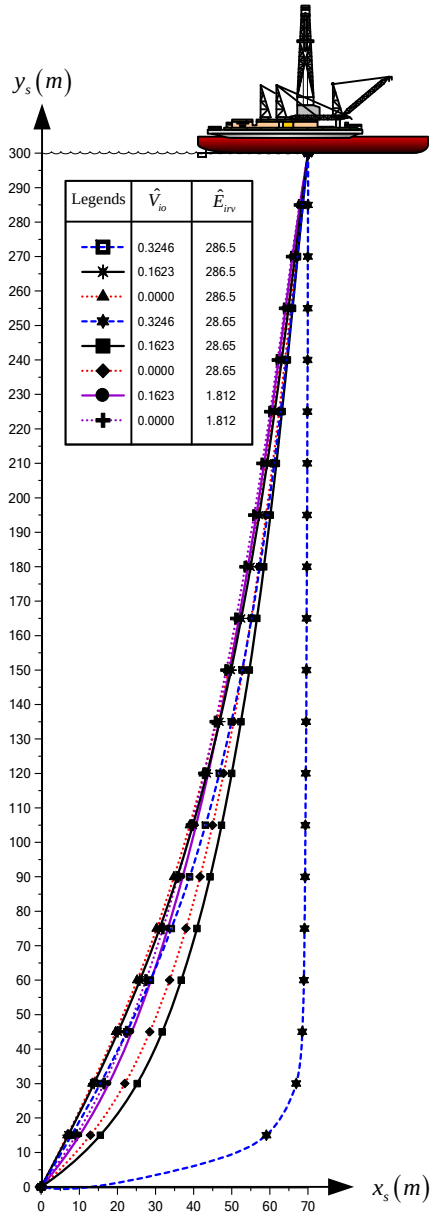

Figure 4.4 Effects of axial extensibility and internal flow on static configurations of marine risers

The transition behavior is occurred due to the variation of the structural stiffness domination from the bending stiffness domination to the pretensioned stiffness (Figure 4.3). The structural stiffness of the low extensible riser is governed by the bending strain energy, and the riser behaves like a tensioned beam.

On the contrary, when the condition of high extensibility such as $\hat{E}_{irv} = 1.81$ is applied, the riser received high axial tension and the axial strain become large. In this case, the

axial strain energy or the pretensioned stiffness becomes the main stiffness of riser as well as the tensioned cable. For a moderate extensibility riser $\left(10.00 \le \hat{E}_{irv} \le 28.65\right)$, the riser has large amount of both axial strain energy and bending strain energy. Consequently, the riser is under the coupled axial-bending stiffness domination and the transition of tensioned beam behavior to tensioned cable behavior is occurred in this state.

Form the above discussions, it can be found that the effect of axial extensibility of the riser induces the lateral displacements when the bending stiffness controls. However, the effect of axial extensibility of the riser reduces the lateral displacements when the pretensioned stiffness controls.

4.4 Effect of Internal Flow Velocity on Dynamic Properties of Marine Riser

In this section, the properties of the deep water riser in Table 4.5 are used to show the effect of internal flow velocity on dynamic properties of marine riser in different static offsets. It is observed that the internal flow velocity induces the tangential load which has the effect on the natural frequencies and the corresponding mode shapes of the marine riser.

Table 4.5 The input data utilized for study the effect of internal flow velocity on dynamic properties of marine riser.

Parameters	Value
1. Riser top tension	340 kN
2. Water depth	300 m
3. Offset of the vessel	0%-20%
4. Outside diameter	0.25 m
5. Inside diameter	0.21 m
6. Density of riser	7850 kg/m^3
7. Density of sea water	1025 kg/m^3
8. Density of mud	998 kg/m^3
9. Young's modulus	2.07x10^{11} N/m^2
10. Poisson’s ratio	0.30
11. Internal flow velocity	0-20 m/sec
12. Current velocity at mean sea level	1.0 m/sec
13. Angle between current direction and x-axis	0^o
14. Normal drag coefficient	1.00
15. Tangential friction coefficient	0.05
16. Added mass coefficient	1.00

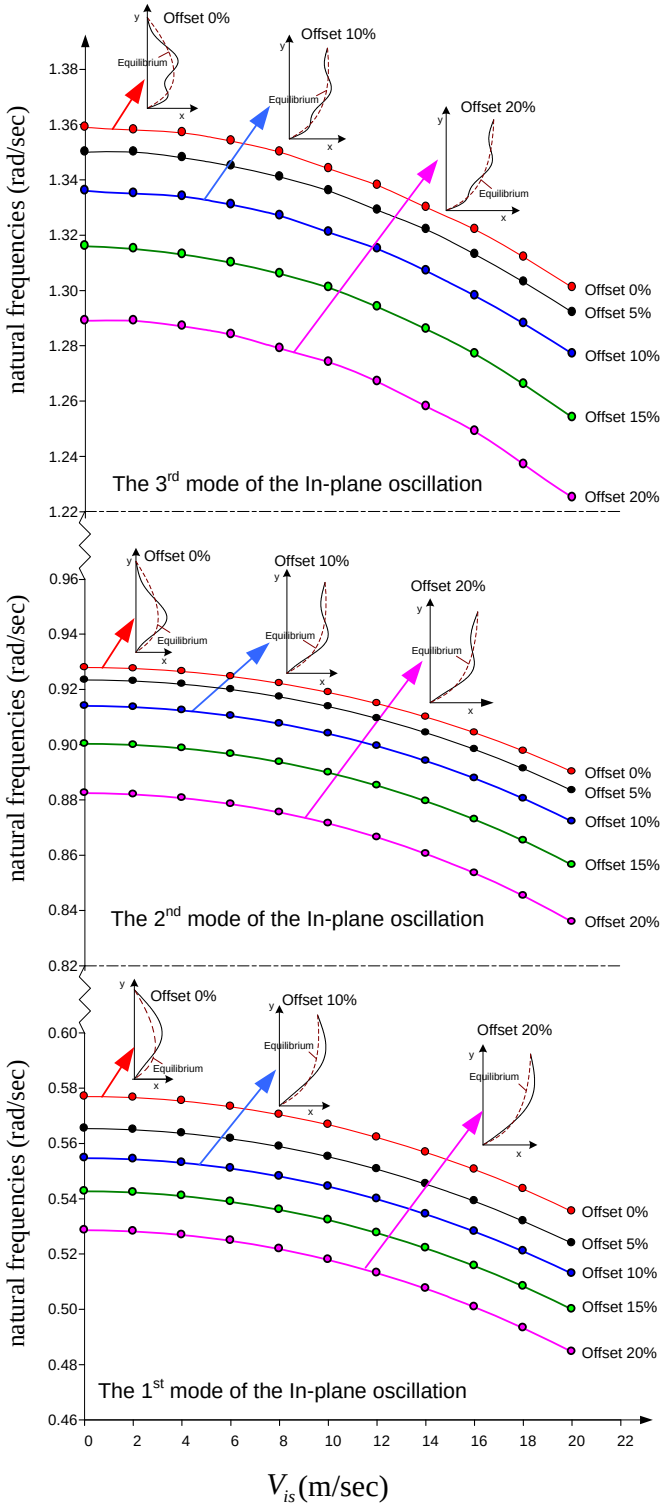

Figure 4.5 The effect of fluid transportation rate on in-plane natural frequencies and mode shapes of the three-dimensional riser in various offsets

The effect of internal flow velocity on in-plane natural frequencies of marine riser is illustrated in figure 4.5. Figure 4.5 shows that the increase in velocity of internal fluid reduces the in-plane natural frequencies of marine riser. If the internal flow velocity is increased continuously, the natural frequencies will be closed to zero. The internal flow velocity that induces the zero value of natural frequencies is called as the critical velocity. However, the critical velocity of fluid transportation is generally higher than 20 m/s which is out of the practical range.

The mode shapes of in-plane oscillation are also illustrated in figure 4.5. This figure shows that the velocity of internal fluid in the range of 0 to 20 m/s has an insignificant effect on the mode shapes of in-plane oscillation. However, the shapes of in-plane oscillation could change the number of curvature if the internal flow speed is continuously increased and reach the critical value [31].

Figure 4.5 indicates that the increase in percent of static offset reduces the in-plane natural frequencies of marine riser. The mode shapes of in-plane oscillation are slightly different when the percent of static offset is increased.

5. Conclusions

This report presents the effect of interaction between internal fluid and pipe wall on large displacement and dynamic properties of marine riser. The kinematics of marine riser and internal fluid are thoroughly addressed. The acceleration of the internal fluid are derived in terms of the riser displacement and internal flow speed. The model formulation of extensible marine riser is developed by the variational approach based on the extensible elastica theory and the work-energy principle. The outstanding feature of the model formulation presented in this report is the use of independent variable α to provide the flexibility in the choice of parameters defining elastic curves. Therefore, the formulation allows users to select independent variable that is suitable for their applications.

The finite element method is used to obtain the numerical solutions. The effect of internal flow on maximum displacement is investigated. It is observed that the maximum displacement increases as the internal flow velocity increases. Moreover, the increase in velocity of transporting fluid changes the position of the maximum displacement down to the seabed.

The increase in velocity of transporting fluid increases the maximum bending moment until the velocity reaches a value which gives a peak value of maximum bending moment. Beyond this velocity the maximum bending moment no longer increases, but decreases, however the maximum displacement continuously increases and the riser tends to have a divergence instability. The direction of the internal flow velocity has no effect on the nonlinear static behavior of the marine riser but the increase in the absolute value of the internal flow velocity induces the large displacement and reduces riser stability. The internal flow velocity has an insignificant effect on axial strain, true-wall tension, and the apparent tension.

The couple effect of axial extensibility and internal flow on maximum displacement and dynamic properties of extensible marine riser is also investigated. The results indicate that the strength of low extensibility riser is dominated by bending stiffness of marine riser. Consequently, the axial extensibility reduces the stability of the riser system. On the contrary, the strength of the high extensibility riser is dominated by the pretensioned

stiffness. Therefore, the high extensibility riser performs the tensioned cable behavior, on which the axial extensibility increases the stability of the riser system. For the riser with moderate extensibility, the riser is in the transition state.

The influence of internal flow on dynamic properties of three-dimensional extensible marine riser is also presented. It is observed that the fluid transportation induces the tangential force which has the effect on the natural frequencies of the riser. The fluid transportation reduces the natural frequencies and the structural stability of the marine riser. The shapes of in-plane oscillations could change the number of curvature when the internal flow velocity reaches the critical values. The effect of the internal flow can be reduced by increasing the axial deformation.

References

1. St. Denis, M. and Armijo, L., 1955, “On Dynamic Analysis of the Mohole Riser”, **Proceeding of Ocean Science and Ocean Engineering Conference**, Vol. 1, pp. 325-330.
2. Chakrabarti, S.K. and Frampton, R.E., 1982, “Review of Riser Analysis Techniques”, **Applied Ocean Research**, Vol. 4, No. 2, pp. 73-90.
3. Ertas, A. and Kozik, T.J., 1987, “A Review of Approaches to Riser Modeling”, **Journal of Energy Resources Technology**, **ASME**, Vol. 109, No. 3, pp. 155-160.
4. Jain, A.K., 1994, “Review of Flexible Risers and Articulated Storage Systems”, **Ocean Engineering**, Vol. 21, No. 8, pp. 733-750.
5. Patel, M.H. and Seyed, F.B., 1995, “Review of Flexible Riser Modelling and Analysis Techniques”, **Engineering Structures**, Vol. 17, No. 4, pp. 293-304.
6. Housner, G.W., 1952, “Bending Vibrations of a Pipe Line Containing Flowing Fluid”, **Journal of Applied Mechanics**, **ASME**, Vol. 19, pp. 205-208.
7. Gregory, R.W. and Païdoussis, M.P., 1966, “Unstable Oscillation of Tubular Cantilevers Conveying Fluid. I. Theory”, **Proceedings of the Royal Society (London) A**, Vol. 293, pp. 512-537.
8. Païdoussis, M.P., 1970, “Dynamics of Tubular Cantilevers Conveying Fluid”, **Journal of Mechanical Engineering Science**, Vol. 12, pp. 85-103.
9. Doll, R.W. and Mote, C.D., 1976, “On the Dynamic Analysis of Curved and Twisted Cylinders Transporting Fluids”, **Journal of Pressure Vessel Technology**, **ASME**, Vol. 98, pp. 143-150.
10. Thompson, J.M.T. and Lunn, T.S., 1981, “Static Elastica Formulations of a Pipe Conveying Fluid”, **Journal of Sound and Vibration**, Vol. 77, pp. 127-132.
11. Païdoussis, M.P., 1998, **Fluid-Structure Interactions**, Slender Structures and Axial Flow, Vol. 1, Academic Press, New York.
12. Irani, M.B., Modi, V.J. and Weit, F., 1987, “Riser Dynamics with Internal Flow and Nutation Damping”, **Proceedings 6th International Offshore Mechanics and Arctic Engineering Symposium**, Vol. 3, pp. 119-125.
13. Patel, H.M. and Seyed, F.B., 1989, “Internal Flow-Induced Behaviour of Flexible Risers”, **Engineering Structures**, Vol. 11, No. 3, pp. 266-280.

14. Moe, G. and Chucheepsakul, S., 1988, “The Effect of Internal Flow on Marine Risers”, **Proceedings 7th International Offshore Mechanics and Arctic Engineering Symposium**, Vol. 1, pp. 375-382.
15. Wu, M.C. and Lou, J.Y.K., 1991, “Effects of Rigidity and Internal Flow on Marine Riser Dynamics”, **Applied Ocean Research**, Vol. 13, No. 5, pp. 235-244.
16. Chucheepsakul, S. and Huang, T., 1994, “Influence of Transported Mass on the Equilibrium Configuration of Risers”, **Proceeding of 4th International Offshore and Polar Engineering Conference**, Vol. 2, pp. 246-249.
17. Chucheepsakul, S., Huang, T. and Monprapussorn, T., 1999, “Influence of Transported Fluid on Behavior of an Extensible Flexible Riser/Pipe”, **Proceedings of 9th International Offshore and Polar Engineering Conference**, Vol. 2, pp. 286-293.
18. Chucheepsakul, S. and Monprapussorn, T., 2001, “Nonlinear Buckling of Marine Elastica Pipes Transporting Fluid”, **International Journal of Structural Stability and Dynamics**, Vol. 1, No. 3, pp. 333-365.
19. Bernitsas, M.M., 1982, “A Three-Dimensional Nonlinear Large-Deflection Model for Dynamic Behavior of Risers, Pipelines, and Cables”, **Journal of Ship Research**, Vol. 26, No. 1, pp. 59-64.
20. Patrikarakis, N.M. and Kriezis, G.A., 1987, “Linear Dynamics of Flexible Risers”, **Journal of Offshore Mechanics and Arctic Engineering**, **ASME**, vol. 109, pp. 254-262.
21. Felippa, C.A. and Chung, J.S., 1981, “Nonlinear Static Analysis of DeepOcean Mining Pipe – Part 1: Modeling and Formulation”, **Journal of Energy Resources Technology**, **ASME**, Vol. 103, No. 1, pp. 11-15.
22. Chai, Y.T. and Varyani, K.S., 2006, “An Absolute Coordinate Formulation for Three-Dimensional Flexible Pipe Analysis”, **Ocean Engineering**, Vol. 33, pp. 23-58.
23. Chucheepsakul, S., Monprapussorn, T. and Huang, T., 2003, “Large Strain Formulations of Extensible Flexible Marine Pipes Transporting Fluid”, **Journal of Fluids and Structures**, Vol. 17, No. 2, pp. 185-224.
24. Streeter, V.L. and Wylie, E.B., 1981, **Fluid Mechanics,** First SI Metric Edition, McGraw-Hill, Singapore.
25. Chakrabarti, S.K., 1990, **Nonlinear Methods in Offshore Engineering,** Developments in Marine Technology Vol. 5, Elsevier, Netherlands.

26. Larsen, C.M., 1976, “Marine Riser Analysis”, **Norwegian Maritime Research**, Vol. 4, pp. 15-26.
27. Dawson, T.H., 1983, **Offshore Structure Engineering,**Prentice-Hall, New Jersey.
28. Sparks, C.P., 1984, “The Influence of Tension, Pressure and Weight on Pipe and Riser Deformations and Stresses”, **Journal of Energy Resources Technology**, **ASME**, Vol. 106, pp. 46-54.
29. Timoshenko, S.P. and Goodier, J.N., 1982, **Theory of Elasticity**, McGraw-Hill, Singapore.
30. Huang, T., 1993, “Kinematics of Transported Mass Inside Risers and Pipes”, **Proceeding of 3rd International Offshore and Polar Engineering Conference**, Vol. 2, pp. 331-336.
31. More, J., Garbow, B.S. and Hillstrom, H., 1980, **User guide for MINPACK-1**, Argonne National Laboratories, Illinois.
32. Meirovitch, L., 1997, **Principles and Techniques of Vibrations**, Prentice Hall, New Jersey.
33. Press, W.H., Teukolsky, S.A., Vettering, W.T. and Flannery, B.P., 1992, **Numerical Recipes in Fortran**, 2nd ed., Cambridge University Press, New York.
34. Smith, B.T., Boyle, J.M., Dongarra, J.J., Garbow, B.S., Ikebe, Y., Klema, V.C. and Moler, C.B., 1976, **Matrix Eigensystem Routines - EISPACK Guide**, Springer-Verlag, New York.
35. Monprapussorn, T., Athisakul, C. and Chucheepsakul, S., 2007, “Nonlinear Vibrations of an Extensible Flexible Marine Riser Carrying a Pulsatile Flow”, **Journal of Applied Mechanics, ASME**. Vol. 74, pp. 754-769.
36. Hover, F.S., Triantafyllou, M.S., 1999, “Linear dynamics of curved tensioned elastic beams”, **Journal of Sound and Vibration**, Vol. 228, pp. 923-930.

Output

ผลงานวิจัยตีพิมพ์ที่ได้จากโครงการนี้ในรอบ 2 ปีที่ผ่านมาสรุปโดยรวมได้ดังนี้ ผลงานวิจัยที่ตีพิมพ์ในวารสารวิชาการระดับนานาชาติ จำนวน 3 ฉบับ และผลงานวิจัยที่นำเสนอผลงานในที่ประชุมวิชาการระดับนานาชาติ จำนวน 1 ฉบับ โดยผลงานทั้งหมดสามาระแจกแจงได้ตามรายละเอียดต่อไปนี้

ผลงานวิจัยที่ตีพิมพ์ในวารสารวิชาการระดับนานาชาติ จำนวน 3 ฉบับได้แก่

1. Athisakul, C., Monprapussorn, T., and Chucheepsakul, S., 2011, “A Variational Formulation for Three-Dimensional Analysis of Extensible Marine Riser Transporting Fluid,” Ocean Engineering, Vol. 38, pp. 609-620.
   (Impact factor = 0.857)
2. Athisakul, C., Phanyasahachart, T., Klaycham, K., and Chucheepsakul, S., 2012, “Static Equilibrium Configruations and Appropriate Applied Top Tension of Extensible Marine Riser with Specified Total Arc-Length using Finite Element Method,” Engineering Structures Vol. 34, pp. 271-277.
   (Impact factor = 1.363)
3. Athisakul, C., Phungpaingam, B., Chatanin, W., and Chucheepsakul, S., 2012, “Critical Weight of Flexible Pipe Converying Fluid Subjected to End Moments”, The IES Journal Part A: Civil & Structural Engineering, Vol. 5, pp. 90-94.
   (ผลงานนี้เป็นผลงานที่ได้รับคัดเลือกให้ตีพิมพ์จากงาน International Conference on Advances in Steel Structures, 14-16 April 2012, Nanjing, China)

ผลงานวิจัยที่นำเสนอผลงานในที่ประชุมวิชาการระดับนานาชาติ จำนวน 1 ฉบับได้แก่

1. Athisakul, C., Phungpaingam, B., Chatanin, W., and Chucheepsakul, S., 2012, “Finite Element Method to Determine Critical Weight of Flexible Pipe Converying Fluid Subjected to End Moments”, Proceedings of 7 th International Conference on Advances in Steel Structures, 14-16 April 2012, Nanjing, China.

Appendix

ภาคผนวกประกอบด้วยสำเนาผลงานวิจัยที่ได้รับการตีพิมพ์ตามรายการดังต่อไปนี้

1. ผลงานวิจัยที่ตีพิมพ์ในวารสารวิชาการระดับนานาชาติ จำนวน 3 ฉบับ
2. ผลงานวิจัยที่นำเสนอผลงานในที่ประชุมวิชาการระดับนานาชาติ จำนวน 1 ฉบับ

Ocean Engineering 38 (2011) 609–620

Contents lists available at ScienceDirect

Ocean Engineering

journal homepage: www.elsevier.com/locate/oceaneng

A variational formulation for three-dimensional analysis of extensible marine riser transporting fluid

Chainarong Athisakul, Tinnakorn Monprapussorn, Somchai Chucheepsakul *

Department of Civil Engineering, Faculty of Engineering, King Mongkut's University of Technology Thonburi, Bangkok 10140, Thailand

ARTICLE INFO

Article history:
Received 20 April 2010
Accepted 7 December 2010
Editor-in-Chief: A.I. Incecik
Available online 24 December 2010

Keywords:
Extensible marine riser
Free vibration
Transporting fluid
Variational formulation
Finite element method

ABSTRACT

This paper presents a model formulation for static and dynamic analysis of three-dimensional extensible marine riser transporting fluid. A variational model formulation is developed based on the principle of virtual work–energy and the extensible elastica theory. The virtual work–energy functional is composed of the virtual strain energy due to axial stretching, bending, and torsion and the virtual work done by the external and internal fluid. The governing dynamic equilibrium equations are derived in the Cartesian coordinate. The finite element method is used to obtain the numerical solutions. The numerical examples are provided to demonstrate interesting effects of fluid transportation and axial deformation on large displacements and dynamic properties of the three-dimensional extensible marine riser.

1. Introduction

The marine riser is a flexible pipe that links the floating drilling/production platform and the seabed. It is a very important structural component used in offshore engineering operations. Over the past several years, the analysis of marine riser has received considerable attention. During the years 1960–1979, the model formulation of marine riser was introduced with the simplified small deflection model in the planar coordinate. Examples of this model can be found in several works such as NESCO (1965), Fischer and Ludwig (1966), Gosse and Barksdale (1969), Morgan (1972), Burke (1974), Young et al. (1978), Kirk et al. (1979), and Daring and Huang (1979).

From 1980 to present, the model formulations have been developed continually for the large displacement and nonlinear dynamic analysis. Researchers have begun to focus on the three-dimensional model formulations that can be used in deep ocean operations. Felippa and Chung (1981) presented the nonlinear static analysis of deep ocean mining pipe or riser suspended from moving vessels with free end at the bottom. Bernitsas (1982) developed a three-dimensional model formulation for large displacement analysis of marine riser. According to this formulation, the numerical solutions for static and dynamic analysis of three-dimensional marine riser were presented by Bernitsas et al. (1985), Kokarakis and Bernitsas (1987), and Bernitsas and Kokarakis (1988). A variational model formulation for three-dimensional analysis of inextensible marine riser was introduced by Huang and Kang (1991). Chai et al. (2002) presented a three-dimensional lump-mass formulation for static and dynamic analysis of a catenary riser. A rather general model formulation for three dimensional analysis of flexible riser using an absolute coordinate was presented by Chai and Varyani (2006).

A large strain formulation of two-dimensional marine riser using two different coordinate systems, namely, Cartesian and Natural coordinates, was presented by Chucheepsakul et al. (2003). The large axial strain can be considered based on three different definitions (total Lagrangian, updated Lagrangian, and Eulerian). Their model formulation can be applied not only for large strain analysis of flexible marine riser, but also for any kind of highly flexible structures such as flexible pipe, marine cable, elastic rod, elastic column, and elastic beam. Monprapussorn et al. (2007) used this formulation to investigate the effect of internal pulsating flow on static and dynamic behaviors of the extensible marine riser. Athisakul and Chucheepsakul (2008) used this formulation for analysis of variable-arc-length beam. Although there are many excellent works that deal with the model formulation of marine riser, the general model formulation that can be applied for large deformation analysis of three-dimensional extensible marine riser is rarely found.

The main purpose of this study is to present a variational model formulation of three-dimensional extensible marine riser transporting fluid. The strain energy due to large axial deformation, bending and twisting are taken into account. A generalized independent variable α is introduced to the model formulation for the sake of generality. The following assumptions are used to stipulate the present formulation:

1. The material of the marine riser is linearly elastic.
2. At the undeformed state, the marine riser is straight, and has no residual stresses.

* Corresponding author. Tel.: +66 2 470 9146; fax: +66 2 427 9063.
E-mail address: somchai.chu@kmutt.ac.th (S. Chucheepsakul).

0029-8018/$ - see front matter © 2010 Elsevier Ltd. All rights reserved.
doi:10.1016/j.oceaneng.2010.12.012

3. The riser's cross sections remain circular after the change of cross-sectional size due to the effect of axial deformation.
4. The longitudinal strain is large, while the effect of the shear strain is small and can be neglected.
5. Every cross-section remains plane perpendicular to the axis.
6. Radial lines of the sections remain straight.

The numerical examples of the special problems such as a catenary cable, three-dimensional cable, and vertical riser are considered. The effects of axial extensibility and internal flow on large displacement and dynamic properties of three-dimensional extensible marine riser are also presented in this paper.

2. Model formulation

2.1. Kinematics and deformation

Globally, the riser's behavior may follow elementary beam or rod theories, while locally, it can be considered as a cylindrical shell. However, the length of the riser is very large as compared to its cross-sectional diameter. Therefore, the riser is usually modeled as a three-dimensional rod rather than three-dimensional shell and the centroidal line of the riser is used to represent the overall riser configurations in both static and dynamic states.

The centroidal line of the riser can be described by three orthogonal coordinate systems. The fixed Cartesian coordinate system x, y, z with unit vectors $\hat{i},\hat{j},\hat{k}$ is used as a global coordinate. The orthogonal coordinate system $\hat{t},\hat{n},\hat{b}$ and the cross-sectional principal axes system x_1, x_2, x_3 with unit vectors $\hat{e}_1,\hat{e}_2,\hat{e}_3$ are used as the local coordinate.

The three states of the marine riser configurations are illustrated by Fig. 1. The first configuration of the riser is the undeformed configuration, which is an ideal configuration. This configuration can be defined by the position vector $\vec{r}_o$ as shown below:

$$\vec{\mathbf{r}}_o(\alpha) = x_o(\alpha)\hat{i} + y_o(\alpha)\hat{j} + z_o(\alpha)\hat{k} \tag{1}$$

The parameter α, which is a scalar parameter, is used to define the curve of riser's centroidal line. This parameter is employed in the formulation for the sake of generality. Therefore, the parameter α can be represented any convenient coordinates such as $x_o,x_s,x,y_o,y_s,y,z_o,z_s,z,s_o,s_s,s$ used to define the centroidal curve.

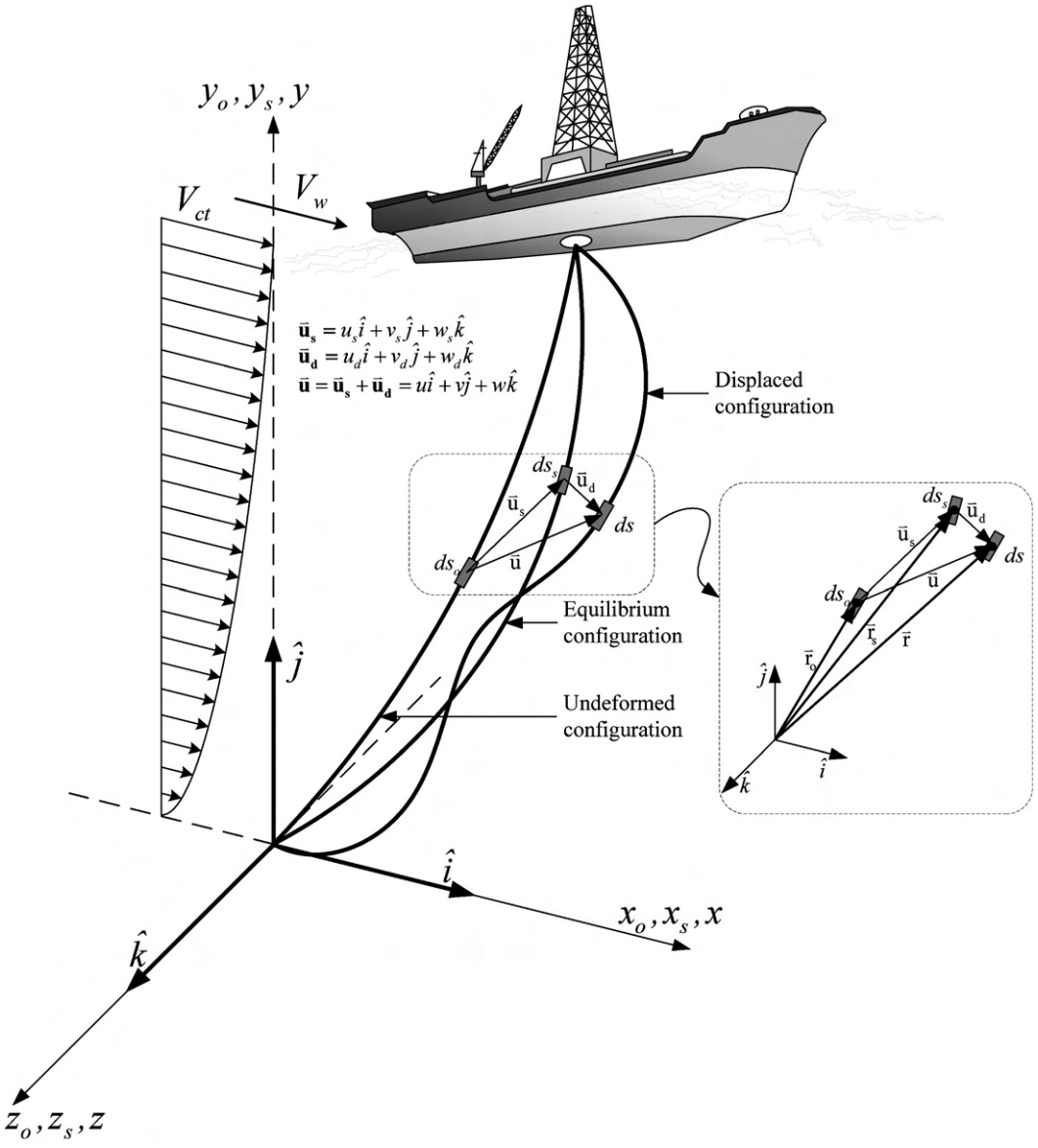

Fig. 1. Three configurations of a three-dimensional marine riser.

The second configuration is the equilibrium configuration. At this configuration, the riser is subjected to the time independent loads such as the apparent weight, quasi-static load from the steady current, and load due to the internal fluid flow. The position vector of the point on the centroidal line of marine riser at equilibrium state is

$$\vec{\mathbf{r}}_s(\alpha)=\vec{\mathbf{r}}_o(\alpha)+\vec{\mathbf{u}}_s(\alpha)=x_s(\alpha)\hat{i}+y_s(\alpha)\hat{j}+z_s(\alpha)\hat{k} \tag{2}$$

The vector $\vec{\mathbf{u}}_s(\alpha)$ is a displacement vector of a point on the equilibrium configuration measured with respect to the undeformed configuration

$$\vec{\mathbf{u}}_s(\alpha)=u_s(\alpha)\hat{i}+v_s(\alpha)\hat{j}+w_s(\alpha)\hat{k} \tag{3}$$

If the riser at the equilibrium state is disturbed from wave and unsteady flows of the transporting fluid, the riser will change its position from equilibrium to displaced configuration. As shown in Fig. 1, at any time t, the total displacement vector $\vec{\mathbf{u}}\ (\alpha,t)$ of the point on the centroidal line of marine riser at the displaced state can be expressed as

$$\vec{\mathbf{u}}\ (\alpha,t)=\vec{\mathbf{u}}_s(\alpha)+\vec{\mathbf{u}}_d(\alpha,t)=u(\alpha,t)\hat{i}+v(\alpha,t)\hat{j}+w(\alpha,t)\hat{k} \tag{4}$$

The vector $\vec{\mathbf{u}}_d(\alpha,t)$ is a displacement vector of the point on the displaced configuration measured with respect to the equilibrium configuration and it is defined as

$$\vec{\mathbf{u}}_d(\alpha,t)=u_d(\alpha,t)\hat{i}+v_d(\alpha,t)\hat{j}+w_d(\alpha,t)\hat{k} \tag{5}$$

Therefore, the position vector for the displaced configuration can be expressed by the following equations:

$$\vec{\mathbf{r}}\ (\alpha,t)=\vec{\mathbf{r}}_s(\alpha)+\vec{\mathbf{u}}_d(\alpha,t)=(x_s+u_d)\hat{i}+(y_s+v_d)\hat{j}+(z_s+w_d)\hat{k} \tag{6}$$

Based on the differential geometry, the differential arc-length for the undeformed state (s_o), the equilibrium state (s_s), and the displaced state (s) can be expressed by the following equations:

$$s_o'=\sqrt{x_o'^2+y_o'^2+z_o'^2} \tag{7}$$

$$s_s'=\sqrt{x_s'^2+y_s'^2+z_s'^2}=\sqrt{(x_o'+u_s')^2+(y_o'+v_s')^2+(z_o'+w_s')^2} \tag{8}$$

$$s'=\sqrt{x'^2+y'^2+z'^2}=\sqrt{(x_o'+u')^2+(y_o'+v')^2+(z_o'+w')^2} \tag{9}$$

The curvature (κ) and torsion (τ_1) of the centroidal line of the three-dimensional riser can be expressed as

$$\kappa=\frac{d\theta}{ds}=\frac{1}{s'^3}\sqrt{(x''y'-x'y'')^2+(y''z'-y'z'')^2+(x''z'-x'z'')^2} \tag{10}$$

$$\tau_1=\frac{d\phi}{ds}=\left[\frac{x'(y''z'''-y'''z'')-y'(x''z'''-x'''z'')+z'(x''y'''-x'''y'')}{(x''y'-x'y'')^2+(y''z'-y'z'')^2+(x''z'-x'z'')^2}\right] \tag{11}$$

where the infinitesimal angles $d\theta$ and $d\phi$ are the angles between successive tangents and successive binormals, respectively. The superscript ($'$) denotes the partial derivative with respect to parameter α.

The orientation of the riser cross-section is defined by an angle $\psi(s,t)$, which is the angle between the principal axis of the cross-section ($\hat{e}_2$) and the principal normal of the centroidal curve ($\hat{n}$) (see Fig. 2). According to the assumption that the riser cross-section remains plane and perpendicular to the axis of the riser, the rotations of the riser cross-section around both principal axes are sufficiently small and can be neglected. Thus, the rotation vector of the riser's cross-section can be defined as

$$\vec{\boldsymbol{\psi}}\ =\psi(\alpha,t)\hat{t}=(\psi_s(\alpha)+\psi_d(\alpha,t))\hat{t} \tag{12}$$

It has to be noted that the torsion of the riser is composed of the torsion of the centerline curve (τ_1) and the rate of change of the twisting angle ($d\psi/ds$). Therefore, the torsion of the riser can be expressed as

$$\tau=\tau_1+\frac{d\psi}{ds} \tag{13}$$

The velocity $\vec{\mathbf{V}}_p(\alpha,t)$ and acceleration $\vec{\mathbf{a}}_p(\alpha,t)$ of the riser can be derived by differentiating Eq. (4) with respect to time (t). Therefore

$$\vec{\mathbf{V}}_p=\dot{\vec{\mathbf{r}}}(\alpha,t)=\dot{u}_d(\alpha,t)\hat{i}+\dot{v}_d(\alpha,t)\hat{j}+\dot{w}_d(\alpha,t)\hat{k} \tag{14}$$

$$\vec{\mathbf{a}}_p=\ddot{\vec{\mathbf{r}}}(\alpha,t)=\ddot{u}_d(\alpha,t)\hat{i}+\ddot{v}_d(\alpha,t)\hat{j}+\ddot{w}_d(\alpha,t)\hat{k} \tag{15}$$

The angular velocity and angular acceleration can be expressed as follows:

$$\dot{\vec{\boldsymbol{\psi}}}=\dot{\psi}(\alpha,t)\hat{t}=\dot{\psi}_d(\alpha,t)\hat{t} \tag{16}$$

$$\ddot{\vec{\boldsymbol{\psi}}}=\ddot{\psi}(\alpha,t)\hat{t}=\ddot{\psi}_d(\alpha,t)\hat{t} \tag{17}$$

The notation $(\dot{\cdot})$ denotes the partial derivative with respect to time (t).

According to the updated Lagrangian description, the total, static, and dynamic axial strains can be defined as follows:

$$\textit{Total strain}:\ \varepsilon_t=\frac{s'-s_o'}{s_s'}=\sqrt{1+2\upsilon_d}-\sqrt{1-2\upsilon_s} \tag{18a}$$

$$\textit{Static strain}:\ \varepsilon_s=\frac{s_s'-s_o'}{s_s'}=1-\frac{s_o'}{s_s'}=1-\sqrt{1-2\upsilon_s} \tag{18b}$$

$$\textit{Dynamic strain}:\ \varepsilon_d=\frac{s'-s_s'}{s_s'}=\frac{s'}{s_s'}-1=\sqrt{1+2\upsilon_d}-1 \tag{18c}$$

The updated Green strains (υ_s,υ_d) in each state in Eqs. (18) can be derived in the terms of displacements of the riser as follows:

$$\upsilon_s=\frac{1}{s_s'^2}\left(x_s'u_s'+y_s'v_s'+z_s'w_s'-\frac{u_s'^2}{2}-\frac{v_s'^2}{2}-\frac{w_s'^2}{2}\right) \tag{19a}$$

$$\upsilon_d=\frac{1}{s_s'^2}\left(x_s'u_d'+y_s'v_d'+z_s'w_d'+\frac{u_d'^2}{2}+\frac{v_d'^2}{2}+\frac{w_d'^2}{2}\right) \tag{19b}$$

2.2. Apparent weight and apparent tension

According to Chucheepsakul et al. (2003), the apparent weight (W_a) and the apparent tension (N_a) can be expressed as

$$W_a=(\rho_pA_{ps}-\rho_eA_{es}+\rho_iA_{is})g \tag{20}$$

$$N_a=N_e+N_{tri}=N+2\nu(p_eA_{es}-p_iA_{is})=EA_{ps}\varepsilon_t \tag{21}$$

in which ρ_p, ρ_e, ρ_i are densities of riser, external fluid, and internal fluid, respectively, A_{ps} is the cross-sectional area of the riser, A_{es}, A_{is} are the outside and inside cross-sectional areas of the riser, respectively, p_e, p_i are the external and internal pressures, respectively, and ν is Poisson's ratio. The axial tension N is a true wall tension of the riser.

2.3. Hydrodynamic forces due to current and wave

For slender structure such as marine riser, the hydrodynamic forces due to current and wave can be computed by the following

expression:

$$\vec{\mathbf{F}}_H = \begin{Bmatrix} f_{Ht} \\ f_{Hn} \\ f_{Hbn} \end{Bmatrix} = \underbrace{0.5\rho_e D_e \begin{Bmatrix} \pi C_{Dt}\gamma_t|\gamma_t| \\ C_{Dn}\gamma_n|\gamma_n| \\ C_{Dbn}\gamma_{bn}|\gamma_{bn}| \end{Bmatrix}}_{\text{Viscous drag force}} + \underbrace{\rho_e A_e C_a \begin{Bmatrix} \dot{\gamma}_t \\ \dot{\gamma}_n \\ \dot{\gamma}_{bn} \end{Bmatrix}}_{\text{Hydrodynamic mass force}} + \underbrace{\rho_e A_e \begin{Bmatrix} \dot{V}_{Ht} \\ \dot{V}_{Hn} \\ \dot{V}_{Hbn} \end{Bmatrix}}_{\text{Froude-Krylov force}} \tag{22}$$

The coefficients C_{Dt}, C_{Dn}, C_{Dbn}, and C_a represent the tangential friction, normal drag, binormal drag, and the added mass coefficients, respectively. The variables V_{Ht},V_{Hn}, and V_{Hbn} are the tangential, normal, and binormal velocities of currents and waves, respectively. The relative velocities $\gamma_t = V_{Ht} - \dot{u}_t$, $\gamma_n = V_{Hn} - \dot{v}_n$, and $\gamma_{bn} = V_{Hbn} - \dot{w}_{bn}$ represent the velocities of currents and waves related to the riser velocity in tangential ($\dot{u}_t$), normal ($\dot{v}_n$), and binormal ($\dot{w}_{bn}$) directions, respectively.

2.4. Hydrodynamic forces due to fluid transportation

Based on the Newton's law of momentum conservation, the inertial force per unit length of the riser induced by the internal fluid flow is written as

$$\vec{f}_i = m_i \vec{a}_F \tag{23}$$

where $\vec{\mathbf{f}}_i$ is the inertial force vector, m_i is the transported mass per unit length of the riser, and $\vec{\mathbf{a}}_F$ is the acceleration vector of the transported fluid.

The acceleration of the transported fluid can be derived by considering the kinematics of transported fluid inside the risers. According to kinematics of transporting mass inside the moving riser (Huang, 1993), the acceleration of transported fluid can be expressed as

$$\vec{\mathbf{a}}_F = \frac{\partial^2(\vec{\mathbf{r}}_p)}{\partial t^2} + \left(\frac{2V_i}{s'}\right)\frac{\partial^2(\vec{\mathbf{r}}_p)}{\partial\alpha\partial t} + \left(\frac{V_i}{s'}\right)^2\frac{\partial^2(\vec{\mathbf{r}}_p)}{\partial\alpha^2} + \left[\frac{\dot{V}_i}{s'} + \frac{V_i V_i'}{s'^2} - \frac{V_i\dot{s}'}{s'^2} - \frac{V_i^2 s''}{s'^3}\right]\frac{\partial(\vec{\mathbf{r}}_p)}{\partial\alpha} \tag{24}$$

where V_i is a relative velocity of the fluid inside the riser.

2.5. Virtual strain energy

According to the extensible elastica theory (Chucheepsakul et al., 2003), the virtual strain energy of the marine riser is written as

$$\delta U = \int_\alpha [N_a\delta s' + B\kappa\delta\theta' + C\tau\delta\phi' + C\tau\delta\psi']d\alpha \tag{25}$$

where $B = EI_p(1+\varepsilon_d)$ is the bending rigidity, $C = GJ_p(1+\varepsilon_d)$ is torsion rigidity, ψ is the twisting angle, s is the arc-length, ε_d is the dynamic strain, I_p is the moment of inertia of the riser, J_p is the polar moment of inertia of the riser. The expressions of the variation of s',θ' and ϕ' are given in Appendix A.

2.6. External virtual work

The external virtual work of the riser system is

$$\delta W = \delta W_w + \delta W_H + \delta W_I \tag{26}$$

where δW_w, δW_H, and δW_I are the virtual work done by the apparent weight, hydrodynamic forces, and inertial forces of the riser and transported fluid, respectively. In the Cartesian coordinates, the expressions of these virtual works can be written as

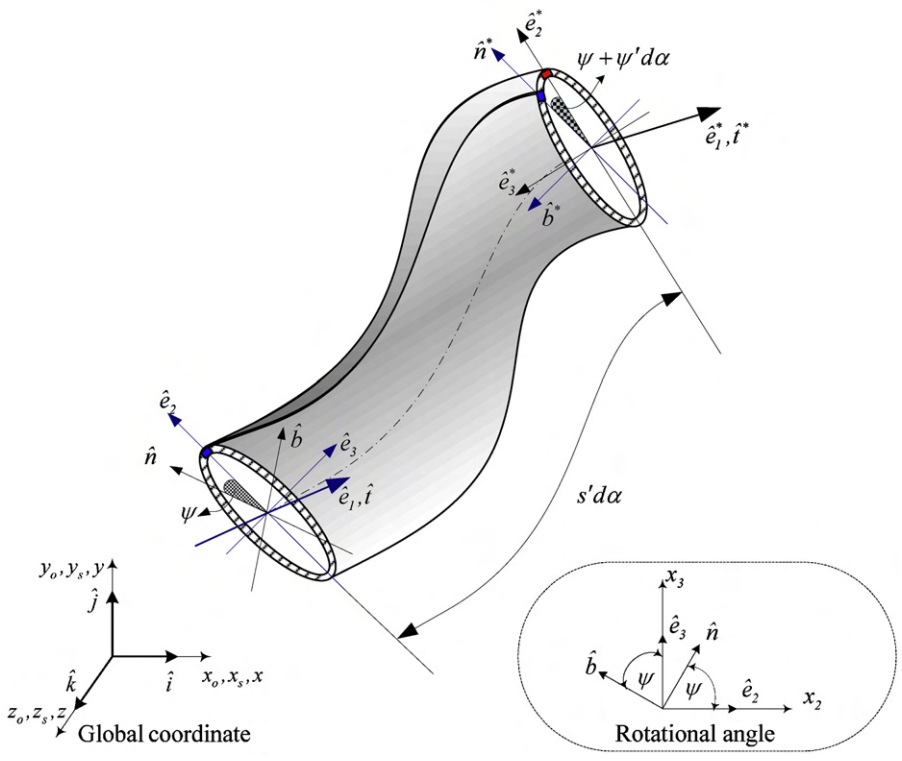

Fig. 2. The orientation of the riser cross-section.

follows:

$$\delta W_w = -\int_\alpha w_a s' \delta v d\alpha \tag{27}$$

$$\delta W_H = \int_\alpha [f_{Hx} s' \delta u + f_{Hy} s' \delta v + f_{Hz} s' \delta w] d\alpha \tag{28}$$

$$\delta W_I = -\int_\alpha [(m_p a_{px} + m_i a_{ix}) s' \delta u + (m_p a_{py} + m_i a_{iy}) s' \delta v + (m_p a_{pz} + m_i a_{iz}) s' \delta w + (\rho_p J_p \ddot{\psi}) s' \delta \psi] d\alpha \tag{29}$$

The components of the hydrodynamic forces vector (f_{Hx}, f_{Hy}, f_{Hz}) can be derived by transforming Eq. (22) to the fixed Cartesian coordinate system. The variables m_p and m_i represent the mass per unit length of the riser and transporting fluid, respectively.

2.7. Total virtual work

In this study, the sea water level (y_s) is used as an independent variable (α). Based on the principle of virtual work, the riser system is in equilibrium if the total virtual work energy of the riser system is zero

$$\delta\pi = \delta U - \delta W_w - \delta W_H - \delta W_I = 0 \tag{30}$$

Substituting Eqs. (25), (27), (28), and (29) into Eq. (30) with some manipulations, one obtains

$$\begin{aligned}\delta\pi = &\int_{y_s} \left\{ \left[N_a \left(\frac{x'}{s'}\right) - B\left(\frac{\kappa^2 x'}{s'} + \frac{s''}{s'^3}\frac{\partial}{\partial y_s}\left(\frac{x'}{s'}\right)\right) + C\tau\kappa b_x \right] \delta u' \right.\\ &+ \left[N_a \left(\frac{y'}{s'}\right) - B\left(\frac{\kappa^2 y'}{s'} + \frac{s''}{s'^3}\frac{\partial}{\partial y_s}\left(\frac{y'}{s'}\right)\right) + C\tau\kappa b_y \right] \delta v' \\ &\left. + \left[N_a \left(\frac{z'}{s'}\right) - B\left(\frac{\kappa^2 z'}{s'} + \frac{s''}{s'^3}\frac{\partial}{\partial y_s}\left(\frac{z'}{s'}\right)\right) + C\tau\kappa b_z \right] \delta w' \right\} dy_s \\ &+ \int_{y_s} \left\{ \left[\frac{B}{s'^2}\frac{\partial}{\partial y_s}\left(\frac{x'}{s'}\right)\right] \delta u'' + \left[\frac{B}{s'^2}\frac{\partial}{\partial y_s}\left(\frac{y'}{s'}\right)\right] \delta v'' \right.\\ &\left. + \left[\frac{B}{s'^2}\frac{\partial}{\partial y_s}\left(\frac{z'}{s'}\right)\right] \delta w'' \right\} dy_s + \int_{y_s} \{T \delta\psi'\} dy_s \\ &- \int_{y_s} \{s'[f_{Hx} - m_p a_{px} - m_i a_{Fx}]\delta u\}\, dy_s \\ &- \int_{y_s} \{s'[-w_a + f_{Hy} - m_p a_{py} - m_i a_{Fy}]\delta v\}\, dy_s \\ &- \int_{y_s} \{s'[f_{Hz} - m_p a_{pz} - m_i a_{Fz}]\delta w\}\, dy_s + \int_{y_s} \{s'[\rho_p J_p \ddot{\psi}]\delta(\psi)\}\, dy_s = 0 \end{aligned} \tag{31}$$

The apparent tension in Eq. (31) can be evaluated by considering the equilibrium condition of forces applied on the riser element in tangential direction. One obtains

$$N_a(y_s) = N_a(y_{sH}) + \int_{y_s}^{y_{sH}} \left[(B\kappa)'\kappa + s'\left(\frac{-w_a}{s'} + f_{Ht} - m_p a_{pt} - m_i a_{Ft}\right)\right] dy_s \tag{32}$$

where f_{Ht} is the hydrodynamic forces in the tangential direction, a_{pt} is the tangential acceleration of the riser, a_{Ft} is the tangential acceleration of transporting fluid. In this study, the finite element method is used to solve the system of Eqs. (31) and (32).

3. Finite element model

Because the top end of the riser can slide through the slip joint, the total stretched arc-length of the riser measured from the seabed to the slip joint may not be known until the equilibrium configuration is determined. Therefore, the discretization along the unstretched arc-length may not be convenient to set up the boundary condition at the top end. In order to eliminate this problem, the discretization of the riser element along the sea water level is applied instead of the total unknown arc-length as shown in Fig. 3.

3.1. Nonlinear static analysis

In general, the riser will vibrate around its static configuration which is commonly nonlinear. Therefore, the nonlinear static solutions have to be evaluated before calculating the dynamic properties of the riser. The hybrid finite element model formulation for nonlinear static analysis of three-dimensional marine riser can be derived by eliminating the time-dependent terms in Eq. (31). One obtains

$$\begin{aligned}\delta\pi_s = &\int_{y_s} \left\{ \left[N_{as} \left(\frac{x'_s}{s'_s}\right) - B_s\left(\frac{\kappa_s^2 x'_s}{s'_s} + \frac{s''_s}{s'^3_s}\frac{\partial}{\partial y_s}\left(\frac{x'_s}{s'_s}\right)\right) + C_s\tau_s\kappa_s b_{xs} \right] \delta u'_s \right.\\ &\left. + \left[N_{as} \left(\frac{z'_s}{s'_s}\right) - B_s\left(\frac{\kappa_s^2 z'_s}{s'_s} + \frac{s''_s}{s'_s 3}\frac{\partial}{\partial y_s}\left(\frac{z'_s}{s'_s}\right)\right) + C_s\tau_s\kappa_s b_{zs} \right] \delta w'_s \right\} dy_s \\ &+ \int_{y_s} \left\{ \left[\frac{B_s}{s'^2_s}\frac{\partial}{\partial y_s}\left(\frac{x'_s}{s'_s}\right)\right] \delta(u''_s) + \left[\frac{B_s}{s'^2_s}\frac{\partial}{\partial y_s}\left(\frac{z'_s}{s'_s}\right)\right] \delta w''_s \right\} dy_s \\ &+ \int_{y_s} \{(C_s\tau_s)'\delta\psi_s\}\, dy_s + \int_{y_s} \{s'_s[-f_{Hxs} + m_i a_{Fxs}]\delta u_s\}\, dy_s \\ &+ \int_{y_s} \{s'_s[-f_{Hzs} + m_i a_{Fzs}]\delta w_s\}\, dy_s = 0 \end{aligned} \tag{33}$$

where $x_s = x_o + u_s$, $z_s = z_o + w_s$. The subscript (s) of each parameters in Eq. (33) represents the static quantities. The nonlinear static

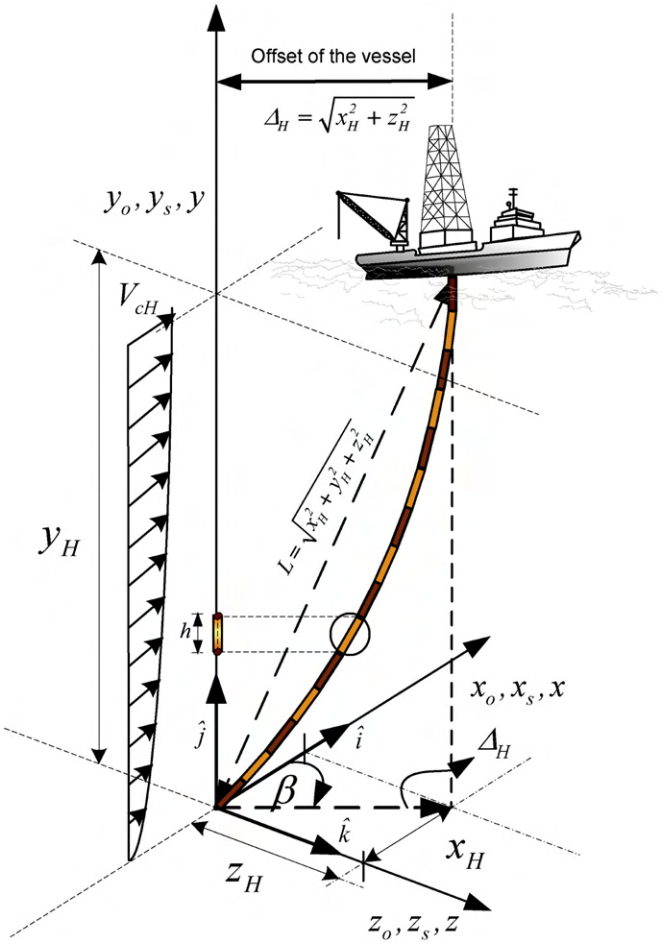

Fig. 3. The discretization of the riser along the water depth.

displacement u_s and w_s are approximated by the fifth order polynomial. It has to be noted that the static displacement u_s and w_s are referenced to the fixed Cartesian coordinate x, y, z, and the undeformed configuration of the riser is arbitrary. Therefore, the axial static strain ε_s is approximated by the linear interpolation and can be calculated from the constrain condition between Eqs. (21) and (32). According to Eq. (33), the derivative of torque is equal to zero ($(C_s\tau_s)'=0$) and the rate of change of the static twisting angle $(d\psi_s/ds)$ can be found from Eq. (13). Therefore, the static twisting angle can be calculated by the direct integration. Consequently, it is not necessary to include the twisting angle to the displacement vector. Therefore, the displacement vector can be expressed as

$$\{\vec{\mathbf{d}}_s\}=\{\,u_s \quad w_s \quad \varepsilon_s\,\}^T=[\mathbf{N}_s]\{\vec{\mathbf{d}}_{ns}\} \tag{34}$$

where the nodal displacements of each element are

$$\left\{\vec{\mathbf{d}}_{\mathbf{ns}}\right\}=\{u_{1s} \quad u'_{1s} \quad u''_{1s} \quad w_{1s} \quad w'_{1s} \quad w''_{1s} \quad \varepsilon_{1s} \mid u_{2s} \quad u'_{2s} \quad u''_{2s} \quad w_{2s} \quad w'_{2s} \quad w''_{2s} \quad \varepsilon_{2s}\} \tag{35}$$

The shape function matrix at the equilibrium state is

$$[\mathrm{N_s}]=\left[\begin{array}{ccccccc|ccccccc} N_{51} & N_{52} & N_{53} & 0 & 0 & 0 & 0 & N_{54} & N_{55} & N_{56} & 0 & 0 & 0 & 0 \\ 0 & 0 & 0 & N_{51} & N_{52} & N_{53} & 0 & 0 & 0 & 0 & N_{54} & N_{55} & N_{56} & 0 \\ 0 & 0 & 0 & 0 & 0 & 0 & N_{11} & 0 & 0 & 0 & 0 & 0 & 0 & N_{12} \end{array}\right] \tag{36}$$

The elements of shape function matrix are defined in Appendix B. According to the calculus of variation, one can find

$$\delta\pi_s^{(e)}=\sum_{i=1}^{14}\left[\frac{\partial\pi_s^{(e)}}{\partial d_{nsi}}\right]\delta d_{nsi}=0 \tag{37}$$

Since $\delta d_{nsi}\neq 0$, one obtains the system of nonlinear equations as

$$\frac{\partial\pi_s}{\partial d_{nis}}=\int_0^h\left[[\mathbf{N}_s'']^T\begin{Bmatrix} BTx_s \\ BTz_s \\ 0 \end{Bmatrix}+[\mathbf{N}_s']^T\begin{Bmatrix} NBTx_s \\ NBTz_s \\ 0 \end{Bmatrix}+[\mathbf{N}_s]^T\begin{Bmatrix} ffx_s \\ ffz_s \\ EA_{ps}\varepsilon_s-N_{as} \end{Bmatrix}\right]dy_s=0 \tag{38}$$

where

$$BTx_s=\frac{B_s}{s_s'^2}\frac{\partial}{\partial y_s}\left(\frac{x_s'}{s_s'}\right)=\frac{B_s}{s_s'^2}\left(\frac{x_s''}{s_s'}-\frac{x_s's_s''}{s_s'^2}\right) \tag{39a}$$

$$BTz_s=\frac{B_s}{s_s'^2}\frac{\partial}{\partial y_s}\left(\frac{z_s'}{s_s'}\right)=\frac{B_s}{s_s'^2}\left(\frac{z_s''}{s_s'}-\frac{z_s's_s''}{s_s'^2}\right) \tag{39b}$$

$$NBTx_s=N_{as}\left(\frac{x_s'}{s_s'}\right)-B_s\left(\frac{\kappa_s^2x_s'}{s_s'}+\frac{s_s''}{s_s'^3}\frac{\partial}{\partial\alpha}\left(\frac{x_s'}{s_s'}\right)\right) \tag{39c}$$

$$NBTz_s=N_{as}\left(\frac{z_s'}{s_s'}\right)-B_s\left(\frac{\kappa_s^2z_s'}{s_s'}+\frac{s_s''}{s_s'^3}\frac{\partial}{\partial\alpha}\left(\frac{z_s'}{s_s'}\right)\right) \tag{39d}$$

$$ffx_s=s_s'[-f_{Hxs}+m_ia_{Fxs}]-(C_s\tau_s\kappa_sb_{xs})' \tag{39e}$$

$$ffz_s=s_s'[-f_{Hzs}+m_ia_{Fzs}]-(C_s\tau_s\kappa_sb_{zs})' \tag{39f}$$

The boundary conditions of the riser system are

$$(at\ y_s=0) \qquad u_s=0, \quad w_s=0, \quad \psi_s=0 \tag{40a–c}$$

$$(at\ y_s=y_{sH}) \qquad u_s=0, \quad w_s=0, \quad N_{as}=N_{asH}, \quad \varepsilon_s=\frac{N_{asH}}{EA_{psH}} \tag{40a–d}$$

The system of the nonlinear equations (Eq. (38)), which is constrained by boundary conditions (Eq. (39)) is solved numerically by the iterative procedure (Monprapussorn et al., 2004).

3.2. Natural frequency analysis

The assumed dynamic displacements of each element are approximated by

$$\{\vec{\mathbf{d}}\}=\{\,u_d \quad v_d \quad w_d \quad \psi_d\,\}^T=[N(y_s)]\{\vec{\mathbf{d}}_{nd}(t)\} \tag{41}$$

The nodal displacement vector $\{\vec{\mathbf{d}}_{nd}\}$ in Eq. (41) is a function of time only and can be expressed as

$$\left\{\vec{\mathbf{d}}_{\mathbf{nd}}\right\}=\{u_1 \quad u_1' \quad u_1'' \quad v_1 \quad v_1' \quad v_1'' \quad w_1 \quad w_1' \quad w_1'' \quad \psi_1 \quad \psi_1' \quad \psi_1'' \mid u_2 \quad u_2' \quad u_2'' \quad v_2 \quad v_2' \quad v_2'' \quad w_2 \quad w_2' \quad w_2'' \quad \psi_2 \quad \psi_2' \quad \psi_2''\} \tag{42}$$

The shape function matrix $[N(y_s)]$, which is a function of y_s, can be expressed as

$$[N]=\left[\begin{array}{cccccccccccc|cccccccccccc} N_{51} & N_{52} & N_{53} & 0 & 0 & 0 & 0 & 0 & 0 & 0 & 0 & 0 & N_{54} & N_{55} & N_{56} & 0 & 0 & 0 & 0 & 0 & 0 & 0 & 0 & 0 \\ 0 & 0 & 0 & N_{51} & N_{52} & N_{53} & 0 & 0 & 0 & 0 & 0 & 0 & 0 & 0 & 0 & N_{54} & N_{55} & N_{56} & 0 & 0 & 0 & 0 & 0 & 0 \\ 0 & 0 & 0 & 0 & 0 & 0 & N_{51} & N_{52} & N_{53} & 0 & 0 & 0 & 0 & 0 & 0 & 0 & 0 & 0 & N_{54} & N_{55} & N_{56} & 0 & 0 & 0 \\ 0 & 0 & 0 & 0 & 0 & 0 & 0 & 0 & 0 & N_{51} & N_{52} & N_{53} & 0 & 0 & 0 & 0 & 0 & 0 & 0 & 0 & 0 & N_{54} & N_{55} & N_{56} \end{array}\right] \tag{43}$$

The elements of the above matrix are the fifth degree polynomial shape functions, which is defined in Appendix B. Then, substituting Eq. (41) into Eq. (31) together with some manipulations, the equation of motion for free vibration analysis of three-dimensional marine riser element can be written in the matrix form as

$$[\mathbf{m}^e]\{\ddot{\mathbf{d}}_{nd}\}+[\mathbf{g}^e]\{\dot{\mathbf{d}}_{nd}\}+[\mathbf{k}^e]\{\mathbf{d}_{nd}\}=\{\mathbf{0}\} \tag{44}$$

where $[\mathbf{m}^e]$, $[\mathbf{g}^e]$, and $[\mathbf{k}^e]$ are the element mass matrix, the element gyroscopic matrix, and the element stiffness matrix, which are shown in Appendix C.

Then, assembling the element equations of motion (Eq. (44)), one obtains the equation of motion for entire riser as

$$[\mathbf{M}]\{\ddot{\mathbf{D}}_{nd}\}+[\mathbf{G}]\{\dot{\mathbf{D}}_{nd}\}+[\mathbf{K}]\{\mathbf{D}_{nd}\}=\{\mathbf{0}\} \tag{45}$$

where $\{\mathbf{D}_{nd}\}=\sum_{i=1}^{nelem}\{\mathbf{d}_{nd}\}$is the global nodal displacement vector; $[\mathbf{M}]=\sum_{i=1}^{nelem}[\mathbf{m}^e]$ is the total mass matrix; $[\mathbf{G}]=\sum_{i=1}^{nelem}[\mathbf{g}^e]$ is the total gyroscopic matrix; $[\mathbf{K}]=\sum_{i=1}^{nelem}[\mathbf{k}^e]$ is the total stiffness matrix. The abbreviation 'nelem' represents the number of finite element.

In order to evaluate Eq. (45), the identity $\{\dot{\mathbf{D}}_{nd}\}=\{\dot{\mathbf{D}}_{nd}\}$ has to be added into Eq. (45). Therefore, the equation of motion for entire riser can be rearranged into the following form (Meirovitch, 1997):

$$\begin{bmatrix}\mathbf{I} & \mathbf{0}\\ \mathbf{0} & \mathbf{M}\end{bmatrix}\begin{Bmatrix}\dot{\mathbf{D}}_{nd}\\ \ddot{\mathbf{D}}_{nd}\end{Bmatrix}+\begin{bmatrix}\mathbf{0} & -I\\ \mathbf{K} & \mathbf{G}\end{bmatrix}\begin{Bmatrix}\mathbf{D}_{nd}\\ \dot{\mathbf{D}}_{nd}\end{Bmatrix}=\begin{Bmatrix}\mathbf{0}\\ \mathbf{0}\end{Bmatrix} \tag{46}$$

Eq. (46) can be cast in the state form as

$$\{\dot{\mathbf{X}}_{nd}\}=[\mathbf{A}]\{\mathbf{X}_{nd}\} \tag{47}$$

where $\{\mathbf{X}_{nd}\}_{2n\times 1}=\{\mathbf{D}_{nd}\quad \dot{\mathbf{D}}_{nd}\}^T$ is the $2n$-dimensional state vector, and the matrix $[\mathbf{A}]$ is the $2n\times 2n$ real nonsymmetric coefficient matrix. The matrix $[\mathbf{A}]$ can be expressed as follows:

$$[\mathbf{A}]=\begin{bmatrix}\mathbf{0} & \mathbf{I}\\ -\mathbf{M}^{-1}\mathbf{K} & -\mathbf{M}^{-1}\mathbf{G}\end{bmatrix}_{2n\times 2n} \tag{48}$$

The solution of Eq. (47) can be written in the following form:

$$\{\mathbf{X}_{nd}\}=e^{\lambda t}\{\mathbf{X}_{na}\} \tag{49}$$

The parameter λ is a complex value and $\{\mathbf{X}_{na}\}$ is a $2n$ complex vector. Substituting Eq. (49) into Eq. (47), one obtains the general algebraic eigenvalue problem as follows:

$$[\mathbf{A}]\{\mathbf{X}_{nd}\}=\lambda\{\mathbf{X}_{nd}\} \tag{50}$$

The general form of the eigenvalue λ can be expressed as

$$\lambda=\alpha\pm i\omega \tag{51}$$

where ω represents the natural frequency of the riser system. The eigenvalue problem of Eq. (50) can be solved numerically by the implicit double-shifted QR algorithm based on the EISPACK routine HQR2 (Smith et al., 1976).

4. Numerical examples

In this study, the computer program for large displacement analysis and free vibration analysis of three-dimensional extensible marine riser is developed in the Fortran-90 language. The special test cases such as the configuration of catenary cable, the free vibration analysis of three-dimensional cable (Henghold et al., 1977), and the free vibration analysis of extensible marine riser transporting fluid (Moe and Chucheepsakul, 1988) are presented in order to verify the accuracy of the numerical results.

4.1. Catenary cable

The numerical approximation of the catenary cable configuration can be evaluated by eliminating the bending and torsional rigidity from Eq. (38). The cable weight is equal to 5 N/m. The axial tensions in cable at top and bottom end are equal to 1574.32 and 1074.32 N, respectively. Fig. 4 shows that the numerical solutions and shape of cable are identical to those carried out by the exact formula.

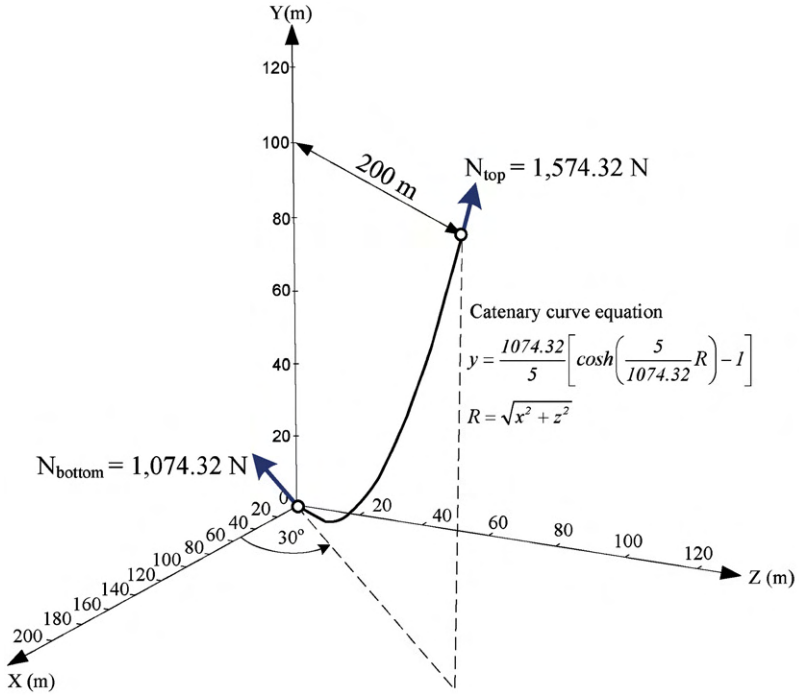

Y (m)	This study (FEM)		Exact solutions	
	X (m)	Z (m)	X (m)	Z (m)
100	173.20	100	173.20	100
80	155.90	90.01	155.97	90.05
60	135.86	78.44	136.01	78.53
40	111.59	64.43	111.85	64.58
20	79.20	45.73	79.68	46.00
0	0	0	0	0

Fig. 4. Configuration of the catenary cable.

Table 1
Comparisons of the first four dimensionless frequencies of an inclined extensible cable for a value of $EA_o/w_aS_s=5000$.

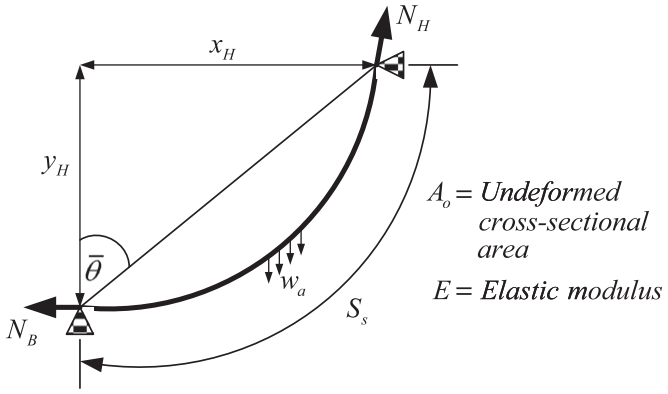

Mode	Dimensionless frequencies of cable ($\hat{\omega}_c$)			
	Henghold et al. (1977)	Chucheepsakul and Srinil (2002)	**This study (20 elements)**	%Difference from Henghold et al. (1977)
Incline angle ($\bar{\theta}$) is equal to 30°				
1 (O)	2.24	2.24	2.24	0.00
2 (I)	3.65	3.57	3.61	1.10
3 (O)	4.53	4.45	4.48	1.10
4 (I)	6.30	6.01	6.07	3.65
Incline angle ($\bar{\theta}$) is equal to 60°				
1 (O)	2.83	2.84	2.84	0.35
2 (I)	5.17	5.28	5.29	2.32
3 (O)	5.67	5.63	5.64	0.53
4 (I)	8.17	8.34	8.35	2.20

Table 2
Input parameters and the in-plane fundamental natural frequencies of the rigid production riser transporting fluid with various speeds of internal flow.

Input parameters used for the rigid production riser transporting fluid	
1. Riser top tension, N_{aH}	476,200 N
2. Water depth, y_H	300 m
3. Excursion of the vessel in x-direction, x_H	0 m
4. Excursion of the vessel in z direction, z_H	0 m
5. Outside diameter, D_{epo}	0.26 m
6. Inside diameter, D_{ipo}	0.20 m
7. Density of riser, ρ_p	7850 kg/m^3
8. Density of sea water, ρ_e	1025 kg/m^3
9. Density of mud, ρ_i	998 kg/m^3
10. Young's modulus, E	2.07×10^{11} N/m^2
11. Poisson's ratio, v	0.50
12. Current velocity at mean sea level, V_{cH}	0 m/sec
13. Angle between current direction and x-direction	0°
14. Normal drag coefficient, C_{Dn}	0.70
15. Tangential drag coefficient, C_{Dt}	0.03
16. Added mass coefficient, C_a	1.00

Numerical results

Internal flow velocity (V_{io})(m/s)	The in-plane fundamental natural frequencies of production riser (rad/sec)					
	Moe and Chucheepsakul (1988) (IA,EBR)		Monprapussorn et al. (2007) (EA)		**This study (20 elements)** (3-D,EA)	
	Analytical solution	Numerical solution	EBR	IBR	EBR	IBR
0	0.2878	0.2890	0.2891	0.3001	0.2892	0.2988
5	–	–	0.2881	0.2994	0.2883	0.2980
10	0.2838	0.2853	0.2853	0.2972	0.2854	0.2957
15	–	–	0.2804	0.2934	0.2805	0.2917
20	0.2706	0.2730	0.2731	0.2880	0.2732	0.2860
25	–	–	0.2627	0.2809	0.2629	0.2783
30	0.2413	0.2478	0.2478	0.2717	0.2481	0.2684
35	–	–	0.2224	0.2603	0.2230	0.2559

Note: IA=inextensible analysis, EA=extensible abiicnalysis, 3-D=3-D analysis, EBR=excluding bending rigidity, IBR=including Bending Rigidity.

4.2. Free vibration of three-dimensional cable

The special case of an inclined extensible cable subjected to its uniform self-weight is presented. The cable is suspended in the air with the incline angle ($\overline{\theta}$) of 30° and 60°. Table 1 shows the in-plane (I) and out-of-plane (O) dimensionless frequencies ($\hat{\omega}_c = \omega\sqrt{S_s/g}$) for the first four modes of the cable with a value of cable stiffness to weight ratio (EA_o/w_aS_s) of 5000. The FEM solutions for 20 elements obtained in this study are in a very good agreement with the studies of Henghold et al. (1977) and Chucheepsakul and Srinil (2002).

4.3. Free vibration of vertical riser transporting fluid

The parameters used and the natural frequencies of a vertical riser transporting fluid are shown in Table 2. The natural frequencies of the vertical riser are compared with the analytical solutions and the numerical solutions that were reported by Moe and Chucheepsakul (1988) and Monprapussorn et al. (2007), respectively. The numerical results, which are obtained from this study, are in good agreement with the previous report.

4.4. Effect of axial extensibility and internal flow on maximum displacement of extensible marine riser

According to the validation of previous examples, the authors are confident that the model formulation developed herein is applicable and give the sufficient accuracy of the numerical results. In this section, the couple effect of axial extensibility and internal flow on maximum displacement of extensible marine riser is presented.

The data in Table 3 is utilized for this example. In the case of extensible riser, the flexural rigidity is small as compared with the applied top tension. Therefore, the applied top tension (N_{aH}) is used as the basis for the parametric normalization. The following dimensionless parameters are introduced in order to comprehend the effect of axial extensibility:

$$\hat{E}_{irv} = \left(\frac{w_a L}{N_{aH}}\right)\sqrt{\frac{EA_{po}}{N_{aH}}}, \quad \hat{V}_{io} = V_{io}\sqrt{\frac{m_{io}}{N_{aH}}}, \quad \hat{\omega} = \omega L\sqrt{\frac{m_{to}}{N_{aH}}},$$
$$\hat{y}_s = \frac{y_s}{L}, \quad \hat{\Delta}_s = \frac{\Delta_s}{L} \qquad (52a\text{–}e)$$

The parameter $\hat{E}_{irv}$ is recognized as the Irvine's first parameter (Hover and Triantafyllou, 1999) in cable mechanics. It is utilized to describe the effect of riser' extensibility. The high value of $\hat{E}_{irv}$ implied the low extensibility, but the low value of $\hat{E}_{irv}$ implied the high extensibility condition of the riser. The parameter $\hat{V}_{io}$ denotes the effect of the mean flow velocity of transported fluid. The parameter $\hat{\omega}$ is the nondimensional form of the natural frequency (ω) of the riser. The parameter $\hat{y}_s$ represents the position of maximum displacement from seabed. The parameter $\hat{\Delta}_s$ is the nondimensional form of the lateral displacement $\left(\Delta_s = \sqrt{u_s^2 + w_s^2}\right)$ of the riser where the span length $L = \sqrt{x_H^2 + y_H^2 + z_H^2}$.

Table 3
The input data utilized for study the effect of axial extensibility and internal flow on maximum displacement of marine riser.

Parameters	Value
Offset of the vessel $\left(\sqrt{x_H^2 + z_H^2}\right)$	70 m
Water depth, y_H	300 m
Normal drag coefficient, C_{Dn}	0.70
Tangential drag coefficient, C_{Dt}	0.03
Added mass coefficient, C_a	1.00
Current velocity at mean sea level, V_{cH}	0.20 m/s
Elastic modulus, E	2.07×10^{11} N/m^2
Outside diameter, D_{epo}	0.26 m
Inside diameter, D_{ipo}	0.20 m
Density of pipes/risers, ρ_p	7850 kg/m^3
Density of sea water, ρ_e	1025 kg/m^3
Density of internal fluid, ρ_i	998 kg/m^3

The combination effect of axial extensibility and internal flow on the maximum displacement of extensible marine riser is shown in Fig. 5. It is evident that the internal flow of transported fluid increases the lateral displacements. The internal flow induces a tangential loading, which destabilizes the riser system. Consequently, the divergent instability could be occurred when speed of internal flow reaches the value of $\hat{V}_{is} = 0.3246$ as shown in Fig. 5.

Fig. 5 also shows that an increase in axial extensibility, by reducing $\hat{E}_{irv}$ from 286.50 to 28.65, enlarges the lateral displacements due to the reduction of bending stiffness. However, the turning point occurs when $\hat{E}_{irv}$ is reduced passing 10.00 to 1.81. In this range, the increase in axial extensibility reduces the lateral displacements.

The transition behavior is occurred due to the variation of the structural stiffness domination from the bending stiffness domination to the pretensioned stiffness (Fig. 5). The structural stiffness of the low extensible riser is governed by the bending strain energy, and the riser behaves like a tensioned beam.

On the contrary, when the condition of high extensibility such as $\hat{E}_{irv} = 1.81$ is applied, the riser received high axial tension and the axial strain become large. In this case, the axial strain energy or the pretensioned stiffness becomes the main stiffness of riser as well as the tensioned cable. For a moderate extensibility riser ($10.00 \le \hat{E}_{irv} \le 28.65$), the riser has large amount of both axial strain energy and bending strain energy. Consequently, the riser is under the coupled axial–bending stiffness domination and the transition of tensioned beam behavior to tensioned cable behavior is occurred in this state.

From the above discussions, it can be found that the effect of axial extensibility of the riser induces the lateral displacements when the bending stiffness controls. However, the effect of axial

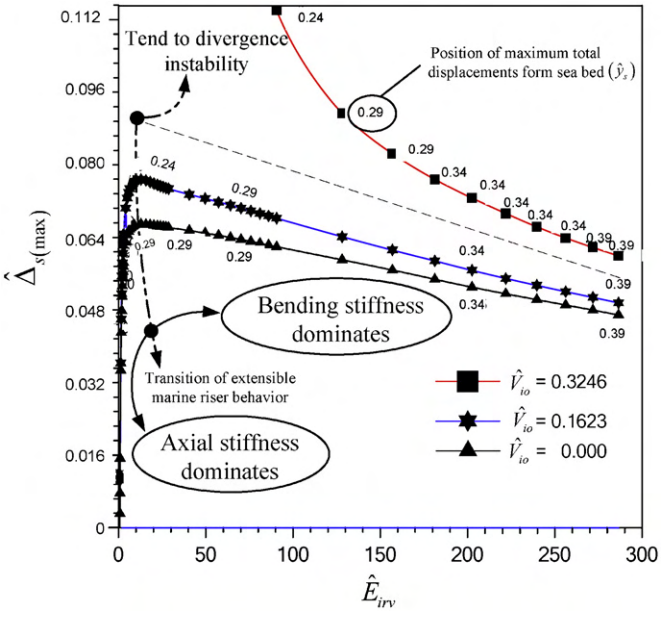

Fig. 5. Effect of axial extensibility and internal flow on maximum displacement ($\hat{\Delta}_s$) of extensible marine risers and their positions from seabed.

extensibility of the riser reduces the lateral displacements when the pretensioned stiffness controls.

4.5. Effect of axial extensibility and internal flow on natural frequencies and mode shapes of extensible marine riser

Figs. 6 and 7 show that the increase in internal flow velocity reduces the natural frequencies of the extensible marine riser. The

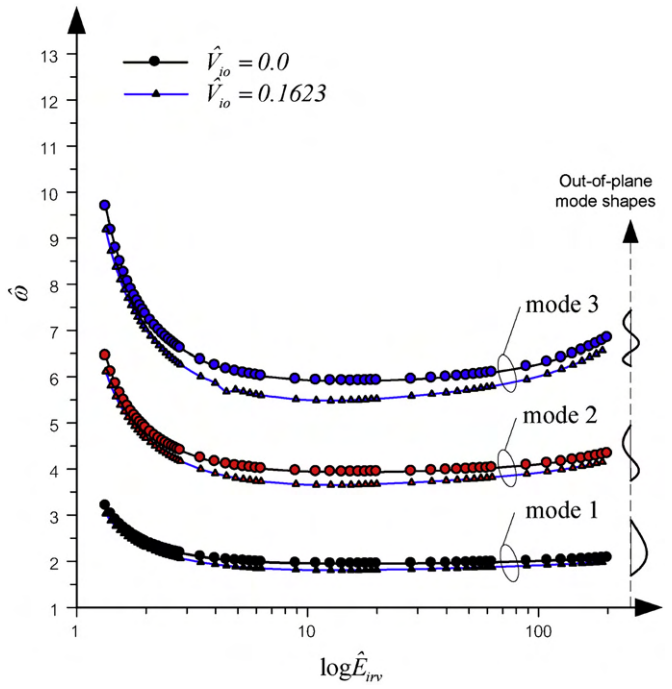

Fig. 6. Effect of axial extensibility on the out-of-plane natural frequencies of the extensible marine riser.

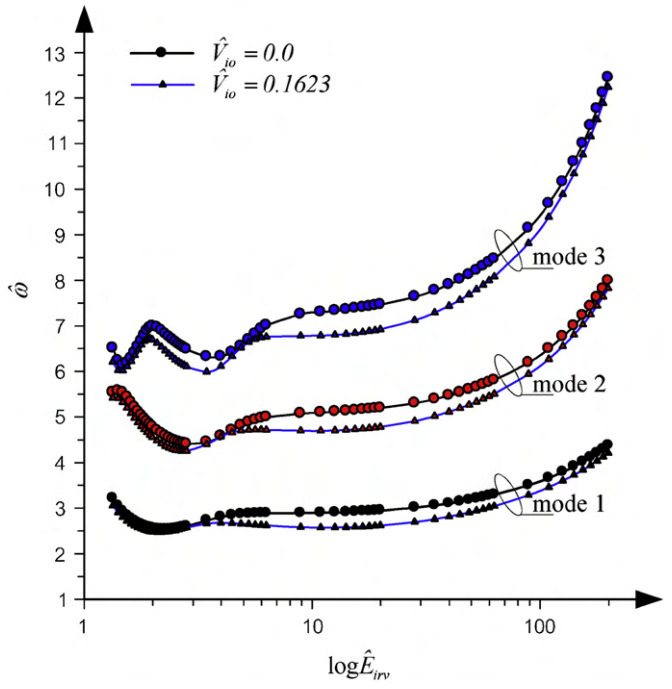

Fig. 7. Effect of axial extensibility on the in-plane natural frequencies of the extensible marine riser.

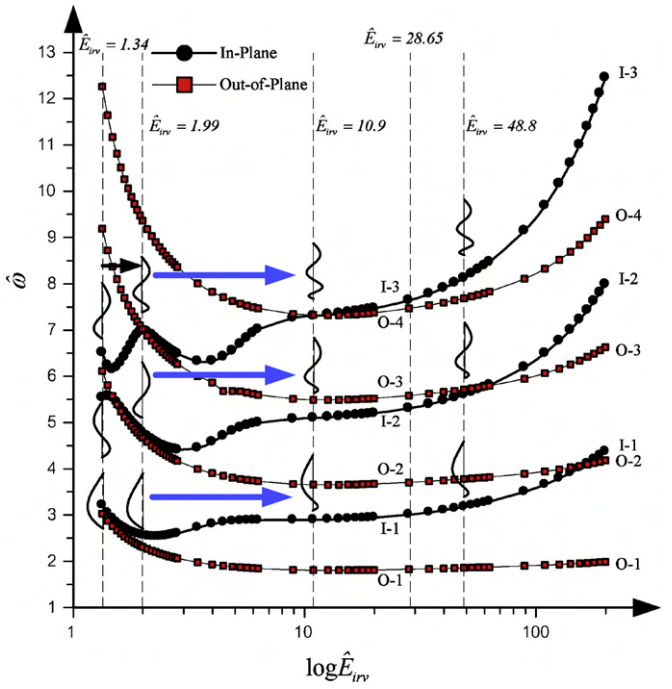

Fig. 8. Effect of axial extensibility on modal transition of the in-plane oscillation of the extensible marine riser.

increase in axial extensibility reduces the values of out-of-plane and in-plane natural frequencies when the bending stiffness domination ($\hat{E}_{irv} > 28.65$) as shown in Figs. 6 and 7. This result corresponds to the tensioned beam behavior (Hover and Triantafyllou, 1999). Moreover, the shape of in-plane oscillation does not change in this range.

On the contrary, the increase in axial extensibility increases the values of out-of-plane and in-plane natural frequencies when the pretensioned stiffness control ($\hat{E}_{irv} < 1.81$) as shown in Figs. 6 and 7. This result corresponds to the tensioned string behavior. In this range, the riser is very taut and the in-plane natural frequencies are close to the out-of-plane natural frequencies as shown in Fig. 8. Same as the three-dimensional marine cable (Chucheepsakul and Srinil, 2002), the fundamental natural frequencies of the marine riser represent the first mode of out-of-plane natural frequencies (Fig. 8).

In the transition state ($1.812 \leq \hat{E}_{irv} \leq 28.65$), the extensible riser behavior is changed from the tensioned beam to the tensioned string behavior (Russell and Lardner, 1998). The shapes of in-plane oscillation are changed by crossing from single curvature curve to double curvature curve of from two curvatures curve to three curvatures curve and so on as shown in Fig. 8. The avoided crossing of the extensible riser is occurred due to the hybrid mode formation between the in-plane oscillation and out-of-plane oscillation (Burgess and Triantafyllou, 1988).

5. Conclusions

The three-dimensional model formulation of the extensible marine riser is developed by variational approach based on the extensible elastica theory and the work–energy principle. The outstanding feature of the model formulation presented in this work is the use of independent variable α to provide the flexibility in the choice of parameters defining elastic curves. Therefore, the formulation allows users to select independent variable that is suitable for their applications.

Several of numerical examples are presented to verify the model formulation. The finite element method is used to obtain the

numerical solutions. The couple effect of axial extensibility and internal flow on maximum displacement and dynamic properties of three-dimensional marine riser are also investigated.

The results indicate that the strength of low extensibility riser is dominated by bending stiffness of marine riser. Consequently, the axial extensibility reduces the stability of the riser system. On the contrary, the strength of the high extensibility riser is dominated by the pretensioned stiffness. Therefore, the high extensibility riser performs the tensioned cable behavior, on which the axial extensibility increases the stability of the riser system. For the riser with moderate extensibility, the riser is in the transition state. In this state, the variation of riser extensibility could induce the avoided crossing of the in-plane mode shapes due to the hybrid mode formation between the in-plane and out-of-plane oscillation.

Acknowledgements

The authors gratefully acknowledge the financial support by the Thailand Research Fund (TRF) under Contract no. MRG5380034.

Appendix A

According to Eqs. (9)–(11), the variation of s',θ' and ϕ' can be expressed as follows:

$$\delta s' = \left(\frac{x'}{s'}\right)\delta u' + \left(\frac{y'}{s'}\right)\delta v' + \left(\frac{z'}{s'}\right)\delta w' \tag{A1}$$

$$\begin{aligned}\delta\theta' = {} & \left[\frac{1}{\kappa s'^2}\frac{\partial}{\partial\alpha}\left(\frac{x'}{s'}\right)\right]\delta u'' + \left[\frac{1}{\kappa s'^2}\frac{\partial}{\partial\alpha}\left(\frac{y'}{s'}\right)\right]\delta v'' + \left[\frac{1}{\kappa s'^2}\frac{\partial}{\partial\alpha}\left(\frac{z'}{s'}\right)\right]\delta w'' \\ & - \left[\frac{\kappa x'}{s'} + \frac{s''}{\kappa s'^3}\frac{\partial}{\partial\alpha}\left(\frac{x'}{s'}\right)\right]\delta u' - \left[\frac{\kappa y'}{s'} + \frac{s''}{\kappa s'^3}\frac{\partial}{\partial\alpha}\left(\frac{y'}{s'}\right)\right]\delta v' \\ & - \left[\frac{\kappa z'}{s'} + \frac{s''}{\kappa s'^3}\frac{\partial}{\partial\alpha}\left(\frac{z'}{s'}\right)\right]\delta w'\end{aligned} \tag{A2}$$

$$\begin{aligned}\delta\phi' = {} & \left[\frac{\tau x'}{s'} + \frac{s'}{\Im}(y''z''' - y'''z'') + \frac{2s'\tau}{\Im}((x''y' - x'y'')y'' + (x''z' - x'z'')z'')\right]\delta u' \\ & + \left[\frac{\tau y'}{s'} + \frac{s'}{\Im}(z''x''' - z'''x'') + \frac{2s'\tau}{\Im}((y''z' - y'z'')z'' + (y''x' - y'x'')x'')\right]\delta v' \\ & + \left[\frac{\tau z'}{s'} + \frac{s'}{\Im}(x''y''' - x'''y'') + \frac{2s'\tau}{\Im}((y''z' - y'z'')y'' + (x''z' - x'z'')x'')\right]\delta w' \\ & + \frac{s'}{\Im}\left[(z'y''' - y'z''') - 2(\tau)\{(x''y' - x'y'')y' + (x''z' - x'z'')z'\}\right]\delta u'' \\ & + \frac{s'}{\Im}\left[(x'z''' - z'x''') - 2(\tau)\{(y''z' - y'z'')z' - (x''y' - x'y'')x'\}\right]\delta v'' \\ & + \frac{s'}{\Im}\left[(y'x''' - x'y''') - 2(\tau)\{-(x''z' - x'z'')x' - (y''z' - y'z'')y'\}\right]\delta w'' \\ & + \frac{s'}{\Im}(y'z'' - z'y'')\delta u''' + \frac{s'}{\Im}(z'x'' - x'z'')\delta v''' + \frac{s'}{\Im}(x'y'' - y'x'')\delta w'''\end{aligned} \tag{A3}$$

where

$$\Im = (s')^6(\kappa)^2 \tag{A4}$$

Appendix B

The elements of shape function matrix are defined as follows:

$$N_{51} = 1 - 10\frac{y_s^3}{h^3} + 15\frac{y_s^4}{h^4} - 6\frac{y_s^5}{h^5} \tag{B1}$$

$$N_{52} = y_s - 6\frac{y_s^3}{h^2} + 8\frac{y_s^4}{h^3} - 3\frac{y_s^5}{h^4} \tag{B2}$$

$$N_{53} = \frac{y_s^2}{2} - \frac{3y_s^3}{2h} + \frac{3y_s^4}{2h^2} - \frac{y_s^5}{2h^3} \tag{B3}$$

$$N_{54} = 10\frac{y_s^3}{h^3} - 15\frac{y_s^4}{h^4} + 6\frac{y_s^5}{h^5} \tag{B4}$$

$$N_{55} = -4\frac{y_s^3}{h^2} + 7\frac{y_s^4}{h^3} - 3\frac{y_s^5}{h^4} \tag{B5}$$

$$N_{56} = \frac{y_s^3}{2h} - \frac{y_s^4}{h^2} + \frac{y_s^5}{2h^3} \tag{B6}$$

$$N_{11} = 1 - \frac{y_s}{h} \tag{B7}$$

$$N_{12} = \frac{y_s}{h} \tag{B8}$$

Appendix C

The element mass matrix is

$$[\mathbf{m}^e]_{24\times24} = \int_0^h \left\{ [N]_{24\times4}^T(s_s') \begin{bmatrix} m^* & 0 & 0 & 0 \\ 0 & m^* & 0 & 0 \\ 0 & 0 & m^* & 0 \\ 0 & 0 & 0 & \rho_p J_{Ps} \end{bmatrix} [N]_{4\times24} \right\} dy_s \tag{C1}$$

Note that, $m^* = m_{ps} + m_{is} + C_a m_{es}$

The element gyroscopic matrix is

$$[\mathbf{g}^e]_{24\times24} = \int_0^h \left\{ [N]_{24\times4}^T(m_{is}V_{is}) \begin{bmatrix} \left(2-\frac{x_s'^2}{s_s'^2}\right) & -\left(\frac{x_s'}{s_s'^2}\right) & -\left(\frac{x_s'z_s'}{s_s'^2}\right) & 0 \\ -\left(\frac{x_s'}{s_s'^2}\right) & \left(2-\frac{1}{s_s'^2}\right) & -\left(\frac{z_s'}{s_s'^2}\right) & 0 \\ -\left(\frac{x_s'z_s'}{s_s'^2}\right) & -\left(\frac{z_s'}{s_s'^2}\right) & \left(2-\frac{z_s'^2}{s_s'^2}\right) & 0 \\ 0 & 0 & 0 & 0 \end{bmatrix} [N']_{4\times24} \right\} dy_s \tag{C2}$$

The element stiffness matrix is

$$[\mathbf{k}^e]_{24\times24} = [_{b1}\mathbf{k}] + [_{b2}\mathbf{k}] + [_{N1}\mathbf{k}] + [_{N2}\mathbf{k}] + [_{T1}\mathbf{k}] + [_{T2}\mathbf{k}] \tag{C3}$$

in which the bending stiffness matrix of the fourth order derivative is

$$[_{b1}\mathbf{k}]_{24\times24} = \int_0^h \left\{ [N'']_{24\times4}^T \frac{B_s}{s_s'^5} \begin{bmatrix} (1+z_s'^2) & -(x_s') & -(x_s'z_s') & 0 \\ -(x_s') & (x_s'^2+z_s'^2) & -(z_s') & 0 \\ -(x_s'z_s') & -(z_s') & (x_s'^2+1) & 0 \\ 0 & 0 & 0 & 0 \end{bmatrix} [N'']_{4\times24} \right\} dy_s \tag{C4}$$

The bending stiffness matrix of the third order derivative is

$$[_{b2}\mathbf{k}]_{24\times24} = \int_0^h \left\{ [N']_{24\times4}^T(-1) \begin{bmatrix} {}_{b2}k_{11s} & {}_{b2}k_{12s} & {}_{b2}k_{13s} & 0 \\ {}_{b2}k_{21s} & {}_{b2}k_{22s} & {}_{b2}k_{23s} & 0 \\ {}_{b2}k_{31s} & {}_{b2}k_{32s} & {}_{b2}k_{33s} & 0 \\ 0 & 0 & 0 & 0 \end{bmatrix} [N'']_{4\times24} \right\} dy_s \tag{C5}$$

where

$${}_{b2}k_{11s} = \frac{B_s}{s_s'^7}[2x_s''x_s' + 2(x_s''z_s' - x_s'z_s'')x_s'z_s'] \tag{C6a}$$

$${}_{b2}k_{22s} = \frac{B_s}{s_s'^7}[2(-z_s'')z_s' - 2x_s''x_s'] \tag{C6b}$$

$$_{b2}k_{33s}=\frac{B_s}{s_s'7}[-2(x_s''z_s'-x_s'z_s'')x_s'z_s'-2(-z_s'')z_s'] \quad \text{(C6c)}$$

$$_{b2}k_{12s}=_{b2}k_{21s}=\frac{B_s}{s_s'7}\left[x_s''(1-x_s'^2)+(x_s''z_s'-x_s'z_s'')z_s'+(-z_s'')x_s'z_s'\right] \quad \text{(C6d)}$$

$$_{b2}k_{13s}=_{b2}k_{31s}=\frac{B_s}{s_s'7}\left[(x_s''z_s'-x_s'z_s'')(z_s'^2-x_s'^2)-(-z_s'')x_s'+x_s''z_s'\right] \quad \text{(C6e)}$$

$$_{b2}k_{23s}=_{b2}k_{32s}=\frac{B_s}{s_s'7}\left[(-z_s'')(z_s'^2-1)-(x_s''z_s'-x_s'z_s'')x_s'-x_s''x_s'z_s'\right] \quad \text{(C6f)}$$

The axial stiffness matrix of the second order derivative is

$$[_{N1}\mathbf{k}]_{24x24}=\int_0^h\left\{[N']_{24\times4}^T\left(\frac{N_{as}}{s_s'}-\frac{m_{is}V_{is}^2}{s_s'}\right)\begin{bmatrix}1&0&0&0\\0&1&0&0\\0&0&1&0\\0&0&0&0\end{bmatrix}[N']_{4\times24}\right\}dy_s$$
$$+\int_0^h\left\{[N']_{24\times4}^T\frac{EA_{ps}}{s_s'^3}\begin{bmatrix}x_s'^2&x_s'&x_s'z_s'&0\\x_s'&1&z_s'&0\\x_s'z_s'&z_s'&z_s'^2&0\\0&0&0&0\end{bmatrix}[N']_{4\times24}\right\}dy_s \quad \text{(C7)}$$

The axial stiffness matrix of the first order derivative is

$$[_{N2}\mathbf{k}]_{24\times24}=\int_0^h\left\{[N]_{24x4}^T\left(-\frac{m_{is}V_{is}V_{is}'}{s_s'}\right)\begin{bmatrix}1&0&0&0\\0&1&0&0\\0&0&1&0\\0&0&0&0\end{bmatrix}[N']_{4\times24}\right\}dy_s \quad \text{(C8)}$$

The torsional stiffness matrix of the fourth order derivative is

$$[_{T1}\mathbf{k}]_{24\times24}=\int_0^h\left\{[N']_{24\times4}^T\begin{bmatrix}_{T1}k_{11s}&_{T1}k_{12s}&_{T1}k_{13s}&0\\_{T1}k_{21s}&_{T1}k_{22s}&_{T1}k_{23s}&0\\_{T1}k_{31s}&_{T1}k_{32s}&_{T1}k_{33s}&0\\0&0&0&0\end{bmatrix}[N''']_{4\times24}\right\}dy_s \quad \text{(C9)}$$

The torsional stiffness matrix of the second order derivative is

$$[_{T2}\mathbf{k}]\int_{y_s}\left\{[N']_{24\times4}^T\begin{bmatrix}0&0&0&_{T2}k_{14s}\\0&0&0&_{T2}k_{24s}\\0&0&0&_{T2}k_{34s}\\_{T2}k_{41s}&_{T2}k_{42s}&_{T2}k_{43s}&_{T2}k_{44s}\end{bmatrix}[N']_{4\times24}\right\}dy_s \quad \text{(C10)}$$

where

$$_{T1}k_{11s}=\frac{C_sz_s'^2}{s_s'9\kappa_s^2},\quad _{T1}k_{22s}=\frac{C_s}{s_s'^9\kappa_s^2}(z_s'x_s''-x_s'z_s'')^2,\quad _{T1}k_{33s}=\frac{C_sx_s''^2}{s_s'^9\kappa_s^2} \quad \text{(C11a–c)}$$

$$_{T1}k_{12s}=_{T1}k_{21s}=\frac{C_s}{s_s'^9\kappa_s^2}z_s''(z_s'x_s''-z_s''x_s') \quad \text{(C11d)}$$

$$_{T1}k_{13s}=_{T1}k_{31s}=\frac{C_s}{s_s'^9\kappa_s^2}(-x_s''z_s'') \quad \text{(C11e)}$$

$$_{T1}k_{23s}=_{T1}k_{32s}=\frac{C_s}{s_s'^9\kappa_s^2}(z_s'x_s''-z_s''x_s')(-x_s'') \quad \text{(C11f)}$$

$$_{T2}k_{14s}=\frac{C_sz_s''}{s_s'^4},\quad _{T2}k_{24s}=\frac{C_s}{s_s'^4}(z_s'x_s''-z_s''x_s'),\quad _{T2}k_{34s}=\frac{C_s(-x_s'')}{s_s'^4} \quad \text{(C11g–i)}$$

$$_{T3}k_{41s}=0,\quad _{T3}k_{42s}=C_s\left[\frac{z_s''x_s'''-x_s''z_s'''}{s_s'^6\kappa_s^2}\right],\quad _{T3}k_{43s}=0,\quad _{T2}k_{44s}=\frac{C_s}{s_s'} \quad \text{(C11j–m)}$$

References

Athisakul, C., Chucheepsakul, S., 2008. Effect of inclination on bending of variable-arc-length beams subjected to uniform self-weight. Engineering Structures 30 (4), 902–908.

Bernitsas, M.M., 1982. A three-dimensional nonlinear large-deflection model for dynamic behavior of risers, pipelines, and cables. Journal of Ship Research 26 (1), 59–64.

Bernitsas, M.M., Kokarakis, J.E., Imron, A., 1985. Large deformation three-dimensional static analysis of deep water marine risers. Applied Ocean Research 7 (4), 178–187.

Bernitsas, M.M., Kokarakis, J.E., 1988. Importance of nonlinearities in static riser analysis. Applied Ocean Research 10 (1), 2–9.

Burgess, J.J., Triantafyllou, M.S., 1988. The elastic frequencies of cables. Journal of Sound and Vibration 120, 153–165.

Burke, B.G., 1974. An analysis of marine risers for deep water. Journal of Petroleum Technology 14, 455–465.

Chai, Y.T., Varyani, K.S., Barltrop, N.D.P., 2002. Three-dimensional lump-mass formulation of a catenary riser with bending, torsion, and, irregular seabed interaction effect. Ocean Engineering 29, 1503–1525.

Chai, Y.T., Varyani, K.S., 2006. An absolute coordinate formulation for three-dimensional flexible pipe analysis. Ocean Engineering 33, 23–58.

Chucheepsakul, S., Monprapussorn, T., Huang, T., 2003. Large strain formulations of extensible flexible marine pipes transporting fluid. Journal of Fluids and Structures 17 (2), 185–224.

Chucheepsakul, S., Srinil, N., 2002. Free vibrations of three-dimensional extensible cables with specified top tension via a variational method. Ocean Engineering 29, 1067–1096.

Dareing, D.W., Huang, T., 1979. Marine riser vibration response determined by modal analysis. Journal of Energy Resources Technology, ASME 101 (3), 159–166.

Felippa, C.A., Chung, J.S., 1981. Nonlinear static analysis of deep ocean mining pipe—part 1: modeling and formulation. Journal of Energy Resources Technology, ASME 103 (1), 11–15.

Fischer, W., Ludwig, M., 1966. Design of floating vessel drilling risers. Journal of Petroleum Technology 3 (1), 272–283.

Gosse, C.G., Barksdale, G.L., 1969. The marine riser a procedure for analysis. Offshore Technology Conference, vol. 1, pp. 1080–1085.

Henghold, W.M., Russell, J.J., Morgan, J.D., 1977. Free vibrations of cables in three dimensions. Journal of Structural Division, ASME 103 (ST5), 1127–1136.

Hover, F.S., Triantafyllou, M.S., 1999. Linear dynamics of curved tensioned elastic beams. Journal of Sound and Vibration 228, 923–930.

Huang, T., 1993. Kinematics of transported mass inside risers and pipes. In: Proceeding of the 3rd International Offshore and Polar Engineering Conference, vol. 2, pp. 331–336.

Huang, T., Kang, Q.L., 1991. Three dimensional analysis of a marine riser with large displacements. International Journal of Offshore and Polar Engineering 1 (4), 300–306.

Kirk, C.L., Etok, E.U., Cooper, M.T., 1979. Dynamic and static analysis of a marine riser. Applied Ocean Research 1 (3), 95–105.

Kokarakis, J.E., Bernitsas, M.M., 1987. Nonlinear three-dimensional dynamic analysis of marine risers. Journal of Energy Resources Technology, ASME 109 (5), 105–111.

Meirovitch, L., 1997. Principles and Techniques of Vibrations. Prentice-Hall, New Jersey.

Moe, G., Chucheepsakul, S., 1988. The effect of internal flow on marine risers. In: Proceedings of the 7th International Offshore Mechanics and Arctic Engineering Symposium, vol. 1, pp. 375–382.

Monprapussorn, T., Athisakul, C., Chucheepsakul, S., 2007. Nonlinear vibrations of an extensible flexible marine riser carrying a pulsatile flow. Journal of Applied Mechanics, ASME 74, 754–769.

Monprapussorn, T., Chucheepsakul, S., Huang, T., 2004. The coupled radial-axial deformation analysis of flexible pipes conveying fluid. International Journal of Numerical Methods in Engineering 59 (11), 1399–1452.

Morgan, G.W., 1972. Riser Dynamic Analysis. Sun Oil Production Research Laboratory, Texas.

NESCO Report, 1965. Structural dynamic analysis of the riser and drill string for project mohole, National Engineering and Science Company.

Russell, J.C., Lardner, T.J., 1998. Experimental determination of frequencies and tension for elastic cables. Journal of Engineering Mechanics, ASCE 124, 1067–1072.

Smith, B.T., Boyle, J.M., Dongarra, J.J., Garbow, B.S., Ikebe, Y., Klema, V.C., Moler, C.B., 1976. Matrix Eigensystem Routines—EISPACK Guide. Springer-Verlag, New York.

Young, R.D., Fowler, J.R., Fisher, E.A., Luke, R.R., 1978. Dynamic analysis as an aid to the design of marine risers. Journal of Pressure Vessel Technology, ASME 100, 200–205.

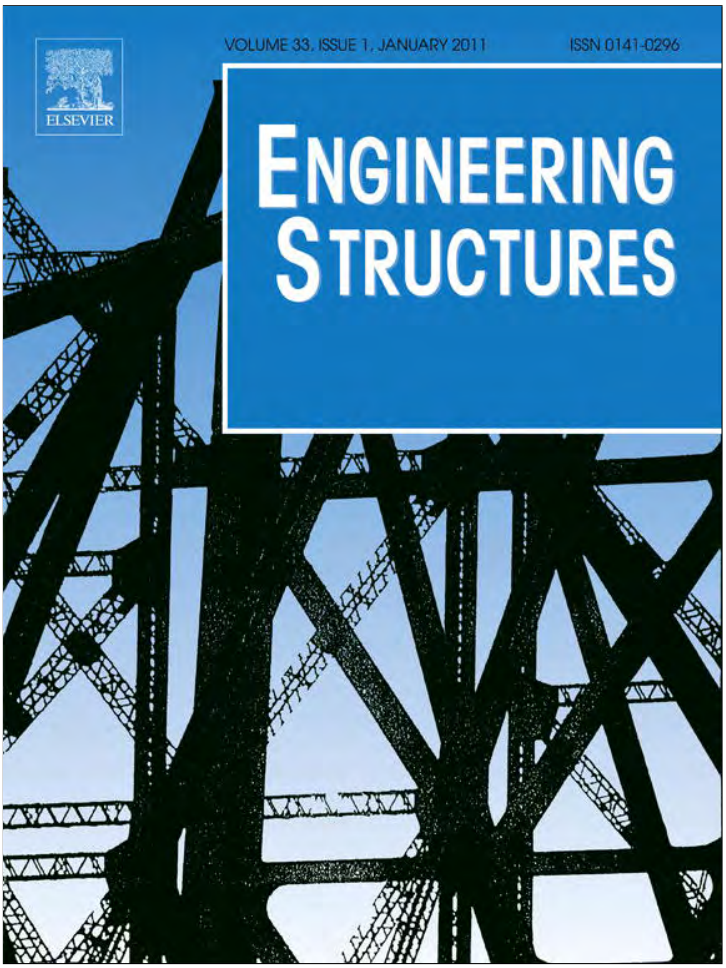

(This is a sample cover image for this issue. The actual cover is not yet available at this time.)

Engineering Structures 34 (2012) 271–277

Contents lists available at SciVerse ScienceDirect

Engineering Structures

journal homepage: www.elsevier.com/locate/engstruct

Static equilibrium configurations and appropriate applied top tension of extensible marine riser with specified total arc-length using finite element method

Chainarong Athisakul, Thongchai Phanyasahachart, Karun Klaycham, Somchai Chucheepsakul *

Department of Civil Engineering, Faculty of Engineering, King Mongkut's University of Technology Thonburi, Bangkok 10140, Thailand

ARTICLE INFO

Article history:
Received 11 November 2010
Revised 15 August 2011
Accepted 19 August 2011

Keywords:
Extensible marine riser
Applied top tension
Constraint condition
Lagrange multipliers
Static configurations
Finite element method

ABSTRACT

This paper presents a finite element method for calculating the static equilibrium configurations and applied top tension of extensible marine riser with specified total arc-length. A variational formulation of an extensible marine riser is formulated based on the work-energy principle. The variational model formulation involves strain energy due to bending and axial stretching, and virtual work done by hydrostatic pressures and other external forces. The total unstretched arc-length of marine riser is specified while the top tension is not yet exactly known at the equilibrium position. A Lagrange multiplier is introduced in order to impose the constraint condition, which is the specified total arc-length of the riser. The system unknowns are composed of the nodal degrees of freedom and the Lagrange multiplier. The system of nonlinear finite element equations is derived based on the finite element procedure. The numerical solutions of the nonlinear system are obtained by the iterative method. The results show that the Lagrange multiplier is identified as the parameter for adjusting the top tension to a proper value that satisfies the constraint condition.

1. Introduction

At present, the technologies for exploration and production of oil and gas in the ultra-deep water has currently been developed. One of a key component for offshore production is the marine riser. As the water depth for offshore operations is increasing, the riser system becomes more important. A failure of the riser system causes not only the severe environmental pollutions but also the significant financial consequences. Therefore, the appropriate applied top tension corresponding to the riser configuration has to be determined with more degree of accuracy.

In general, the riser is a long slender vertical structure connecting between the floating production facility and subsea wellhead. Therefore, the riser behaves like a flexible structure which can be experienced large displacement. Since this problem is highly nonlinear, the nonlinear analysis technique is required. The nonlinear analysis method of flexible structure has been developed continuously over the past 50 years as found in literature [1–4].

Felippa and Chung [5,6] presented a static analysis procedure for determination of nonlinear static equilibrium configurations of marine riser. They modeled the riser as the three-dimensional beam elements. The numerical solutions were obtained by using the incremental load iterative procedure. McNamara et al. [7] used the hybrid finite elements, which the axial force is independently interpolated and combined with the corresponding axial displacements, for static and dynamic analysis of flexible risers. Moe and Arntsen [8] proposed an analytic model for static analysis of catenary risers. The particular three-dimensional model formulations and analysis techniques for deep water riser have been developed by several investigators [9–15]. The development of flexible riser modeling and analysis techniques was reviewed by Patel and Seyed [16].

Most of research works mentioned above assumed that the total length of riser is constant, therefore the total arc-length of the riser is normally discretized to be a finite length and the riser configurations are determined along the arc-length of riser. However, in most cases, the top end of the riser can slip through the slip joint. Consequently, the total stretched arc-length of the riser measured from the seabed to the slip joint may not be known until the equilibrium configuration is evaluated. Therefore, the use of the unstretched arc-length to be the independent variable may not convenient to set up the boundary condition at the slip joint.

In order to reduce the complexity of the problem discussed above, the vertical distance is used as the independent variable instead of the unstretched arc-length [17]. This technique eliminates a number of iterations that are required to adjust the total unstretched arc-length until the boundary conditions at the top end are satisfied. Moreover, in finite element analysis, the

* Corresponding author. Tel.: +66 2 470 9146; fax: +66 2 427 9063.
E-mail address: somchai.chu@kmutt.ac.th (S. Chucheepsakul).

0141-0296/$ - see front matter © 2011 Elsevier Ltd. All rights reserved.
doi:10.1016/j.engstruct.2011.08.031

discretization of the riser elements along the arc-length requires more nodal variables than the discretization along the sea depth [18]. Some other examples of research works, which were adopted this technique for large displacement analysis, can be found in Huang and Kang [19], Chucheepsakul et al. [20], Athisakul et al. [21–23], Monprapussorn et al. [24,25], and Kaewunruen et al. [26].

For the case of the applied top tension is specified, the discretization along the sea depth (y_s) is suitable for the numerical solutions. The stretched arc-length and unstretched arc-length can be easily found by direct integration along the vertical coordinate of the riser configurations. On the contrary, if the unstretched arc-length is specified, the applied top tension will be adjusted to satisfy the equilibrium and boundary conditions. A trial error in estimating the proper value of the applied top tension may be used, but it is a time consuming process. A better approach to solve this constraint problem is to use the Lagrange multiplier method.

The purpose of this paper is to present the finite element method for large displacement and large deformation analysis of marine riser with a constraint condition (a specified total unstretched arc-length). The model formulation is developed by using the variational approach. The strain energy due to bending, axial stretching and virtual work done by hydrostatic pressure and other external forces are involved in the variational model. A Lagrange multiplier is introduced in order to impose the constraint condition. The numerical examples are provided to explain the physical meaning of the Lagrange multiplier. The relations between the top tension and the unstretched arc-length in different water depth and static offset are investigated herein.

2. Strain–displacement relations

The marine riser configurations and the infinitesimal elements of marine riser in three states of the riser configurations are depicted in Fig. 1. The parameters ds_o, ds_s, and ds represent the differential arc-lengths at undeformed, equilibrium, and displaced configurations, respectively.

According to the updated Lagrangian description, the motions and deformations of riser body are described with respect to the equilibrium position. Therefore, the definition of the total axial strain, static strain, and dynamic strain can be defined as shown in Table 1.

Based on the differential geometry of curve in plane, the differential arc-lengths in three states of the riser configurations can be defined as follows.

At the undeformed state, the differential arc-length is defined by

$$ds_o = \sqrt{x_o'^2 + y_o'^2}\,d\alpha = (1-\varepsilon_s)\sqrt{x_s'^2 + y_s'^2}\,d\alpha \tag{1}$$

at the equilibrium state, the differential arc-length is defined by

$$ds_s = \sqrt{x_s'^2 + y_s'^2}\,d\alpha = \sqrt{(x_o' + u_s')^2 + (y_o' + v_s')^2}\,d\alpha \tag{2}$$

and at the displaced state, the differential arc-length is defined by

$$\begin{aligned} ds &= \sqrt{x'^2 + y'^2}\,d\alpha = \sqrt{(x_s' + u')^2 + (y_s' + v')^2}\,d\alpha \\ &= (1+\varepsilon_d)\sqrt{x_s'^2 + y_s'^2}\,d\alpha \end{aligned} \tag{3}$$

where u and v represent the displacement in x and y directions, respectively. The subscript (o) refers to the undeformed position. The subscript (s) denotes the static equilibrium position. The superscript ($'$) represents the derivative of the parameter with respect to the independent variable α.

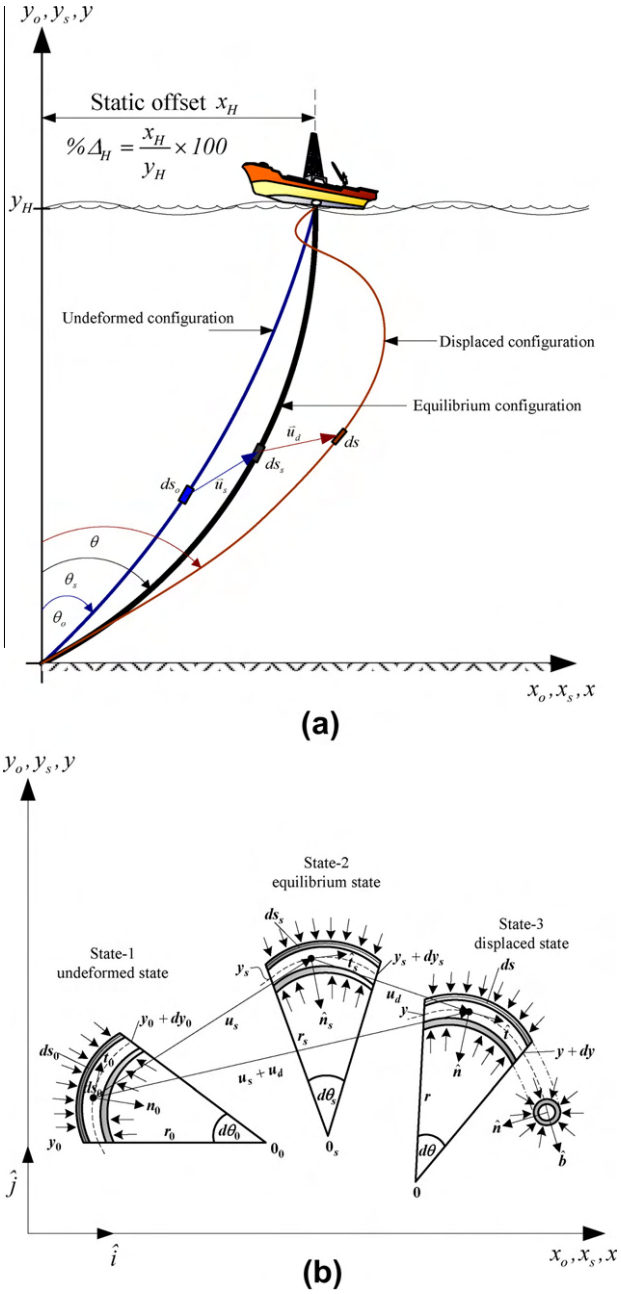

Fig. 1. (a) Three states of marine riser configurations. (b) The infinitesimal elements of marine riser in three states.

Table 1
Definition of the axial strains at each state.

Total strain (1–3)	Static strain (1–2)	Dynamic strain (2–3)
$\varepsilon_t = \frac{ds - ds_0}{ds_s}$	$\varepsilon_s = 1 - \frac{ds_o}{ds_s}$	$\varepsilon_d = \frac{ds}{ds_s} - 1$

3. Variational model

The model formulation used in this study is developed by variational approach. Theoretically, the strain energy includes those contributions from axial deformation and bending deformation. The external virtual work of the riser system is composed of the virtual works done by the effective weight, hydrodynamic loading and inertial forces of the riser mass and the transported fluid mass. These expressions can be shown briefly in the following subtopics.

3.1. Strain energy due to axial deformation

Based on the updated Lagrangian description, the strain energy due to axial deformation of the apparent system of the riser is

$$U_a = \int_0^{s_t} \frac{EA_s\varepsilon_t^2}{2} ds_s \tag{4}$$

Since the riser is a submerged structure, the effect of pressure fields from external and internal fluid has to be considered [18,27–28]. Based on theory of elasticity, the total axial strain $(\varepsilon_t)$for elastic isotropic riser can be expressed in terms of the true wall tension (T) and fluid pressures by Eq. (5).

$$\varepsilon_t = \frac{1}{EA_{ps}}[T + 2v(p_eA_{es} - p_iA_{is})] \tag{5}$$

According to Eq. (5), the apparent tension can be defined by

$$T_{as} = \underbrace{T}_{1} + \underbrace{2v(p_eA_{es} - p_iA_{is})}_{2} = EA_{ps}\varepsilon_t \tag{6}$$

The effect of fluid pressures on the riser is deduced by the second term of Eq. (6), where A_{es} is the outside cross-sectional area of the riser, A_{is} is the inside cross-sectional area of the riser, A_{ps} is the cross sectional area of the risers $(A_{ps} = A_{es} - A_{is})$, p_e represents the external fluid pressure, p_i represents the internal fluid pressure, and v is the Poisson's ratio. In case of $v = 0.5$, the apparent tension is identical to the effective tension [27]. The concept of apparent tension is a convenient mathematical technique for grouping the fluid pressures into the axial tension. Eq. (6) shows that the external fluid pressure induces the axial tension, while the internal fluid pressure induces the axial compression.

By taking the first variation to Eq. (4) and adopting the Eq. (6), one obtains the virtual strain energy due to axial deformation as shown below.

$$\delta U_a = \int_{\alpha_o}^{\alpha_t} \left[T_{as}\frac{x_s'}{s_s'}\delta u_s' + T_{as}\frac{y_s'}{s_s'}\delta v_s'\right] d\alpha \tag{7}$$

3.2. Strain energy due to bending

According to the updated Lagrangian description, the strain energy due to bending can be expressed as

$$U_b = \int_0^{s} \frac{M^2}{2EI_{Ps}} ds_s \tag{8}$$

Based on the elastica theory of extensible risers/pipes [18], the moment–curvature relation of the riser system can be written in the following form:

$$M = EI_{Po}(1 + \varepsilon_s)\kappa \tag{9}$$

By substituting Eq. (9) into Eq. (8), one obtains

$$U_b = \int_0^{s_t} \frac{1}{2} EI_{Po}\kappa^2(1 + \varepsilon_s)^2 ds_s \tag{10}$$

The virtual strain energy due to bending is derived by taking a first variation of Eq. (10) and changing variable ds_s to be $d\alpha$. The virtual strain energy due to bending can be written as

$$\delta U_b = \int_{\alpha_o}^{\alpha_t} M\delta\theta' d\alpha \tag{11}$$

According to the differential geometry of curve, the curvature and the derivative of the angle θ, which is the angle between the displacement curve and y-axis (see Fig. 1), can be expressed in Cartesian coordinate as follows.

$$\kappa = \frac{\theta'}{s'} = \frac{(x''y' - x'y'')}{s'^3} \tag{12}$$

$$\theta' = \frac{(x''y' - x'y'')}{s'^2} \tag{13}$$

The relations between the Cartesian coordinates and the angle θ are

$$\frac{x'}{s'} = \sin\theta, \text{ and } \frac{y'}{s'} = \cos\theta \tag{14}$$

By substituting Eqs. (9), (12), and (13) into Eq. (11) and setting the subscribe variables to be the static equilibrium state, one obtains

$$\begin{aligned}\delta U_b = \int_{\alpha_o}^{\alpha_t} \Bigg\{ & \frac{B_s\kappa_s}{s_s'}\left(\frac{y_s'}{s_s'}\right)\delta u_s'' \\ & + \left[-B_s\kappa_s^2\left(\frac{x_s'}{s_s'}\right) - B_s\kappa_s\frac{s_s''}{s_s'^2}\left(\frac{y_s'}{s_s'}\right)\right]\delta u_s' - \frac{B_s\kappa_s}{s_s'}\left(\frac{x_s'}{s_s'}\right)\delta v_s'' \\ & + \left[-B_s\kappa_s^2\left(\frac{y_s'}{s_s'}\right) + B_s\kappa_s\frac{s_s''}{s_s'^2}\left(\frac{x_s'}{s_s'}\right)\right]\delta v_s'\Bigg\} d\alpha\end{aligned} \tag{15}$$

where $B_s = EI_{po}(1 + \varepsilon_s)$ is the bending rigidity of the riser.

3.3. Work done by apparent weight

The virtual work done by the apparent weight of the riser can be expressed as

$$\delta W_w = -\int_0^{s_t} w_a\delta v_s ds = -\int_{\alpha_o}^{\alpha_t} \frac{w_a s_s'}{1 + \varepsilon_s}\delta v_s d\alpha \tag{16}$$

According to the apparent tension concept, the real system of the submerged riser subjected to external and internal fluid pressures is equivalent to the apparent system of the riser in the air that is subjected to the apparent tension and the apparent weight [18].

The apparent weight per unit length of the riser can be defined as

$$w_a = [\rho_pA_{ps} - \rho_eA_{es} + \rho_iA_{is}]g \tag{17}$$

where ρ_p is the density of the riser, ρ_e is the density of the external fluid/sea water, ρ_i is the density of the internal fluid. It is noted that the outside cross-sectional area of the riser A_{es} can be represented as the cross-sectional area of the external fluid column. In the same manner, the inside cross-sectional area of the riser A_{is} can be represented as the cross-sectional area of the internal fluid column.

3.4. Work done by current force

The current force per unit length is composed of two components. The component in normal direction can be expressed in the following form.

$$f_{Hn} = \frac{1}{2}\rho_eD_eC_{Dn}V_{Hn}^2 \tag{18}$$

The component in tangential direction is given by

$$f_{Ht} = \frac{1}{2}\rho_e\pi D_eC_{Dt}V_{Ht}^2 \tag{19}$$

where D_e is the outside diameter of the riser, V_{Ht} and V_{Hn} are the current velocities in tangential and normal directions, C_{Dn} and C_{Dt} are the normal drag and tangential drag coefficients, respectively. The virtual work done by hydrodynamic force can be expressed as follows:

$$\delta W_H = \int_{\alpha_o}^{\alpha_t} [(f_{Hn}y_s' + f_{Ht}x_s')\delta u_s + (-f_{Hn}x_s' + f_{Ht}y_s')\delta v_s] d\alpha \tag{20}$$

3.5. Work done by inertial forces

Based on the Newton's second law, the inertial force from internal flow velocity is defined as

$$\vec{F} = -\int_{\alpha_o}^{\alpha_t} m_i \vec{a}_i s'_s d\alpha \tag{21}$$

in which the transported fluid mass per unit length at the equilibrium state is $m_i = \rho_i A_{is}$. The virtual work done by inertial force of transporting fluid can be expressed as:

$$\delta W_I = -\int_{\alpha_o}^{\alpha_t} [(m_i a_{ix}) s'_s \delta u_s + (m_i a_{iy}) s'_s \delta v_s] d\alpha \tag{22}$$

By considering the kinematics of transported mass in the moving frame [29], the acceleration of the fluid inside the riser can be expressed in terms of the riser's displacements and the speed of the transported fluid as shown below.

$$a_{ix} = \left(\frac{\kappa_s y'_s}{s'_s}\right) V_i^2 \tag{23}$$

$$a_{iy} = -\left(\frac{\kappa_s x'_s}{s'_s}\right) V_i^2 \tag{24}$$

where V_i is the speed of the internal fluid.

3.6. Total virtual work equation

Based on the virtual work principle, the total virtual work-energy of the riser system is

$$\delta\pi = (\delta U_a + \delta U_b) - (\delta W_w + \delta W_H + \delta W_I) \tag{25}$$

By substituting Eqs. (7), (15), (16), (20), and (22) into Eq. (25), one obtains the total virtual work equation as shown below.

$$\begin{aligned}\delta\pi = &\int_{\alpha_o}^{\alpha_t} \left\{\frac{B_s\kappa_s}{s'_s}\left(\frac{y'_s}{s'_s}\right)\delta u''_s + \left[(T_{as} - B_s\kappa_s^2)\left(\frac{x'_s}{s'_s}\right) - B\kappa\frac{s''}{s_s'^2}\left(\frac{y'_s}{s'_s}\right)\right]\delta u'_s\right\} d\alpha \\ &+ \int_{\alpha_o}^{\alpha_t} \left\{-\frac{B_s\kappa_s}{s'_s}\left(\frac{x'_s}{s'_s}\right)\delta v''_s + \left[(T_{as} - B_s\kappa_s^2)\left(\frac{y'_s}{s'_s}\right) + B_s\kappa_s\frac{s''_s}{s_s'^2}\left(\frac{x'_s}{s'_s}\right)\right]\delta v'_s\right\} d\alpha \\ &+ \int_{\alpha_o}^{\alpha_t} -\left[f_{Hn}y'_s + f_{Ht}x'_s - m_i\kappa_s y'_s V_i^2\right]\delta u_s d\alpha \\ &+ \int_{\alpha_o}^{\alpha_t} -\left[-\frac{w_a s'_s}{1+\varepsilon_s} - f_{Hn}x'_s + f_{Ht}y'_s + m_i\kappa_s x'_s V_i^2\right]\delta v_s d\alpha\end{aligned} \tag{26}$$

Eq. (26) is used for calculating the static equilibrium configuration of marine riser. This equation is suitable for the case of the applied top tension is specified and the total unstretched arc-length of riser is an unknown. The unstretched arc-length of the riser depends on the coordinate of the riser configuration and it can be determined by integrating Eq. (1).

In the case of the unstretched arc-length is specified, the top tension that is sufficient to maintain the equilibrium of riser is an unknown. The assumed top tension may be guessed and then adjust the value until the arc-length reaches to the specified value. However, this method is not efficient for numerical computation. Therefore, a better technique, which is the Lagrange multiplier method, is used.

Table 2
Properties of the riser used in the numerical analysis.

Property	Value
Outside diameter	0.26 m
Inside diameter	0.20 m
Offset of the top end ($\%\Delta_H$)	5–40%
Density of riser	7850 kg/m^3
Density of sea water	1025 kg/m^3
Density of internal fluid	998 kg/m^3
Young's modulus	2.07×10^{11} N/m^2

Table 3
Numerical results of the deep water riser for water depth of 900 m, 10% offset, and the specified top tension of 1500 kN.

Top tension (kN)	1500
Unstretched total arc-length (m)	906.05
Stretched total arc-length (m)	906.23
Top angle (degree)	2.46
Bottom angle (degree)	17.10

3.7. Constraint equation

According to Eq. (1), the total unstretched arc-length of the riser can be calculated as shown below.

$$\int_{\alpha_o}^{\alpha_t} ds_o = \int_{\alpha_o}^{\alpha_t} \left\{(1-\varepsilon_s)\sqrt{y_s'^2 + x_s'^2}\right\} d\alpha = S_{\text{total}} \tag{27}$$

In the procedure, a Lagrange multiplier is introduced in the constraint condition. When the value of unstretched arc-length (S_{total}) is specified, this introduces the constraint condition which is written as

$$g = \int_{\alpha_o}^{\alpha_t} \left\{(1-\varepsilon_s)\sqrt{y_s'^2 + x_s'^2}\right\} d\alpha - S_{total} = 0 \tag{28}$$

3.8. Modified total virtual work equation

Based on the virtual work principle, the total virtual work of the riser system is equal to zero when the riser system is in equilibrium. Therefore, Eq. (26) has to be minimized to zero with the constraint Eq. (28). According to the Lagrange multiplier technique [30], the unknown variable λ is added to the system and the total virtual work equation is modified as follows.

$$\delta\pi^* = \delta\pi + \delta(\lambda g) \tag{29}$$

where $\delta\pi^*$ is the modified total virtual work. After performing variation of the second term in Eq. (29), one obtains

$$\begin{aligned}\delta\pi^* = &\int_{\alpha_o}^{\alpha_t} \left\{\frac{B_s\kappa_s}{s'_s}\left(\frac{y'_s}{s'_s}\right)\delta u'' + \left[(T_{as} - B_s\kappa_s^2)\left(\frac{x'_s}{s'_s}\right) - B\kappa\frac{s''}{s_s'^2}\left(\frac{y'_s}{s'_s}\right)\right]\delta u'_s\right\} d\alpha \\ &+ \int_{\alpha_o}^{\alpha_t} \left\{-\frac{B_s\kappa_s}{s'_s}\left(\frac{x'_s}{s'_s}\right)\delta v''_s + \left[(T_{as} - B_s\kappa_s^2)\left(\frac{y'_s}{s'_s}\right) + B_s\kappa_s\frac{s''_s}{s_s'^2}\left(\frac{x'_s}{s'_s}\right)\right]\delta v'_s\right\} d\alpha \\ &+ \int_{\alpha_o}^{\alpha_t} -\left[f_{Hn}y'_s + f_{Ht}x'_s - m_i\kappa_s y'_s V_i^2\right]\delta u_s d\alpha \\ &+ \int_{\alpha_o}^{\alpha_t} -\left[-\frac{w_a s'_s}{1+\varepsilon_s} - f_{Hn}x'_s + f_{Ht}y'_s + m_i\kappa_s x'_s V_i^2\right]\delta v_s d\alpha \\ &+ \int_{\alpha_o}^{\alpha_t} \left\{\lambda(1-\varepsilon_s)\left[\left(\frac{x'_s}{s'_s}\right)\delta u'_s + \left(\frac{y'_s}{s'_s}\right)\delta v'_s\right]\right\} d\alpha \\ &+ \left(\int_{\alpha_o}^{\alpha_t} \left\{(1-\varepsilon_s)\sqrt{x_s'^2 + y_s'^2}\right\} d\alpha - S_{\text{total}}\right)\delta\lambda\end{aligned} \tag{30}$$

4. The finite element method

In this study, the nonlinear static solutions can be evaluated by using the finite element method. Based on the finite element pro-

Table 4
Numerical results of the deep water riser for water depth of 900 m, 10% offset, and the specified unstretched arc-length of 910 m.

The assumed top tension (kN)	1500
The Lagrange multiplier λ	−152.77
Unstretched total arc-length (m)	910.00
Stretched total arc-length (m)	910.14
Top angle (degree)	1.63
Bottom angle (degree)	32.66

cedures, the range of the total sea depth is divided into n elements. The sea water level (y_s) is used as an independent variable (α), therefore $\delta v = \delta v' = \delta v'' = 0$. Consequently, then the modified total virtual work equation (Eq. (30)) becomes

$$\delta\pi^* = \int_0^{y_H} \left\{ \frac{B_s\kappa_s}{s_s'^2}\delta u_s'' + \left[\frac{T_{as}x_s'}{s_s'} - 2\frac{B_s\kappa_s x_s'' x_s'}{s_s'^4}\right]\delta u_s' \right\} dy_s + \int_0^{y_H} -\left[f_{Hn} + f_{Ht}x_s' - m_i\kappa_s V_i^2\right]\delta u_s dy_s + \int_0^{y_H} \left\{ \frac{\lambda(1-\varepsilon_s)x_s'}{s_s'}\delta u_s' \right\} dy_s + \left(\int_0^{y_H} \left\{ (1-\varepsilon_s)\sqrt{1+x_s'^2} \right\} dy_s - S_{total} \right)\delta\lambda \tag{31}$$

The large displacement of the riser (x_s) is composed of two components. First is the linear component (x_{sl}), which can be directly calculated by linear interpolation. Second is the nonlinear component (u_s), which is approximated by the fifth degree polynomial. Hence, the large displacement of the riser can be written as shown below.

$$x_s = x_{sl} + u_s \tag{32}$$

$$u_s = [N_s]\{d_i\} \tag{33}$$

A matrix $[N_s]$ contains the fifth order shape function and a vector $\{d_i\}$ contains the nodal displacements of the riser element.

$$\{d_i\}^T = \{u_{1s}\ u_{1s}'\ u_{1s}''|u_{2s}\ u_{2s}'\ u_{2s}''\} \tag{34}$$

According to the virtual work principle, Eq. (31) is equal to zero for equilibrium position. Therefore,

$$\delta\pi^* = \left(\frac{\partial\pi^*}{\partial d_i}\right)\delta d_i + \left(\frac{\partial\pi^*}{\partial\lambda}\right)\delta\lambda = 0 \tag{35}$$

Since δd_i and $\delta\lambda$ are not equal to zero, thus

$$\left(\frac{\partial\pi^*}{\partial d_i}\right) = \int_0^{y_H} \left\{ \frac{[N'']^T B_s\kappa_s}{s_s'^2} + [N']^T\left[\frac{T_{as}x_s'}{s_s'} - 2\frac{B_s\kappa_s x_s'' x_s'}{s_s'^4}\right] \right\} dy_s - \int_0^{y_H} [N]^T\left(f_{Hn} + f_{Ht}x_s' - \rho_i A_{is}\kappa_s V_i^2\right) dy_s + \int_0^{y_H} \left\{ [N']^T\left(\frac{\lambda(1-\varepsilon_s)x_s'}{s_s'}\right) \right\} dy_s = 0 \tag{36}$$

$$\left(\frac{\partial\pi^*}{\partial\lambda}\right) = \left(\int_0^{y_H} (1-\varepsilon_s)\sqrt{1+x_s'^2}\, dy_s - S_{total} \right) = 0 \tag{37}$$

Because Eqs. (36) and (37) are the system of nonlinear equations, the iterative procedure is used to obtain the numerical solutions. According to Taylor's series approximation, Eqs. (36) and (37) can be approximated by neglecting the second-order terms as shown below

$$\left\{\frac{\partial\pi_k^*}{\partial d_i}\right\}^{(n+1)} = \left\{\frac{\partial\pi_k^*}{\partial d_i}\right\}^{(n)} + \left\{\frac{\partial}{\partial d_j}\left(\frac{\partial\pi_k^*}{\partial d_i}\right)\right\}^{(n)}\Delta d^{(n)} + \left\{\frac{\partial}{\partial\lambda}\left(\frac{\partial\pi_k^*}{\partial d_i}\right)\right\}^{(n)}\Delta\lambda^{(n)} = 0 \tag{38}$$

$$\left\{\frac{\partial\pi_k^*}{\partial\lambda}\right\}^{(n+1)} = \left\{\frac{\partial\pi_k^*}{\partial\lambda}\right\}^{(n)} + \left\{\frac{\partial}{\partial d_i}\left(\frac{\partial\pi_k^*}{\partial\lambda}\right)\right\}^{(n)}\Delta d^{(n)} + \left\{\frac{\partial}{\partial\lambda}\left(\frac{\partial\pi_k^*}{\partial\lambda}\right)\right\}^{(n)}\Delta\lambda^{(n)} = 0 \tag{39}$$

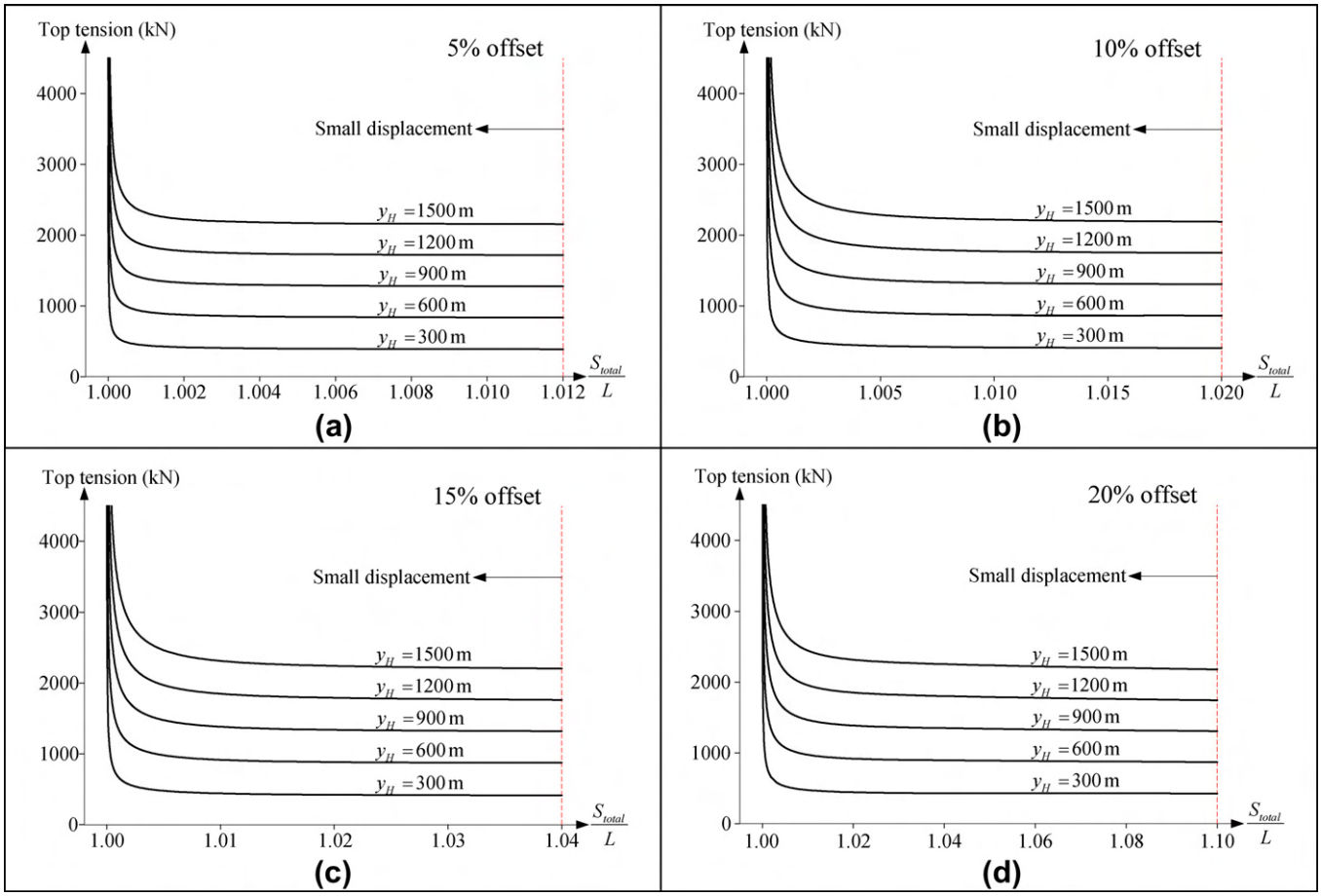

Fig. 2. Relations between the top tension and the unstretched arc-length for water depth of 300, 600, 900, 1200, and 1500 m. (A) 5% offset, (b) 10% offset, (c) 15% offset, (d) 20% offset, (e) 25% offset, (f) 30% offset, (g) 35% offset, (h) 40% offset.

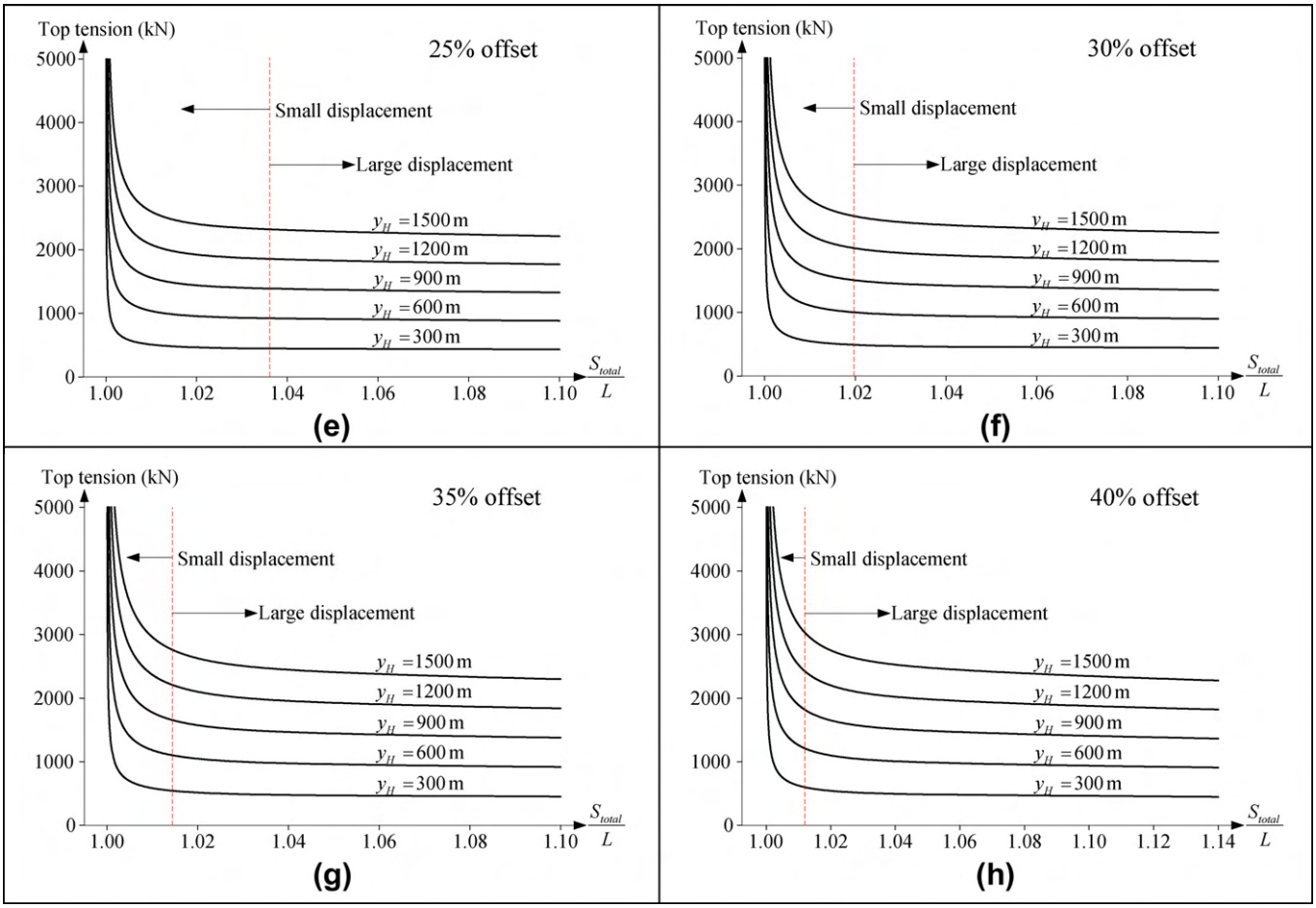

Fig. 2 (*continued*)

where $\{\Delta d\}^n = \{d_i^{n+1}\} - \{d_i^n\}$, $\Delta\lambda^{(n)} = \lambda^{(n+1)} - \lambda^{(n)}$, and n= number of iteration.

Eqs. (38) and (39) can be arranged into the matrix form as follows

$$\begin{bmatrix} [K_{NL}]_{N\times N} & \{K_\lambda\}_{N\times 1} \\ \{K_\lambda\}^T_{1\times N} & 0 \end{bmatrix} \begin{Bmatrix} \{\Delta d_i\} \\ \Delta\lambda \end{Bmatrix} = \begin{Bmatrix} -\{R_i\} \\ -R_\lambda \end{Bmatrix} \tag{40}$$

The integer value N is the number of nodal displacements of the riser system. The matrix $[K_{NL}]$ is the assemblage of the matrices $\{\partial^2\pi_k^*/\partial d_i\partial d_j\}$ from all elements. The vector $\{K_\lambda\}$ represents the assemblage of the element vectors $\{\partial^2\pi_k^*/\partial\lambda\partial d_i\}$. The vector $\{R_i\}$ is the element vectors $\{\partial\pi_k^*/\partial d_i\}$. The parameter R_λ is the value of $\partial\pi^*/\partial\lambda$. The increment vector of nodal displacements $\{\Delta d_i\}$ and the increment value $\Delta\lambda$ are the unknown to be determined. By adding the increment vector $\{\Delta d_i\}$ to $\{d_i\}$ and adding the value of $\Delta\lambda$ to λ, the adjusted values of $\{d_i\}$ and λ are obtained. Use these values for computation the next iteration. Repeat this process until it is terminated when $\{\Delta d_i\}$ and $\Delta\lambda$ approach zero.

5. Numerical solutions

In this section, the numerical examples are presented to identify the physical meaning of the Lagrange multiplier. The relations between the top tension and the unstretched arc-length of the risers, which are subjected to the apparent weight only, are provided for water depth of 300, 600, 900, 1200, and 1500 m. The numerical result from this study has been verified with the classical catenary cable, and found that the results are conformable. The basic properties of the marine riser shown in Table 2 are used to evaluate the numerical examples.

5.1. Physical meaning of the Lagrange multiplier

Considering the case of the specified top tension of 1500 kN is applied to the deep water riser for 900 m water depth and 10% offset. The numerical solutions for this case are shown in Table 3.

If the unstretched total arc-length of 910 m is specified as the constraint condition, the iterative procedure will be used to evaluate Eq. (40). The numerical results for this constraint problem are shown in Table 4.

Calculation of top tension based on Table 4 can be simply explained as follows, if the top tension of 1347.23 kN is applied instead of 1500 kN, the unstretched total arc-length will become 910.00 m. It can be seen that the applied top tension is equal to the assumed top tension minus the Lagrange multiplier (1500–152.77 = 1347.23 kN).

According to the numerical results presented above, one can identify that the Lagrange multiplier is a parameter for adjusting the value of applied top tension in order to satisfy the equilibrium and the constraint condition.

5.2. Relations between the top tension and the unstretched arc-length

The relations between the top tension and the unstretched arc-length for the water depth of 300, 600, 900, 1200 and 1500 m are shown in Fig. 2. The risers are subjected to the apparent weight

only, like steel catenary risers (SCR). The percentage of static offsets ($\%\Delta_H$) is varied in the range of 5–40%.

The numerical results in Fig. 2a–d show that the riser behaves like a tension beam for the nearly vertical marine riser with the static offset less than 20%. The displacements of the riser are small when the shapes of static configuration are kept to have the free hanging configurations without a contact portion on the seabed.

For a free hanging configuration with 25% static offset, the risers experience large displacement (the angles between the span length and the equilibrium configuration are larger than 10 degrees) when the ratios of total unstretched arc-length (S_{total}) to the span length (L) are more than 1.036 as shown in Fig. 2e.

The riser configurations are close to the catenary shape when the percentage of static offsets is increased. Fig. 2f–h indicate that the risers experience the large displacement when the ratios of total unstretched arc-length to the span length are larger than 1.02, 1.014, and 1.012 for 30%, 35%, and 40% static offset, respectively. Fig. 2 also shows that the applied top tensions decreased as the specified unstretched arc-length increased. However, the applied top tensions are not less than the minimum values, which are close to the values of the total of apparent weight of riser, as shown in Fig. 2. If the applied top tensions are less than those minimum values, the riser can no longer maintain its stability and will collapse.

6. Conclusions

This paper presents a numerical procedure to obtain the static configuration of marine riser with the constraint condition, which is the specified total unstretched arc-length. The model formulation is developed by the variational approach. The Lagrange multiplier is applied to impose the constraint condition. The finite element method with the iterative procedure is used for large displacement analysis of marine riser. The numerical results indicate that the Lagrange multiplier represents the parameter for adjusting the applied top tension in order to maintain the riser in equilibrium position under the constraint condition. The relations between the top tension and the unstretched arc-length in different water depth and static offset are also presented.

Acknowledgements

The authors gratefully acknowledge the financial support by the Thailand Research Fund (TRF) under Contract No. MRG5380034.

References

[1] Cook RD, Malkus DS, Plesha ME. Concepts and applications of finite element analysis. 3rd ed. New York: John Wiley & Sons; 1989.
[2] Bathe KJ. Finite Element Procedures. New Jersey; Prentice-Hall; 1996.
[3] Belytschko T, Liu WK, Moran B. Nonlinear finite elements for continua and structures. New York: John Wiley & Sons; 2000.
[4] Crisfield MA. An arc-length method including line searches and accelerations. Int J Numer Methods Eng 1983;19:1269–89.
[5] Felippa CA, Chung JS. Nonlinear static analysis of deep ocean mining pipe – Part 1: modeling and formulation. J Energy Res Technol 1981;103:11–5.
[6] Chung JS, Felippa CA. Nonlinear static analysis of deep ocean mining pipe – Part 2: numerical studies. J Energy Res Technol 1981;103:16–25.
[7] McNamara JF, O'Brien PJ, Gilrory SG. Nonlinear analysis of flexible risers using hybrid finite elements. J Offshore Mech Arct Eng 1988;110:197–204.
[8] Moe G, Arntsen Ø. An analytic model for static analysis of catenary risers. In: proceeding of 11th international offshore and polar engineering conference, 2001. p. 248–53.
[9] Bernitsas MM, Kokarakis JE. Importance of nonlinearities in static riser analysis. Appl Ocean Res 1988;10:2–9.
[10] O'Brien PJ, McNamara JF. Significant characteristics of three-dimensional flexible riser analysis. Eng Struct 1989;11:223–33.
[11] Chung JS, Cheng BR, Huttelmaier HP. Three-dimensional coupled responses of a vertical deep-ocean pipe: Part I. excitation at pipe ends and external torsion. Int J Offshore Polar Eng 1994;4:320–30.
[12] Chung JS, Cheng BR, Huttelmaier HP. Three-dimensional coupled responses of a vertical deep-ocean pipe: Part II. excitation at pipe top and external torsion. Int J Offshore Polar Eng 1994;4:331–9.
[13] Chung JS, Cheng BR. Effects of elastic joints on 3-d nonlinear responses of a deep-ocean pipe: Modeling and boundary conditions. Int J Offshore Polar Eng 1996;6:203–11.
[14] Chai YT, Varyani KS. An absolute coordinate formulation for three dimensional flexible pipe analysis. Ocean Eng 2006;33:23–58.
[15] Chatjigeorgiou IK. On the effect of internal flow on vibrating catenary risers in three dimensions. Eng Struct 2010;32:3313–29.
[16] Patel MH, Seyed FB. Review of flexible riser modelling and analysis techniques. Eng Struct 1995;17:293–304.
[17] Huang T, Chucheepsakul S. Large displacement analysis of a marine riser. J Energy Res Technol 1985;107:54–9.
[18] Chucheepsakul S, Huang T, Monprapussorn T. Large strain formulations of extensible flexible marine pipes transporting fluid. J Fluids Struct 2003;17:333–65.
[19] Huang T, Kang QL. Three dimensionalanalysis of a marine riser with large displacements. Int J Offshore Polar Eng 1991;1:300–6.
[20] Chucheepsakul S, Huang T, Monprapussorn T. Influence of transported fluid on behavior of an extensible flexible riser/pipe. In: proceeding of 9th international offshore and polar engineering conference, 1999. p. 286–93.
[21] Athisakul C, Huang T, Chucheepsakul, S. Large strain static analysis of marine risers via a variational approach. In: Proceeding of 12th international offshore and polar engineering conference, 2002. p. 164–70.
[22] Athisakul C, Chucheepsakul S. Effect of inclination on bending of variable-arc-length beams subjected to uniform self-weight. Eng Struct 2008;30:902–8.
[23] Athisakul C, Monprapussorn T, Chucheepsakul S. A variational formulation for three-dimensional analysis of extensible marine riser transporting fluid. Ocean Eng 2011;38:609–20.
[24] Monprapussorn T, Chucheepsakul S, Huang T. The coupled radial-axial deformation analysis of flexible pipes conveying fluid. Int J Num Methods Eng 2004;59:1399–452.
[25] Monprapussorn T, Athisakul C, Chucheepsakul S. Nonlinear vibrations of an extensible flexible marine riser carrying a pulsatile flow. J Appl Mech ASME 2007;74:754–69.
[26] Kaewunruen S, Chiravatchradej J, Chucheepsakul S. Nonlinear free vibrations of marine risers/pipes transporting fluid. Ocean Eng 2005;32:417–40.
[27] Spark CP. The influence of tension, pressure and weight on pipe and riser deformations and stresses. J Energy Res Technol 1984;106:46–54.
[28] Patel MH, Seyed FB. Internal flow-induced behavior of flexible risers. Eng Struct 1989;11:266–80.
[29] Huang T. Kinematic of transported mass inside risers and pipes. In: Proceeding of 3rd international offshore and polar engineering conference, 1993. p. 331–6.
[30] Langhaar HL. Energy methods in applied mechanics. New York: John Wiley & Sons; 1962.

The IES Journal Part A: Civil & Structural Engineering
Publication details, including instructions for authors and subscription information:
http://www.tandfonline.com/loi/tiea20

Critical weight of flexible pipe conveying fluid subjected to end moments

Chainarong Athisakul [a], Boonchai Phungpaingam [b], Waraporn Chatanin [c] & Somchai Chucheepsakul [a]

[a] Department of Civil Engineering, Faculty of Engineering, King Mongkut's University of Technology, Thonburi, Bangkok, Thailand

[b] Department of Civil Engineering, Rajamangala University of Technology, Thanyaburi, Pathum-thani, Thailand

[c] Department of Mathematics, Faculty of Science, King Mongkut's University of Technology, Thonburi, Bangkok, Thailand

Available online: 19 Apr 2012

To cite this article: Chainarong Athisakul, Boonchai Phungpaingam, Waraporn Chatanin & Somchai Chucheepsakul (2012): Critical weight of flexible pipe conveying fluid subjected to end moments, The IES Journal Part A: Civil & Structural Engineering, 5:2, 90-94

To link to this article: http://dx.doi.org/10.1080/19373260.2012.663743

The IES Journal Part A: Civil & Structural Engineering
Vol. 5, No. 2, May 2012, 90–94

Taylor & Francis
Taylor & Francis Group

TECHNICAL PAPER

Critical weight of flexible pipe conveying fluid subjected to end moments

Chainarong Athisakul[a]*, Boonchai Phungpaingam[b], Waraporn Chatanin[c] and Somchai Chucheepsakul[a]

[a]*Department of Civil Engineering, Faculty of Engineering, King Mongkut's University of Technology, Thonburi, Bangkok, Thailand;* [b]*Department of Civil Engineering, Rajamangala University of Technology, Thanyaburi, Pathum-thani, Thailand;* [c]*Department of Mathematics, Faculty of Science, King Mongkut's University of Technology, Thonburi, Bangkok, Thailand*

(*Received 5 November 2011; final version received 2 February 2012*)

This article aims to evaluate the critical weight of flexible pipe subjected to applied end moments at fixed support locations. The pipe is hinged at one end, while the other end is free to slide over a frictionless support. The horizontal distance between the two supports is fixed. The model formulation is developed by the variational approach, and the finite element method is employed to obtain the numerical solutions. The critical weights are evaluated for various values of end moments and the proportional parameter of the end moments.

Keywords: finite element method; flexible pipe; critical weights; variational approach; end moments; nonlinear

1. Introduction

The failure of flexible pipes used in offshore engineering operations causes severe environmental pollution. To ensure the strength and stability of flexible pipe, accurate determination of the wall thickness of pipe is necessary. There has been considerable amount of research works dealing with the stability of pipes conveying fluids, such as Chen (1971) and Païdoussis and Issid (1974). Thompson and Lunn (1981) presented the static elastic theory for nonlinear analysis of pipe conveying fluid. They found that the internal flow velocity can induce the buckling-type or fluttering-type instabilities. The divergence instability of a variable-arc-length elastica pipe due to steady flow velocity of internal fluid was presented by Chucheepsakul and Monprapussorn (2000). They used the elliptic integral method to obtain analytical solutions. However, this work is focused only on the effect of internal flow velocity by neglecting the weight of the pipe and the internal fluid. A more recent investigation on nonlinear buckling of marine elastic pipes transporting fluid was presented by Chucheepsakul and Monprapussorn (2001). They concluded that the nonlinear buckling of the marine elastica pipe can occur due to insufficient stiffness and overloading. The critical weights of pipes for a particular example were also presented in their works. Athisakul and Chucheepsakul (2008) used the finite element method (FEM) to evaluate the critical loads of the variable-arc-length beam for various inclinations. Their results can be applied as benchmarks for the analysis of free hanging marine pipes/risers. To reduce the stress at both the touchdown point and at the platform connection, a subsea buoy is added to produce the S, Wave and Camel configurations. According to the subsea buoy system, the additional bending moment may occur at the ends of the pipes. Consequently, flexible pipes have to resist the double curvature bending. Chucheepsakul *et al*. (1999) published a paper dealing with the double curvature bending of variable-arc-length elasticas under two applied moments. The elliptic integral method was utilised to obtain the closed-form solutions. However, the weight of structure is neglected.

This article continues in this line of investigation by considering the combination of its uniform self-weight and two applied moments at both ends in the same direction. Since the elliptic integrals method cannot be applied to this kind of problems, the FEM is an alternative method to determine the numerical solutions. The variational approach is employed to develop the model formulation. The first variation of the total potential energy is derived to establish the system of nonlinear finite element equations. The numerical solutions are obtained by an iterative procedure. The second variation of the total potential energy is evaluated to form the tangent stiffness matrix of the pipes. The critical uniform self-weights of the pipe are the maximum value, which the determinant of tangent stiffness matrix is equal to zero. In practice, the critical uniform self-weight can be defined from changing the sign of tangent stiffness matrix from positive to negative.

*Corresponding author. Email: athisakul@gmail.com

ISSN 1937-3260 print/ISSN 1937-3279 online

http://dx.doi.org/10.1080/19373260.2012.663743
http://www.tandfonline.com

2. Variational formulation

Consider a flexible pipe of uniform flexural rigidity EI as shown in Figure 1(a). The pipe is supported by a pin support at end A and by a frictionless support at end B. The constant distance between ends A and B is L. The pipe is subjected to a clockwise moment $M_A = (1-\beta)M_o$ at the end A and a clockwise moment $M_B = \beta M_o$ at the end B. The scalar parameter β represents the proportion of the moment at end B to the total moment M_o. The uniform self-weight of the pipe per unit arc-length is equal to$w$. The internal fluid of density ρ_i is transported from end A to end B with a uniform and steady flow speed U. The internal area of pipe is represented by A_i. Figure 1(b) shows the deformed configuration of the flexible pipe. The total arc-length S_t is an unknown parameter. The overhang length l is small compared with the total arc-length S_t. Therefore, the loads in the portion of overhang length l can be neglected.

According to variational principle (Chucheepsakul *et al*. 2003, Athisakul *et al*. 2011), the total virtual work of the flexible pipe can be expressed as

$$\delta\pi = \int_0^L \left\{ \frac{EIy''}{(1+y'^2)^{5/2}}\delta y'' - \frac{2EIy''^2y'}{(1+y'^2)^{7/2}}\delta y' + \frac{Ny'}{\sqrt{1+y'^2}}\delta y' - w\sqrt{1+y'^2}\delta y + \rho_i A_i \kappa U^2 \delta y \right\} \mathrm{d}x - \frac{M_A}{(1+y'^2)}\delta y'\Big|^{x=0} - \frac{M_B}{(1+y'^2)}\delta y'\Big|^{x=L}. \tag{1}$$

The first two terms represent the virtual strain energy due to bending. The third term represents the virtual strain energy due to axial deformation, where N is the axial force in the pipe section. The fourth term is the virtual work done by pipe's weight. The fifth term is the virtual work done by the internal flow inside the pipe. The last two terms are the virtual work done by the applied end moments.

According to differential geometry of a plane curve, one obtains

$$\frac{\mathrm{d}x}{\mathrm{d}s} = \cos\theta,\ \frac{\mathrm{d}y}{\mathrm{d}s} = \sin\theta,\ \mathrm{d}s = \sqrt{1+y'^2}\mathrm{d}x,\ \kappa = \frac{\theta'}{s'} = \frac{y''}{s'^3}. \tag{2a–d}$$

The prime represents the derivatives with respect to x. Since the beam material is linear elastic, the moment curvature relation becomes

$$M = -EI\kappa = -EI\frac{\mathrm{d}\theta}{\mathrm{d}s}. \tag{3}$$

3. Finite element method

The span length L is divided into n equally spaced regions or elements. Each of these elements has a length l. The displacement of the beam segment is approximated by

$$y(x) = [N]\{q\}. \tag{4}$$

where $[N]$ is the row of fifth-order polynomials shape functions, and $\{q\}$ is the vector containing the values of y and its first and second derivatives at both ends of the element. Consequently, the system of element equations can be expressed as follows:

$$\left\{\frac{\partial\pi}{\partial q_i}\right\} = \int_0^L \left\{ [N'']^T \frac{EIy''}{(1+y'^2)^{5/2}} + [N']^T \left[\frac{Ny'}{\sqrt{1+y'^2}} - \frac{2EIy''^2y'}{(1+y'^2)^{7/2}} \right] - [N]^T \left[w\sqrt{1+y'^2} - \rho_i A_i \kappa U^2 \right] \right\} \mathrm{d}x. \tag{5}$$

The contribution from the applied moments is

$$\left\{\frac{\partial\pi}{\partial q}\right\}_{x=0,x=L} = -[N']^T \frac{M_A}{(1+y'^2)}\Big|^{x=0} - [N']^T \frac{M_B}{(1+y'^2)}\Big|^{x=L}. \tag{6}$$

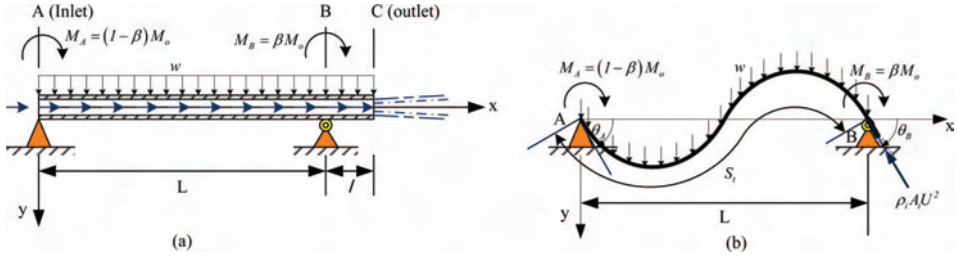

Figure 1. (a) Undeformed configuration of flexible pipe; (b) deformed configurations of flexible pipe.

For equilibrium, the total virtual of the system is zero ($\delta\pi = 0$). Therefore, the nonlinear global equilibrium equation $\{\frac{\partial\pi}{\partial Q}\} = \{0\}$ can be obtained by assembling the element equations. The iterative procedure is used to obtain the numerical solutions of the global degree of freedom Q.

To find the critical configuration of the pipe, the second variation of the total potential energy is derived into the matrix form as (Athisakul and Chucheepsakul, 2008)

$$\delta^2\pi = \{q\}^T[K_T]\{q\}. \tag{7}$$

The critical weight is evaluated by optimising for an increment of load step by step until the determinant of tangent stiffness matrix $[K_T]$ is equal to zero or it changes sign from positive to negative (Athisakul and Chucheepsakul, 2008). The critical weight is the maximum value of pipe weight, which the equilibrium of pipe is still satisfied.

4. Numerical results

The following nondimensional parameters are introduced for the sake of generality.

$$s^* = s/s_t, \hat{x} = x/L, \hat{y} = y/L, \hat{s} = s/L, \tag{8a–d}$$

$$\hat{M} = ML/EI, \hat{Q} = QL^2/EI, \hat{N} = NL^2/EI,\hat{}\quad w = wL^3/EI, \hat{U} = UL\sqrt{\rho_i A_i/EI}. \tag{8e–i}$$

The parameters ρ_i and A_i represent density of internal fluid and internal cross-sectional area of the pipe, respectively.

To validate the numerical results obtained from this study, some numerical solutions for double curvature bending of the variable-arc-length elastica are evaluated as shown in Table 1. It is clearly found that the numerical solutions obtained from this study are in very good agreement with the exact solutions

Table 1. Validation of numerical results fosr elasticas with double curvature bending $\hat{M} = 3$.

	Rotation at end A θ_A (rad)		Rotation at end B θ_B (rad)		Total arc-length $\hat{s}_t$	
β	EIM (Chucheepsakul *et al.* 1999)	FEM (this study)	EIM (Chucheepsakul *et al.* 1999)	FEM (this study)	EIM (Chucheepsakul *et al.* 1999)	FEM (this study)
0.2	0.809178	0.809161	− 0.250095	− 0.250097	1.057947	1.057950
0.4	0.404192	0.404200	0.101105	0.101101	1.010185	1.010183
0.6	0.107839	0.107836	0.389108	0.389121	1.009265	1.009258
0.8	− 0.144274	− 0.144305	0.652506	0.652565	1.031259	1.031254
1.0	− 0.357892	− 0.358003	0.887168	0.887392	1.066052	1.066079

Note: EIM, elliptic integral method; FEM, finite element method.

Table 2. Critical weights of flexible pipe for $\hat{M} = -2, -1, 0, 1, 2$ and $\hat{U} = 0, 0.5, 1.0$.

	$\beta = 0.0$	$\beta = 0.2$	$\beta = 0.4$	$\beta = 0.6$	$\beta = 0.8$	$\beta = 1.0$
Internal flow speed $\hat{U} = 0.0$						
$\hat{M} = -2$	15.3973	12.3742	9.6621	7.3203	5.4136	3.9953
$\hat{M} = -1$	11.7910	10.3329	8.9553	7.6665	6.4751	5.3889
$\hat{M} = 0$	8.2527					
$\hat{M} = 1$	4.7846	6.1236	7.5528	9.0644	10.6511	12.3040
$\hat{M} = 2$	1.3774	3.9242	6.8541	10.099	13.6007	17.3154
Internal flow speed $\hat{U} = 0.5$						
$\hat{M} = -2$	15.1678	12.1258	9.3909	7.0288	5.1015	3.6663
$\hat{M} = -1$	11.5385	10.0692	8.6816	7.3831	6.1820	5.0863
$\hat{M} = 0$	7.9757					
$\hat{M} = 1$	4.4836	5.8316	7.2706	8.7912	10.3857	12.0471
$\hat{M} = 2$	1.0524	3.6166	6.5641	9.8250	13.3420	17.0675
Internal flow speed $\hat{U} = 1.0$						
$\hat{M} = -2$	14.4967	11.3923	8.5905	6.1609	4.1709	2.6823
$\hat{M} = -1$	10.7921	9.2927	7.8735	6.5436	5.3102	4.1840
$\hat{M} = 0$	7.1554					
$\hat{M} = 1$	3.5896	4.9660	6.4326	7.9807	9.6009	11.2874
$\hat{M} = 2$	0.0822	2.7016	5.7040	9.0156	12.5758	16.3385

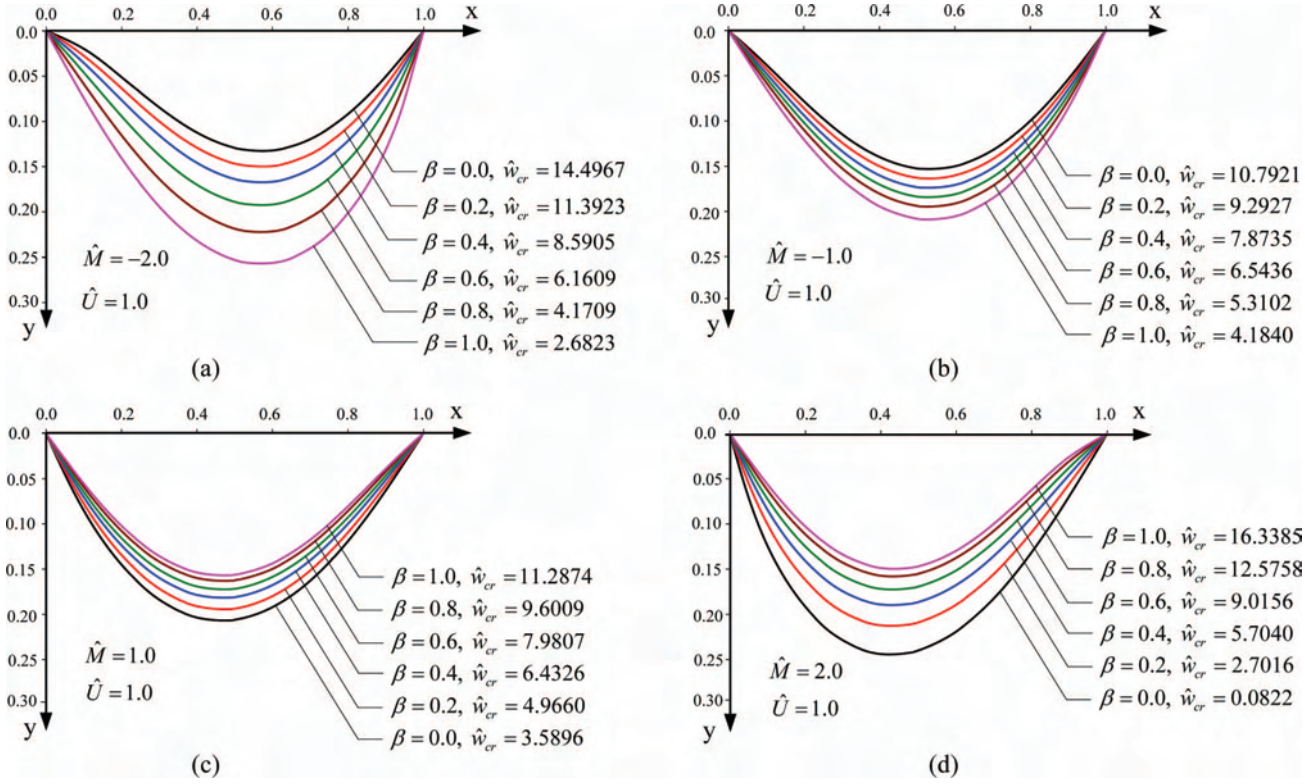

Figure 2. Critical configurations of the pipe for $\hat{U} = 1$.

computed from the elliptic integral method (Chucheepsakul *et al.*, 1999).

The particular problems of flexible pipes with the total end moment $\hat{M}$ from -2 to 2, and the internal flow speed $\hat{U}$ of 0, 0.5 and 1.5 are considered. Table 2 shows the critical weights of the pipe for various values of the proportional parameter β of the end moments. As shown in Table 2, the critical weights depend on the value of total end moments, the direction of end moments and the internal flow speed. For $\hat{M} = 0$ and $\hat{U} = 0$, the critical weight of 8.2527 is identical to the value suggested by Athisakul and Chucheepsakul (2008). In the case where $\hat{M}$ and β are specified, the critical weight of the pipe decreases as the internal flow speed increases. The critical configurations of the pipe for $\hat{U} = 1$ are illustrated in Figure 2. Considering the case of negative end moments, the critical weight decreases as the parameters β increases (see Table 2). According to the positive sign convention of the applied end moments shown in Figure 1, the negative end moment at end A resists the deflection induced by the pipe weight while the negative end moment at end B enlarges the deflection of the pipe. Therefore, the deflection of the pipe at a critical state increases as the parameter β of the negative end moment increases as shown in Figure 2(a,b). On the contrary, the positive end moment at end A enlarges the deflection of pipe while the positive end moment at end B resists the weight of pipe. Consequently, the deflection of the pipe at critical state decreases as the parameter β of the positive end moment increases as shown in Figure 2(c,d). For a given value of positive end moment, the critical weight of pipe increases as the parameter β increases (see Table 2). Table 2 also shows that the equilibrium of the pipe with the positive value of pipe weight may not exist for the case of large end moment.

5. Conclusions

In this article, the critical uniform weight of the flexible pipe subjected to two end moments is determined by using the FEM. The end moments are applied at both ends of the pipe in the same direction. The critical weight of the pipe decreases as the internal flow speed increases. As the parameter β increases, the critical weight increases when the positive end moments are applied. The results are opposite when the negative end moments are applied, as the parameter β increases the critical weight decreases. It is also found that the equilibrium of the pipe with the positive value of pipe weight may not exist when the absolute value of moment becomes large.

Acknowledgements

The authors gratefully acknowledge the financial support by the Thailand Research Fund (TRF) under Contract No. MRG5380034.

References

Athisakul, C. and Chucheepsakul, S., 2008. Effect of inclination on bending of variable-arc-length beams subjected to uniform self-weight. *Engineering Structures*, 30, 902–908.

Athisakul, C., Monprapussorn, T., and Chucheepsakul, S., 2011. A variational formulation for three-dimensional analysis of extensible marine riser transporting fluid. *Ocean Engineering*, 38, 609–620.

Chen, S.S., 1971. Flow-induced instability of an elastic tube. *ASME Paper No. 71*-Vibr.-39.

Chucheepsakul, S. and Monprapussorn, T., 2000. Divergence instability of variable-arc-length elastica pipes transporting fluid. *Journal of Fluids and Structures*, 14, 895–916.

Chucheepsakul, S. and Monprapussorn, T., 2001. Nonlinear buckling of marine elastica pipes transporting fluid. *International Journal of Structural Stability and Dynamics*, 1 (3), 333–365.

Chucheepsakul, S., Monprapussorn, T. and Huang, T., 2003. Large strain formulations of extensible flexible marine pipes transporting fluid. *Journal of Fluids and Structures*, 17, 185–224.

Chucheepsakul, S., Wang, C.M., He, X.Q. and Monprapussorn, T., 1999. Double curvature bending of variable-arc-length elasticas. *Journal of Applied Mechanics, ASME*, 66, 87–94.

Païdoussis, M.P. and Issid, N.T., 1974. Dynamic stability of pipes conveying fluid. *Journal of Sound and Vibration*, 33, 267–294.

Thompson, J.M.T. and Lunn, T.S., 1981. Static elastica formulations of a pipe conveying fluid. *Journal of Sound and Vibration*, 77, 127–132.

FINITE ELEMENT METHOD TO DETERMINE CRITICAL WEIGHT OF FLEXIBLE PIPE CONVEYING FLUID SUBJECTED TO END MOMENTS

* C. Athisakul[1], B. Phungpaingam[2], W. Chatanin[3], S. Chucheepsakul[1]

[1] Department of Civil Engineering, Faculty of Engineering,
King Mongkut's University of Technology Thonburi, Bangkok, Thailand
[2] Department of Civil Engineering, Rajamangala University of Technology Thanyaburi,
Thanyaburi, Pathum-thani, Thailand
[3] Department of Mathematics, Faculty of Science, King Mongkut's University of
Technology Thonburi, Bangkok, Thailand
* Email: Athisakul@gmail.com

KEYWORDS

Finite element method, flexible pipe, critical weights, variational approach, end moments, nonlinear.

ABSTRACT

This paper aims to evaluate the critical weight of flexible pipe subjected to applied end moments at fixed support locations. The pipe is hinged at one end, while the other end is free to slide over a frictionless support. The horizontal distance between the two supports is fixed. The model formulation is developed by the variational approach, and the finite element method is employed to obtain the numerical solutions. The critical weights are evaluated for various values of end moments and the proportional parameter of the end moments.

INTRODUCTION

The failure of flexible pipes used in offshore engineering operations causes severe environmental pollution. In order to ensure the strength and stability of flexible pipe, accurate determination of the wall thickness of pipe is necessary. There has been a considerable amount of research works dealing with the stability of pipes conveying fluids such as Chen [1], and Païdoussis and Issid [2]. Thompson and Lunn [3] presented the static elastic theory for nonlinear analysis of pipe conveying fluid. They found that the internal flow velocity can induce the buckling-type or fluttering-type instabilities. The divergence instability of a variable-arc-length elastica pipe due to steady flow velocity of internal fluid was presented by Chucheepsakul and Monprapussorn [4]. They used the elliptic integral method to obtain analytical solutions. However, this work is focused only on the effect of internal flow velocity by neglecting the weight of the pipe and the internal fluid. A more recent investigation on nonlinear buckling of marine elastic pipes transporting fluid was presented by Chucheepsakul and Monprapussorn [5]. They concluded that the nonlinear buckling of the marine elastica pipe can occur due to insufficient stiffness and

overloading. The critical weights of pipes for a particular example were also presented in their works. Athisakul and Chucheepsakul [6] used the finite element method to evaluate the critical loads of the variable-arc-length beam for various inclinations. Their results can be applied as benchmarks for the analysis of free hanging marine pipes/risers. In order to reduce the stress at both the touchdown point and at the platform connection, a subsea buoy is added to produce the S, Wave, and Camel configurations. According to the subsea buoy system, the additional bending moment may occur at the ends of the pipes. Consequently, flexible pipes have to resist the double curvature bending. Chucheepsakul et al. [7] published a paper dealing with the double curvature bending of variable-arc-length elasticas under two applied moments. The elliptic integral method was utilized to obtain the closed-form solutions. However, the weight of structure is neglected.

This paper continues in this line of investigation by considering the combination of its uniform self-weight and two applied moments at both ends in the same direction. Since the elliptic integrals method cannot be applied to this kind of problems, the finite element method (FEM) is an alternative method to determine the numerical solutions. The variational approach is employed to develop the model formulation. The first variation of the total potential energy is derived to establish the system of nonlinear finite element equations. The numerical solutions are obtained by an iterative procedure. The second variation of the total potential energy is evaluated to form the tangent stiffness matrix of the pipes. The critical uniform self-weights of the pipe are the maximum value, which the determinant of tangent stiffness matrix is equal to zero. In practice, the critical uniform self-weight can be defined from changing the sign of tangent stiffness matrix from positive to negative.

VARIATIONAL FORMULATION

Consider a flexible pipe of uniform flexural rigidity EI as shown in Figure 1(a). The pipe is supported by a pin support at end A and by a frictionless support at end B. The constant distance between ends A and B is L. The pipe is subjected to a clockwise moment $M_A = (1-\beta)M_0$ at the end A and a clockwise moment $M_B = \beta M_0$ at the end B. The scalar parameter β represents the proportion of the moment at end B to the total moment M_0. The uniform self-weight of the pipe per unit arc-length is equal to w. The internal fluid of density ρ_i is transported from end A to end B with a uniform and steady flow speed U. The internal area of pipe is represented by A_i. Figure 1(b) shows the deformed configuration of the flexible pipe. The total arc-length S_t is an unknown parameter. The overhang length l is small compared with the total arc-length S_t. Therefore, the loads in the portion of overhang length l can be neglected.

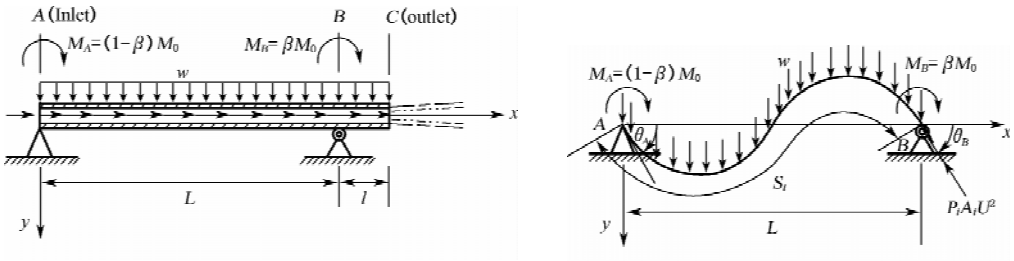

(a) (b)

Figure 1 (a) Undeformed configuration of flexible pipe; (b) Deformed configurations of flexible pipe.

According to variational principle [8, 9], the total virtual work of the flexible pipe can be expressed as

$$\delta\pi = \int_0^L \left\{ \frac{EIy''}{(1+y'^2)^{5/2}}\delta y'' - \frac{2EIy''^2 y'}{(1+y'^2)^{7/2}}\delta y' + \frac{Ny'}{\sqrt{1+y'^2}}\delta y' - w\sqrt{1+y'^2}\delta y + \rho_i A_i \kappa U^2 \delta y \right\} \mathrm{d}x$$
$$- \frac{M_A}{(1+y'^2)}\delta y' \Big|^{x=0} - \frac{M_B}{(1+y'^2)}\delta y' \Big|^{x=L} \tag{1}$$

The first two terms represent the virtual strain energy due to bending. The third term represents the virtual strain energy due to axial deformation, where N is the axial force in the pipe section. The fourth term is the virtual work done by pipe's weight. The fifth term is the virtual work done by the internal flow inside the pipe. The last two terms are the virtual work done by the applied end moments.

According to differential geometry of a plane curve, one obtains

$$\frac{\mathrm{d}x}{\mathrm{d}s} = \cos\theta,\ \frac{\mathrm{d}y}{\mathrm{d}s} = \sin\theta,\ \mathrm{d}s = \sqrt{1+y'^2}\,\mathrm{d}x,\ \kappa = \frac{\theta'}{s'} = \frac{y''}{s'^3} \tag{2 a-d}$$

The prime represents the derivatives with respect to x. Since the beam material is linear elastic, the moment curvature relation becomes

$$M = -EI\kappa = -EI\frac{\mathrm{d}\theta}{\mathrm{d}s} \tag{3}$$

FINITE ELEMENT METHOD

The span length L is divided into n equally spaced regions or elements. Each of these elements has a length l. The displacement of the beam segment is approximated by

$$y(x) = [N]\{q\} \tag{4}$$

where $[N]$ is the row of fifth-order polynomials shape functions, and $\{q\}$ is the vector containing the values of y and its first and second derivatives at both ends of the element. Consequently, the system of element equations can be expressed as follows

$$\left\{\frac{\partial\pi}{\partial q_i}\right\} = \int_0^L \left\{ [N'']^T \frac{EIy''}{(1+y'^2)^{5/2}} + [N']^T \left[\frac{Ny'}{\sqrt{1+y'^2}} - \frac{2EIy''^2 y'}{(1+y'^2)^{7/2}} \right] \right.$$
$$\left. - [N]^T [w\sqrt{1+y'^2} - \rho_i A_i \kappa U^2] \right\} \mathrm{d}x \tag{5}$$

The contribution from the applied moments is

$$\left\{\frac{\partial\pi}{\partial q}\right\}_{x=0,\ x=L} = -[N']^T \frac{M_A}{(1+y'^2)} \Big|^{x=0} - [N']^T \frac{M_B}{(1+y'^2)} \Big|^{x=L} \tag{6}$$

For equilibrium, the total virtual of the system is zero ($\delta\pi = 0$). Therefore, the nonlinear global equilibrium equation $\left\{\frac{\partial\pi}{\partial Q}\right\} = \{0\}$ can be obtained by assembling the element equations. The iterative procedure is used to obtain the numerical solutions of the global degree of freedom Q.

In order to find the critical configuration of the pipe, the second variation of the total potential energy is derived into the matrix form [6] as

$$\delta^2\pi = \{q\}^T [K_T] \{q\} \tag{7}$$

The critical weight is evaluated by optimizing for an increment of load step by step until the determinant of tangent stiffness matrix $[K_T]$ is equal to zero or it changes sign from positive to negative [6]. The

critical weight is the maximum value of pipe weight, which the equilibrium of pipe is still satisfied.

NUMERICAL RESULTS

The following non-dimensional parameters are introduced for the sake of generality.

$$s^* = s/s_t,\ x = x/L,\ y = y/L,\ s = s/L, \tag{8 a-d}$$

$$M = ML/EI,\ \hat{Q} = QL^2/EI,\ N = NL^2/EI,\ \hat{w} = wL^3/EI,\ U = UL\sqrt{\rho_i A_i/EI} \tag{8 e-i}$$

The parameters ρ_i and A_i represent density of internal fluid and internal cross sectional area of the pipe, respectively.

In order to validate the numerical results obtained from this study, some numerical solutions for double curvature bending of the variable-arc-length elastica are evaluated as shown in Table 1. It is clearly found that the numerical solutions obtained from this study are in very good agreement with the exact solutions computed from the elliptic integral method [7].

The particular problems of flexible pipes with the total end moment $\hat{M}$ from -2 to 2, and the internal flow speed $\hat{U}$ of 0, 0.5, and 1.5 are considered. Table 2 shows the critical weights of the pipe for various values of the proportional parameter β of the end moments. As shown in Table 2, the critical weights depend on the value of total end moments, the direction of end moments, and the internal flow speed. For $\hat{M} = 0$ and $\hat{U} = 0$, the critical weight of 8.252 7 is identical to the value suggested by Athisakul and Chucheepsakul [6]. In case where $\hat{M}$ and β are specified, the critical weight of the pipe decreases as the internal flow speed increases. The critical configurations of the pipe for $\hat{U} = 1$ are illustrated in Figure 2. Considering the case of negative end moments, the critical weight decreases as the parameters β increases (see Table 2). According to the positive sign convention of the applied end moments shown in Figure 1, the negative end moment at end A resists the deflection induced by the pipe weight while the negative end moment at end B enlarges the deflection of the pipe. Therefore, the deflection of the pipe at a critical state increases as the parameter β of the negative end moment increases as shown in Figures 2(a) and 2(b). On the contrary, the positive end moment at end A enlarges the deflection of pipe while the positive end moment at end B resists the weight of pipe. Consequently, the deflection of the pipe at critical state decreases as the parameter β of the positive end moment increases as shown in Figures 2(c) and 2(d). For a given value of positive end moment, the critical weight of pipe increases as the parameter β increases (see Table 2). Table 2 also shows that the equilibrium of the pipe with the positive value of pipe weight may not exist for the case of large end moments.

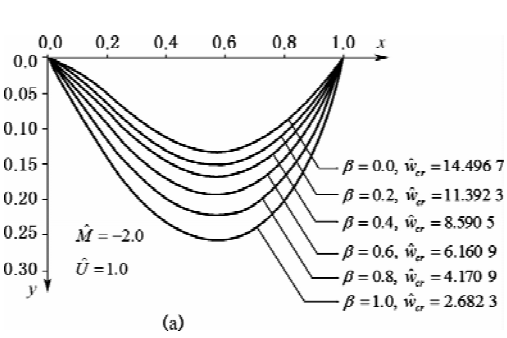

(a)

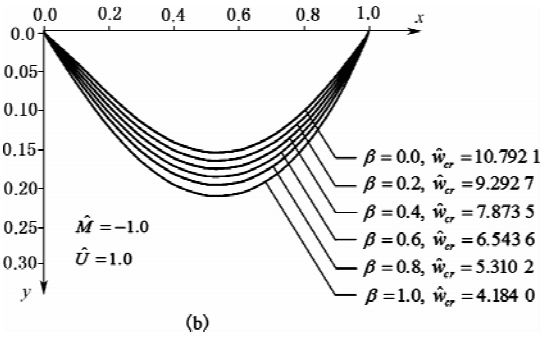

(b)

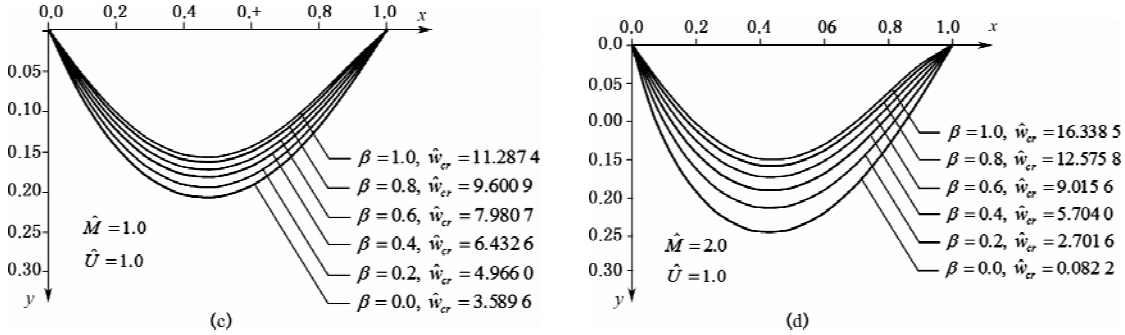

Figure 2 Critical configurations of the pipe for $\hat{U}=1$.

TABLE 1 VALIDATION OF NUMERICAL RESULTS FOR THE PROBLEM OF ELASTICAS WITH DOUBLE CURVATURE BENDING $\hat{M}=3$

	Rotation at end A θ_A (rad)		Rotation at end B θ_B (rad)		Total arc-length $\hat{s}_t$	
β	EIM [7]	FEM (this study)	EIM [7]	FEM (this study)	EIM [7]	FEM (this study)
0.2	0.809 178	0.809 161	−0.250 095	−0.250 097	1.057 947	1.057 950
0.4	0.404 192	0.404 200	0.101 105	0.101 101	1.010 185	1.010 183
0.6	0.107 839	0.107 836	0.389 108	0.389 121	1.009 265	1.009 258
0.8	−0.144 274	−0.144 305	0.652 506	0.652 565	1.031 259	1.031 254
1.0	−0.357 892	−0.358 003	0.887 168	0.887 392	1.066 052	1.066 079

EIM = Elliptic integral method
FEM = Finite element method

TABLE 2 CRITICAL WEIGHTS OF THE FLEXIBLE PIPE FOR $\hat{M}=-2, -1, 0, 1, 2$, AND $\hat{U}=0, 0.5, 1.0$

	Internal Flow Speed $\hat{U}=0.0$					
	$\beta=0.0$	$\beta=0.2$	$\beta=0.4$	$\beta=0.6$	$\beta=0.8$	$\beta=1.0$
$\hat{M}=-2$	15.397 3	12.374 2	9.662 1	7.320 3	5.413 6	3.995 3
$\hat{M}=-1$	11.791 0	10.332 9	8.955 3	7.666 5	6.475 1	5.388 9
$\hat{M}=0$			8.252 7			
$\hat{M}=1$	4.784 6	6.123 6	7.552 8	9.064 4	10.651 1	12.304 0
$\hat{M}=2$	1.377 4	3.924 2	6.854 1	10.099	13.600 7	17.315 4
	Internal Flow Speed $\hat{U}=0.5$					
	$\beta=0.0$	$\beta=0.2$	$\beta=0.4$	$\beta=0.6$	$\beta=0.8$	$\beta=1.0$
$\hat{M}=-2$	15.167 8	12.125 8	9.390 9	7.028 8	5.101 5	3.666 3
$\hat{M}=-1$	11.538 5	10.069 2	8.681 6	7.383 1	6.182 0	5.086 3
$\hat{M}=0$			7.975 7			
$\hat{M}=1$	4.483 6	5.831 6	7.270 6	8.791 2	10.385 7	12.047 1
$\hat{M}=2$	1.052 4	3.616 6	6.564 1	9.825 0	13.342 0	17.067 5

continued

	Internal Flow Speed $\hat{U}=1.0$					
	$\beta=0.0$	$\beta=0.2$	$\beta=0.4$	$\beta=0.6$	$\beta=0.8$	$\beta=1.0$
$\hat{M}=-2$	14.496 7	11.392 3	8.590 5	6.160 9	4.170 9	2.682 3
$\hat{M}=-1$	10.792 1	9.292 7	7.873 5	6.543 6	5.310 2	4.184 0
$\hat{M}=0$			7.155 4			
$\hat{M}=1$	3.589 6	4.966 0	6.432 6	7.980 7	9.600 9	11.287 4
$\hat{M}=2$	0.082 2	2.701 6	5.704 0	9.015 6	12.575 8	16.338 5

CONCLUSIONS

The finite element method for determining the critical uniform weight of the flexible pipe subjected to two end moments is presented. The end moments are applied at both ends of the pipe in the same direction. The critical weight of the pipe decreases as the internal flow speed increases. As the parameter β increases the critical weight increases when the positive end moments are applied. The results are opposite when the negative end moments are applied, as the parameter β increases the critical weight decreases. It is also found that the equilibrium of the pipe with the positive value of pipe weight may not exist when the absolute value of moment becomes large.

ACKNOWLEDGEMENTS

The authors gratefully acknowledge the financial support by the Thailand Research Fund (TRF) under Contract No. MRG5380034.

REFERENCES

[1] Chen, S.S., "Flow-induced instability of an elastic tube", *ASME* Paper No. 71-Vibr.-39, 1971.
[2] Païdoussis, M.P. and Issid, N.T., "Dynamic stability of pipes conveying fluid", *Journal of Sound and Vibration*, 1974, 33, pp. 267-294.
[3] Thompson, J.M.T. and Lunn, T.S., "Static elastica formulations of a pipe conveying fluid", *Journal of Sound and Vibration*, 1981, 77, pp. 127-132.
[4] Chucheepsakul, S. and Monprapussorn, T., "Divergence instability of variable-arc-length elastica pipes transporting fluid", *Journal of Fluids and Structures*, 2000, 14, pp. 895-916.
[5] Chucheepsakul, S. and Monprapussorn, T., "Nonlinear buckling of marine elastica pipes transporting fluid", *International Journal of Structural Stability and Dynamics*, 2001, 1(3), pp. 333-365.
[6] Athisakul, C., and Chucheepsakul, S., "Effect of inclination on bending of variable-arc-length beams subjected to uniform self-weight", *Engineering Structures*, 2008, 30, pp. 902-908.
[7] Chucheepsakul, S., Wang, C.M., He, X.Q. and Monprapussorn, T., "Double curvature bending of variable-arc-length elasticas", *Journal of Applied Mechanics*, *ASME*, 1999, 66, pp. 87-94.
[8] Chucheepsakul, S., Monprapussorn, T. and Huang T., "Large strain formulations of extensible flexible marine pipes transporting fluid", *Journal of Fluids and Structures*, 2003, 17, pp. 185-224.
[9] Athisakul, C., Monprapussorn, T. and Chucheepsakul, S., "A variational formulation for three-dimensional analysis of extensible marine riser transporting fluid", *Ocean Engineering*, 2011, 38, 609-620.